Investigation of Near-Infrared Laser Diodes for Application in Space-Based Spectroscopic Gas Sensing

by

David McInerney

A thesis submitted for the degree of
Doctor of Philosophy
in the University of Dublin

School of Physics,
Trinity College,
Dublin.

October 2006
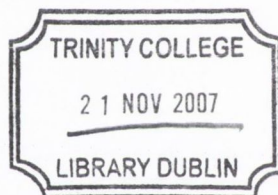
Declaration

This thesis has not been submitted as an exercise for a degree at this or any other university. The work presented is entirely my own, apart from the assistance mentioned in the acknowledgements. I agree that Trinity College Library may lend or copy this thesis upon request.

David McInerney

October, 2006.

Summary

The availability of numerous semiconductor diode lasers that provide wavelength tuneable, high output power, single frequency emission in the near infrared region of the spectrum ($0.7\mu m$ - $2.5\mu m$) provides researchers with a reliable and compact source of monochromatic radiation. Originally, development of this technology was driven by the telecommunications industry, however the fact that the overtone/combination absorption spectra of several gas species match the emission frequency of these laser sources have presented countless benefits for spectroscopic sensing applications.

The overall objective of this thesis is to investigate the critical issues relating to the suitability of two specific laser diodes and their application as injection seed lasers (ISL) for a spaced-based water vapour detection experiment. The importance of water to everyday life on earth is obvious and therefore the capability to accurately detect H_2O in the upper and lower troposphere is of immense benefit for monitoring weather conditions, climate change and pollution levels.

The spectral characteristics of two devices are examined in detail and their suitability for application as ISL's for space-based spectroscopic studies of water vapour is assessed. An external cavity diode laser (ECDL) in the Littrow architecture and a distributed feedback (DFB) diode laser both emitting at 935nm are detailed. Laser characteristics such as wavelength tuning, output power, side mode suppression ratio, spectral linewidth, sensitivity to feedback and operation under vacuum conditions are investigated.

An ECDL was implemented in a frequency stabilization scheme to operate as an ISL, with the output frequency of the laser locked to a H_2O vapour absorption line at 935.684nm. The frequency locking was achieved using a wavelength modulation spectroscopy technique. Continuous tuning of the emission frequency of the ECDL is achieved by a combination of fine tuning an external grating position by means of a piezo electric transducer (PZT), and injection current. By introducing a dual feedback control loop to manage the injection current and PZT voltage settings, the error signal bet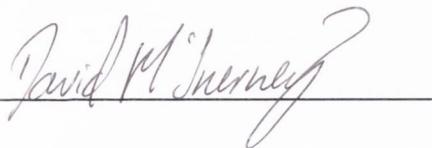ween the desired locking frequency and the output frequency of the laser was minimized. The performance of the overall frequency stabilized laser was examined in terms of accuracy and stability of the laser output frequency and dynamic response of the system. One disadvantage of tuneable diode lasers, due to the complex design of the devices, is the long-term drift and instability. Tuneable laser sources initially require time consuming

and tedious characterization, which dictates the correct operating parameters in terms of injection current control. However, due to ageing, thermal and mechanical instability, periodic re-characterization of these laser sources is necessary to maintain optimum performance in terms of mode-hop free, continuous wavelength tuning and sufficient side mode suppression ratio. With this in mind, a novel mode referencing technique was introduced to the frequency stabilized ECDL so that in-situ monitoring of the lasing mode guarantees optimum spectral performance.

In any laser frequency stabilization system, it is important to determine the free running frequency drift of the laser with no active stabilization in place. This measurement was performed by fixing the output frequency of both the ECDL and DFB laser diode to the wavelength corresponding to the centre of a water vapour absorption line at 935nm and monitoring the variation in the detected signal. From these results it was possible to determine the frequency drift of both laser sources over extended time periods. Consequently, the idea that a gas absorption line could be implemented as a frequency discriminator was applied to a technique to attempt to measure the instantaneous frequency noise and hence the spectral linewidth of a laser diode. The method involved setting the output frequency of a DFB laser, emitting at $1.39\mu m$, to the side of a H_2O vapour absorption line. Frequency variations in the laser output are converted to amplitude variations in the detected signal using the position of maximum slope at the side of the absorption feature. By introducing an auto-balancing photodetector into the experimental set-up it was possible to separately measure the resulting frequency fluctuations and hence determine a value for the linewidth of the laser. The value for the linewidth using this technique was compared to a simultaneous measurement using the delayed self-homodyne procedure.

The results of the various experiments reported in this thesis provide a significant contribution to the investigation of suitable laser diode sources for applications in space-based gas sensing projects, particularly at 935nm. Furthermore, a novel mode referencing technique to control and optimise an ECDL emission wavelength has been demonstrated with the potential to be applied to other tuneable laser diodes, so that time consuming and expensive re-characterization of devices can be avoided.

Acknowledgements

Numerous people have contributed to this thesis over the past few years for which I am truly grateful.

Firstly, I would like to thank my supervisor Professor John Donegan for giving me the opportunity to join the Semiconductor Photonics group here in Trinity and carry out my research. A sincere thank you John, for all your support, advice, and constant encouragement, which made my time as a member of the group a pleasure, and is much appreciated.

I would also like to acknowledge the invaluable contribution of Dr. Vincent Weldon and Mick Lynch to my progress and advancement of knowledge in the field of diode laser based sensing. Their technical expertise and advice on the subject provided vital structure and feedback to my studies. A sincere thanks to both for many interesting and informative discussions about laser based sensing, and to Vincent for the odd game of squash also.

Special thanks to Tom Farrell and Michael Todd for their help in sourcing the ECDL and DFB lasers used throughout the work in this thesis. Thanks also to Dewi Jones for help with my introduction to laser diode simulation techniques.

Thanks to all the members, past and present, of the Photonics group including Canice, Laura, Torsten, Matthais, Severine, Aaron, Wei-Hua, Vamsi, John, Pablo and Diarmuid.

Special thanks also to Seve who always gave me positive words of encouragement and to Richard for the numerous games of squash and rounds of golf with the odd relaxing pint thrown in for good measure, all of which helped to keep me going when the work was stressful.

I am grateful to Mick O'Reilly and Dave Grouse in the mechanical workshop, for all their help with fabrication of pieces over the past few years and a dept of gratitude is also due to John Kelly, Ken Concannon and Marie Kinsella.

I would also like to mention all the lads from the hurling and golf clubs that have helped me stay sane and in good spirits throughout my studies. A special word of thanks to Mark, Dave, Kevin, Marc, Conor, Joc, Trevor and Luke.

Finally, an immense dept of gratitude is due to my parents, my sisters, Celine, Clare, and Meadhbh and my girlfriend Aisling, for their constant love, support and kindness throughout, and to whom this thesis is dedicated.

Publications

D. McInerney, M. Lynch, J.F. Donegan, and V. Weldon, "Spectral linewidth and tuning requirements of sources for gas sensing in space-based applications at 935 nm", *IEE Proc., Optoelectronics*, vol. 153, pp. 33-39, 2006.

D. McInerney, V. Weldon, M. Lynch, and J.F. Donegan, "Frequency stability and tuning requirements of sources for specific gas sensing in space based applications", Lasers and Electro-Optics Europe, (CLEO/Europe) 2005.

V. Weldon, D. McInerney, R. Phelan, M. Lynch, and J.F. Donegan, "Characteristics of several NIR tuneable diode lasers for spectroscopic based gas sensing: A comparison" Journal title: Spectrochimica Acta Part A: Molecular and Biomolecular Spectroscopy, , Pgs 1013-1020, 2006.

Table of Contents

Chapter 1

Introduction

1.1 Introduction

Since the invention of the semiconductor laser diode in the early 1960s [1-3], it has become one of the most influential and useful technologies to date. Its application in so many varied and exciting fields such as optical storage, telecommunications, solid-state laser pumping and sensing applications has produced a technology whose global market value in 2005 was estimated at over \$3 billion [4]. The telecommunications area was the initial driving force for development and research into improving laser diodes. For fibre optic transmission, materials for laser diodes such as InGaAsP/InP were of great interest due to the minimum dispersion of fibres at 1300nm and minimal absorption at 1550nm wavelengths in the near infrared (NIR) region (0.7µm - 2.5µm) of the spectrum. For wavelengths below 900nm, AlGaAs/GaAs materials were also studied in detail as a source material for lasers and detectors.

However, in addition to its use for fibre optic transmission applications, the fortunate presence of vibrational overtone/combination absorption spectra in the NIR wavelength region provides researchers with an affordable, room temperature-operating, source of monochromatic light which can be used for targeting and detecting gas species. Because the absorption strengths of the overtone/combination bands are much less than that of the fundamental vibrational absorption bands, modulation techniques such as wavelength modulation spectroscopy (WMS) and frequency modulation spectroscopy (FMS) were implemented to improve detection sensitivies for laser diode based gas sensing [5]. Consequently, numerous gaseous species, which are of particular interest in industrial and environmental monitoring applications, such as C_2H_2, CH_4, CO_2, HCN, H_2O, and NH_3 can be accurately and quickly measured using tuneable diode laser absorption spectroscopy. By combining the laser technology with modulation techniques, it is possible to realise instruments that can for example, monitor pollution levels, analyse the efficiency of combustion engines in a non-intrusive manner, locate and detect explosives

1

or hazardous materials for security purposes, produce early fire warning systems, and carryout non-invasive medical diagnostics.

In this thesis, a water absorption band at 935nm is targeted using tuneable laser diodes. The interest in H_2O sensing is a result of an investigation and comparison of two different laser sources to act as injection seed lasers (ISL) for a space-based water vapour sensing experiment. The main objective of this work is to provide a frequency stabilized ISL so it can act as a frequency reference for a larger solid state laser. The spectral characteristics and performance of an external cavity diode laser (ECDL) and a distributed feedback laser (DFB) are examined in detail to determine their suitability for application as an ISL for high sensitivity H_2O sensing. The frequency stabilization of the ECDL to a H_2O absorption line at 935.684nm is controlled by the implementation of a dual feedback locking loop scheme [6]. While investigating the dual feedback loop dynamics of the ECDL, a novel mode referencing technique was devised for the laser, which helps develop the frequency locking system by performing in-situ device characterisation. This technique, which monitors the laser output power, forces the laser to operate in an optimum spectral mode and thus avoids any mode hopping which could cause a complete failure of a frequency stabilization scheme. This means that the effect of ageing or external influences on the lasers operation are automatically mitigated and the time consuming task of re-characterisation of an ECDL can be avoided thanks to this technique. This technique also has the potential to be applied to other widely tuneable laser diodes.

Other factors of concern for gas absorption spectroscopy using lasers are also examined. These include the vacuum operation of the ECDL at constant temperature and injection current. The effects of external optical feedback on the spectral characteristics of the ECDL and on a slotted Fabry-Perot device are also studied. Finally, for any frequency stabilization system, knowledge of the free running drift of the laser is essential. By incorporating a water vapour absorption line as a frequency discriminator, it was possible to monitor the frequency drift of both the ECDL and DFB for an extended period. An outcome of this frequency drift measurement led to the development and trial of an alternative technique to measure the spectral linewidth of a diode laser. The spectral linewidth of a DFB laser emitting at 1.39µm was measured by employing a H_2O absorption line as a frequency discriminator. A detailed description of the subsequent chapters is given in section 1.2.

1.2 Thesis overview

Chapter 2

A general introduction into the fundamental theory and basics of absorption spectroscopy are presented in this chapter. The use of semiconductor laser diodes, emitting in the near infrared (700nm-2.5μm) region of the spectrum, for gas sensing applications is outlined. The main absorption linewidth broadening mechanisms and the more prominent modulation spectroscopy methods employed in this work, including wavelength modulation spectroscopy and frequency modulation spectroscopy, are also discussed.

Chapter 3

This chapter provides a general introduction to semiconductor diode laser technology. The design and operation of some of the more popular laser diodes sources available during this work are discussed. The operational dynamics of a Fabry-Perot device are modelled using a series of rate equations to provide the reader with an in-depth understanding of diode laser operation. A more detailed analysis of the design features of an external cavity diode laser (ECDL) and a distributed feedback (DFB) laser diode both of which are extensively used throughout this research are also presented. Properties of these laser diodes such as wavelength tuning range, side mode suppression ratio and output power are detailed. Important issues for successful diode laser operation, such as optical isolation, external optical feedback and spectral degradation are also discussed. Finally, a measurement of the linewidth enhancement factor of a slotted Fabry-Perot laser is presented.

Chapter 4

The spectral characteristics of two laser diodes both emitting in the 935nm region of the spectrum are investigated and compared. The devices are candidates for a space-based gas sensing application where one of the lasers is to act as an injection seed source and frequency reference. An external cavity diode laser operating in the Littrow configuration

and a distributed feedback laser are examined. Various properties of the lasers such as wavelength tuning range, single frequency emission, output power and spectral linewidth are tested. Further tests involving the ECDL such as vacuum and optical feedback sensitivity are also carried out to establish its suitability for space-based operation. Finally a comparison is made between the ECDL and DFB laser diodes to determine the preferred laser source for the injection seed laser role.

Chapter 5

A dual feedback locking loop is implemented for the successful control of the emission wavelength of a frequency stabilized ECDL. The frequency stabilization is achieved by means of locking to a water absorption line at 935.684nm using a wavelength modulation spectroscopy technique [6]. The reason for the introduction of the dual locking loop is outlined and the accuracy and performance of the overall frequency locking system of the laser is also examined. In addition, a mode referencing technique is introduced which enables the laser to operate in continuous frequency locked mode. The mode referencing step ensures that the laser is maintained at its desired locked frequency without any need for time consuming, re-characterisation of the laser device parameters.

Chapter 6

A novel technique to measure the spectral linewidth of a DFB laser diode emitting at 1.39μm is investigated. The method involves using a gas absorption line as a frequency discriminator to measure the frequency noise of a laser. The output frequency of the laser source under test is tuned to the side of a gas absorption line, where any frequency variation in the laser output are converted to an amplitude variation, and detected with a balanced photodetector. The measurement is facilitated by the balanced detection scheme that detects the amplitude variations. A model of the gas absorption line specifics was developed in order to determine the optimum position on the side of the line and the slope of the absorption line. With knowledge of the absorption profile, the slope of the absorption line was determined and hence, the instantaneous frequency noise of the laser can be calculated. This approach is also compared to a more traditional self-homodyne

spectral linewidth measurement technique. The free running frequency drift of an ECDL and DFB laser, are also measured using a gas absorption line.

Chapter 7

The main conclusions and results of the research carried out for the thesis are summarized in this chapter. The most significant results are presented and some proposals based on the findings for future sensing applications are discussed.

1.3   References

[1]   N. Hall, G. E. Fenner, J. D. Kingsley, T. J. Soltys, and R. O. Carlson, "Coherent Light Emission From GaAs Junctions" *Phys. Rev. Lett.*, vol. 9, pp. 366–368, 1962.

[2]   M. G. A. Bernard and G. Duraffourg, "Laser condition in semiconductors", *Physica Status Solidi*, vol. 1, pp. 699, 1961.

[3]   M I Nathan, W P Dumke, G. Burns, FH Dills, G. Lasher. "Stimulated emission of radiation from GaAs pn junctions" *Applied Physics Letters*, vol. 1, pp.62, 1962.

[4]   Steele, Robert V., " Laser Marketplace 2006: Diode doldrums", *Laser Focus World*, Feb. 2006.

[5]   David S. Bomse, D. Christian Hovde, Shin-Juh Chen, and Joel A. Silver, "Early fire sensing using near-IR diode laser spectroscopy" *SPIE Proc.* vol. 4817, Diode Lasers and Applications in Atmospheric Sensing, pp73-81, 2002.

[6]   L.S. Rothmana *et al*, " The HITRAN 2004 molecular spectroscopic database," *Journal of Quantitative Spectroscopy & Radiative Transfer*, vol. 96, pp. 139–204, 2005.

Chapter 2

Fundamentals of Absorption Spectroscopy

2.1 Introduction

The subject of absorption spectroscopy has been studied since the early seventeenth century and is extremely useful in many different areas of research. It has helped to develop our understanding and knowledge of the world we live in from the macroscopic world of stars, to the microscopic world of atoms. The concept of absorption spectroscopy can be defined as the analysis of how electromagnetic radiation interacts with matter. When light of a certain wavelength interacts with matter, the light is either scattered, emitted, or absorbed. In this chapter, we concentrate on explaining the basis for semiconductor diode laser based spectroscopic studies and the dynamics of this light/matter interaction and on how information can be extracted relating to the concentration, composition and the absorbing wavelength of different species. The near infra-red region of the spectrum is explored with specific emphasis on H_2O absorption detection at 935nm. Spectral absorption lineshape analysis and the various lineshape broadening mechanisms that exist are also examined. The advances over the past 25 years with regard to semiconductor diode laser technology has provided researchers with an affordable, reliable instrument that is a source of coherent, monochromatic electromagnetic radiation which may be used to probe and detect various gaseous species [1]. The experimental application of semiconductor diode lasers to gas sensing is discussed. In addition, the theory and experimental results of the various spectroscopic detection schemes used such as wavelength modulation spectroscopy (WMS) and frequency modulation spectroscopy (FMS) are also presented.

2.2 Absorption spectra of gases

An absorption spectrum can occur when tuneable monochromatic radiation passes through a gas and the atoms in that form absorb at certain characteristic frequencies. Of

course, the profile of the spectral absorption will depend on the type of gas species targeted and on the frequency of the incident radiation. In this section, a short introduction is given regarding the basics of how absorption spectroscopy occurs and the application of laser diodes to spectral gas absorption experimental techniques. According to quantum theory, the energy of a molecule or atom is quantized. In other words, a particular molecule or atom can exist in a variety of discrete energy levels and can move from one energy level to another by a transition involving a finite amount of energy. Consider a photon of light passing through a gas of a certain molecule. If the photon contains sufficient energy it may be absorbed by the gas and a transition to a higher energy level can occur. However this process is only possible if the energy of the photon matches the transition energy. It is this resonant energy difference that provides the foundation for tuneable diode laser absorption spectroscopy. For a molecule, the energy levels are unique to each species and are very well defined so that each molecule has its own absorption spectrum. Consequently, it is possible to individually detect various gases using a combination of monochromatic laser radiation and a suitable photodetector. For the case where absorption bands of different molecules overlap at the same frequency, they can be accurately separated and identified by analysing the fine structure of the absorption spectrum.

The most commonly observed molecular spectra involve electronic, rotational, or vibrational, energy transitions. In brief, electronic spectra typically result in absorption in the ultraviolet or visible region of the spectrum and are a result of the movement and redistribution of the electrons in a molecule. In the microwave region of the spectrum ($1mm \leq \lambda \leq 1m$) transitions of pure rotational energy levels of molecules occur. In general, a rotational spectrum from a molecule requires that the molecule has a permanent dipole moment, which must change as the molecule rotates. Rotational transitions occur mostly between rotational levels of the same vibrational state, although there are many examples of combination vibration-rotation transitions for light molecules. The most efficient method to analyse the vibrational state of a molecule is to use infra-red spectroscopy as vibrational transitions typically require an amount of energy that corresponds to the infrared region of the spectrum. Vibrational transitions occur between different vibrational levels of the same electronic state. Vibrational transitions also occur in conjunction with rotational transitions. Therefore, highly-resolved vibrational spectra will contain fine structure corresponding to the rotational transitions that occur at the same time as a vibrational transition. The infrared region of the spectrum

can be divided into three regions; the near-, mid- and far- infrared, named for their relation to the visible spectrum. The far-infrared lies in the region of 25μm – 1mm may be used for pure rotational spectroscopy. The mid-infrared (2.5μm - 25μm) can be used to study the fundamental vibrations and associated rotational-vibational structure, while the near-IR (0.7μm - 2.5μm) can be used to examine the overtone/combination and harmonic absorption features.

For gas sensing applications using semiconductor diode lasers, the near-infrared region of the spectrum is of most interest due to the availibilty of devices that emit radiation at those frequencies. Recently, the fundamental vibrations present in the mid-infrared region are also being analysed due to the latest innovations with quantum cascade (QC) laser technology that emit coherent light at these frequencies and can detect many different gas species [2,3]. For a more detailed discussion of the theory and understanding of molecular spectroscopy and related topics, many excellent and informative books exist [4,5].

2.3 Spectral absorption lineshape assessment

In most diode laser based gas absorption schemes, the emitted radiation from the laser is passed through a reference gas cell, and the resulting absorption as a function of wavelength is recorded with a photodiode. Figure 2.1 illustrates a characteristic Doppler broadened absorption lineshape, with a Gaussian distribution, of an isolated absorption line with the line centre position corresponding to v_0. The concentration of the target gas under investigation may be determined by the area under the absorption profile or by the height of the absorption peak, if the lineshape profile is known. The width of the absorption lineshape is defined by both the half-width at half the maximum peak height (HWHM), and the full-width at half the maximum peak height (FWHM), both of which are commonly used. Obviously, lineshape profiles are susceptible to a number of broadening mechanisms including Doppler or pressure broadening effects or a combination of both. In order to ensure accurate analysis of the absorption line profile, it is therefore essential to differentiate between the relevant broadening effects. The width of a lineshape feature is primarily influenced by Doppler broadening and collisional (or pressure) broadening, both of which are now detailed.
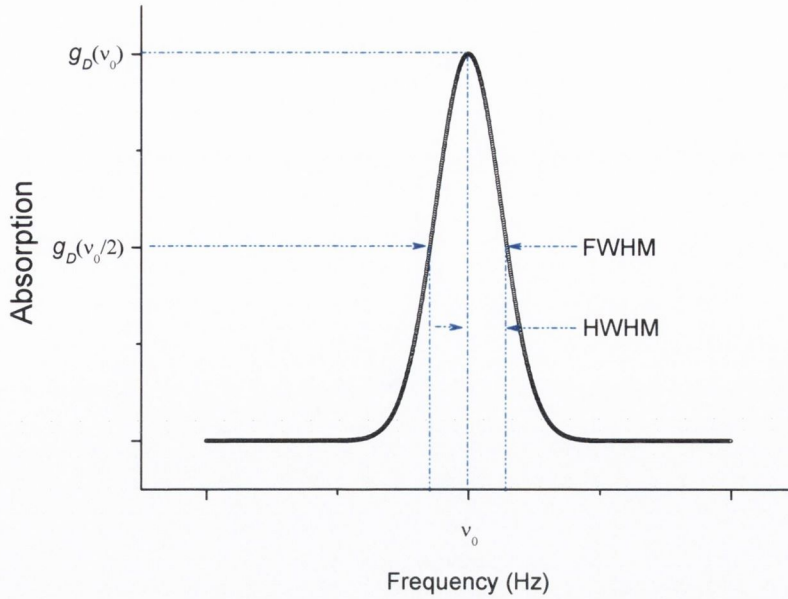
Figure 2.1. *Illustration of spectral lineshape against frequency for an absorption profile with the positions of the FWHM and HWHM indicated clearly.*

For a gas at low pressure (<50mbar), the effect of pressure broadening is less significant than Doppler broadening. Doppler broadening of spectral lines is due to the random, thermal motion of molecules which results in a distribution of velocities of the molecules in the gas. If a molecule has a velocity component in either the opposite or same direction as the propagation direction of the laser radiation beam, there exists a shift in the frequency of the photon that the molecule absorbs. In this manner, there exists some discrepancy between the actual and perceived wavelength of light absorbed by the molecules, which results in many small shifts, the cumulative effect of which is to broaden the absorption line. Doppler broadening is dependent on the wavelength of the line, the molecular mass of the emitting particle and the temperature. Since the spectral line is a combination of all the emitted radiation, the higher the temperature of the gas, the broader the spectral line emitted from that gas.

The velocities of the atoms in the gas follow a Maxwell distribution which gives the probability $P(v)dv$ of an atom having a velocity between v and $v + dv$ as,

$$P(v)dv = \sqrt{(m/2\pi kT)} \ \exp(-mv^2/2kT) \ dv \qquad (2.1)$$

where m is the molecular mass of the molecule, k is the Boltzmann constant, and T is the temperature in Kelvin. This distribution function is then related to a lineshape profile with a Gaussian outline, $g_D(v)$.

$$g_D(v) = (1/\gamma_D)\sqrt{\ln 2/\pi} \exp\left(-\ln 2\left(\frac{v-v_0}{\gamma_D}\right)^2\right) \qquad (2.2)$$

with v_0 is the frequency at line centre and γ_D is the Doppler HWHM given by

$$\gamma_D = (v_0/c)\sqrt{(2kT\ln 2/m)} \qquad (2.3)$$

where c is the speed of light, and has a maximum peak value at,

$$g_D(v_0) = (1/\gamma_D)\sqrt{\ln 2/\pi} \qquad (2.4)$$

To avoid the inconvenience of the ln2 term, the 1/e Doppler width, γ_{ED}, is also used. It is simply defined as,

$$\gamma_{ED} = \frac{\gamma_D}{\left(\sqrt{\ln 2}\right)} \qquad (2.5)$$

so that the 1/e Doppler HWHM is,

$$\gamma_{ED} = (v_0/c)\sqrt{(2kT/m)} \qquad (2.6)$$

The HWHM of the Doppler width can also be further simplified to,

$$\gamma_D(cm^{-1}) = 3.581 \times 10^{-7} v_0 \sqrt{\frac{T}{m}} \qquad (2.7)$$

with v_0 expressed in wavenumbers (cm^{-1}) , T is the temperature in Kelvin and m the molecular mass. For example the HWHM of a H_2O absorption line at 935nm (10695.2 cm^{-1}) and 300K is given by,

$$\gamma_D(cm^{-1}) = (3.581 \times 10^{-7}).(10695.2)\sqrt{\frac{300}{18}} \qquad (2.8)$$

$$\gamma_D = 0.01563 cm^{-1} = 469 MHz \qquad (2.9)$$

Pressure broadening is caused by collisions between molecules in a gas and results in homogeneous broadening. It is the most important source of broadening when pressures are high (>50mbar) and depends on both the density and the temperature of the gas. The continuous motion of molecules in a gas causes them to collide with each other at a rate of $1/\tau_c$, which increases with pressure, where τ_c is defined as the average time between collisions. Vibrational and rotational energies of the molecules are perturbed by these collisions, which interrupt the dipole oscillation resulting in a broadening of the vibrational/rotational lineshape. The importance of pressure broadening effects is significant since many optical detection systems occur at atmospheric pressure where pressure broadening is dominant. The spread in the wavelength of light absorbed by the molecule causes a spread in the absorption spectra. The pressure broadening normalized Lorentzian lineshape is given by [6],

$$L(v) = \left(\frac{1}{\pi}\right)\frac{\gamma_L}{(v-v_0)^2 + \gamma_L^2} \qquad (2.10)$$

where γ_L is the HWHM in wavenumbers (cm^{-1}), with a maximum peak value at,

$$L(v_0) = \frac{1}{\pi\gamma_L} \qquad (2.11)$$

The dependence of pressure and temperature on the Lorentzian linewidth is governed by,

$$\gamma_L = \gamma_L^0 (P/P_0)(T/T_0)^s \qquad (2.12)$$

where P is the gas pressure and γ_L^0 is the HWHM at standard temperature (T_0) and pressure (P_0). The effective power s, is often given as 0.5, but is not always the case as it can be affected by the rotational state and the broadening conditions of either self or foreign gas broadening.

However, at pressures where neither, Doppler or pressure broadening is the dominant broadening effect, the absorption lineshape profile of an absorption species can be described by a combination of both, that results in the Voigt profile [7]. It can be expressed in terms of a convolution of the Doppler and pressure broadening processes as,

$$\phi(v) = \frac{1}{\gamma_D}\sqrt{\frac{\ln 2}{\pi}}K(x,y) \tag{2.13}$$

where $K(x,y)$ is defined as the Voigt function and given by,

$$K(x,y) \equiv \frac{y}{\pi}\int_{-\infty}^{\infty}\frac{e^{-t^2}}{y^2+(x-t)^2}dt \tag{2.14}$$

In equation 2.14, y is defined as the ratio of the Lorentzian to Doppler widths given by,

$$y \equiv \frac{\gamma_L}{\gamma_D}\sqrt{\ln 2} \tag{2.15}$$

and x is the frequency scale in units of Doppler lineshape half-width γ_D, given by,

$$x \equiv \frac{v-v_0}{\gamma_D}\sqrt{\ln 2} \tag{2.16}$$

A plot of all three lineshape functions Gaussian, Lorentzian and Voigt is illustrated in figure 2.2. In general, towards the centre of the absorption line shape, the Voigt profile shows Doppler like behaviour and a Lorentzian like behaviour in the wings of the absorption profile. The absorption profiles in figure 2.2 have been deliberately modelled with different areas under each curve to highlight the contrast in the lineshapes.
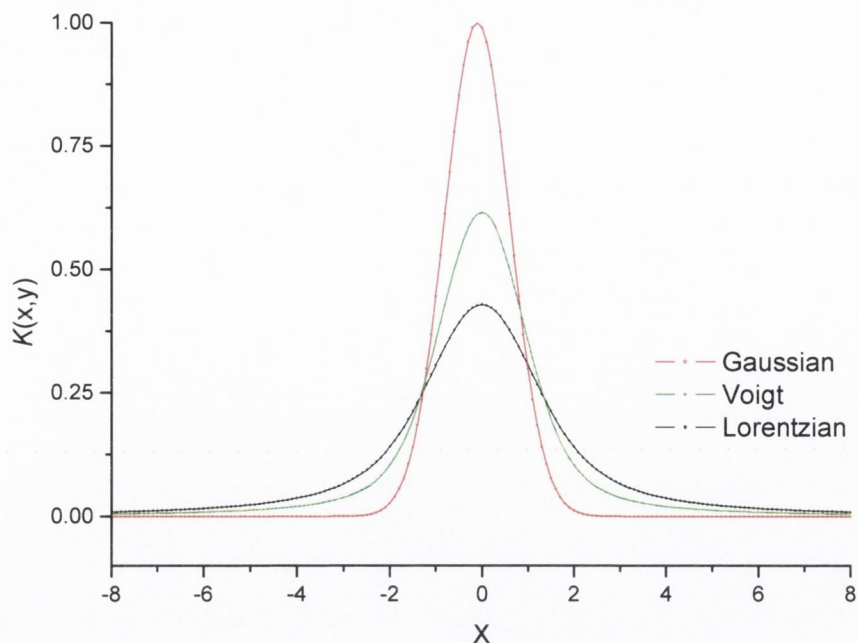
Figure 2.2. *Illustration of comparison of spectral lineshapes of gases calculated to show the difference in the Gaussian, Voigt and Lorentzian absorption profiles.*

2.4 H₂O absorption band

The water absorption spectrum of the 940nm band is central throughout the work performed for this thesis. The significance of water absorption at this wavelength is related to the analysis and characterization of two semiconductor laser diodes both emitting at 935nm. The two devices are candidates to function as injection seed lasers for a space-based water vapour sensing experiment, details of which are given in section 4.1. The key interest in atmospheric water vapour studies at the 940nm H_2O absorption band is a result of the isolation of this H_2O band from additional absorbing species in this region of the spectrum. Consequently, measurements can be accurately made from high altitudes with negligible interference effects from other absorbing species. In short, the abundance of water vapour in the atmosphere means that it has a constant influence on weather and climate conditions. The ability to accurately measure the water vapour content in the atmosphere is therefore crucial to improved understanding and prediction of weather conditions, climate change and pollution monitoring [8]. Stronger water absorption lines present at 1.39μm are also employed in this thesis for a frequency noise measurement of a DFB laser diode, which is described in chapter 6. The trace in figure 2.3 depicts the numerous absorption lines present in the 940nm water vapour band, with a strongly absorbing line at 935.684nm clearly marked [9].
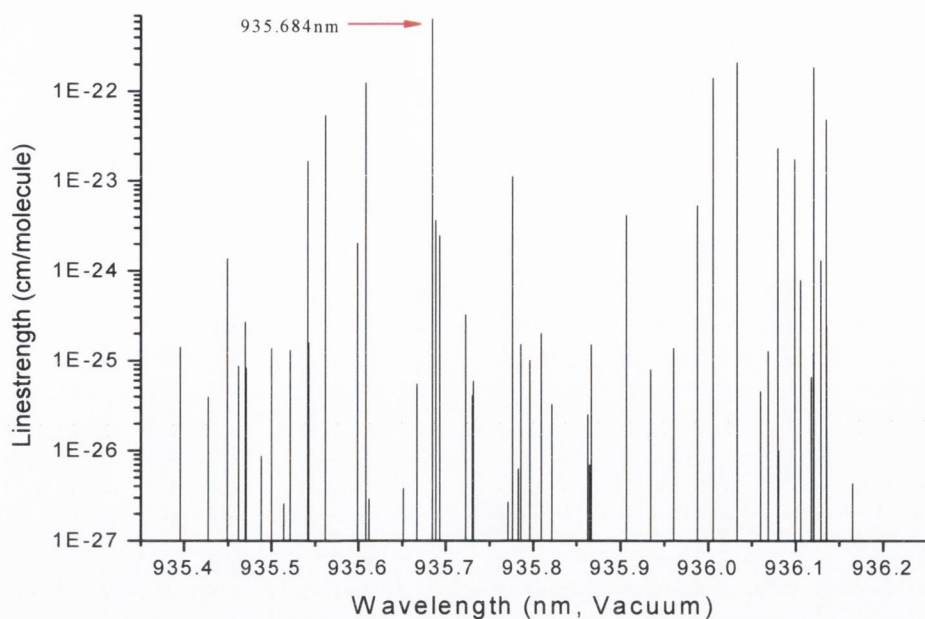
Figure 2.3. *Plot of linestrengths of water vapour absorption lines in the 940nm band with a strongly absorbing line at 935.684nm clearly indicated [9].*

The absorption line at this wavelength has featured throughout the research. It is used as a frequency reference for a laser stabilization scheme and has also been targeted for modulation spectroscopy tests of two laser diode devices.

2.5 Modulation spectroscopy techniques

2.5.1 Introduction

The accuracy and resolution limits of gas sensing applications using laser diode technology in the near-infrared spectrum can be greatly enhanced with the addition of certain modulation spectroscopy techniques. This is due to the fact that the fundamental absorption band of several gases occur in the mid-infrared region of the spectrum where absorption line-strengths are strong. By comparison, gas detection of the vibrational overtone/combination bands using NIR diode lasers needs to be complemented with certain modulation methods because the absorption line-strengths in the near-infrared region are significantly weaker. Therefore, techniques such as wavelength modulation spectroscopy (WMS) and frequency modulation spectroscopy (FMS) have been developed to overcome this problem [10-12]. The main distinction between the two techniques is related the frequency of the modulation. For WMS, the modulation

14

frequency is usually much less than the gas linewidth whereas with FMS, the modulation frequency can be equal to or greater than the gas linewidth and can therefore be several hundred MHz. Because WMS has been the more dominant modulation technique employed during the course of this research it is outlined in detail, whereas a more concise explanation of the FMS technique is given.

2.5.2 WMS

The basics of WMS are to target a gas absorption feature with modulated laser radiation, record the transmission with a photodiode, and process the resultant signal using a lock-in amplifier. The modulation of the laser sources is performed typically at kilohertz frequencies and can achieve sensitivities of 10^{-4} to 10^{-5} fractional absorption [13,14]. Depending of the application involved, whether it is solely for detection purposes or frequency reference, the lock-in amplifier can also be used to detect at higher harmonics of the fundamental modulation frequency. For example, the peak of the *2f* harmonic is often used for gas species detection while the *1f* or higher odd harmonics are commonly employed in frequency reference schemes as they have zero crossing values at the absorption line centre [15]. A more detailed and thorough review of the theory of WMS may be found elsewhere [16].

To begin our appraisal of harmonic detection techniques using laser diodes, the Beer-Lambert law is introduced. For laser radiation entering a sample gas, the Beer-Lambert law describes the relationship between absorbance and concentration of an absorbing species and is given by the following expression,

$$I(\nu) = I_0 \exp\left(-\kappa(\nu)nL\right) \tag{2.17}$$

where $I(\nu)$ is the transmitted laser intensity as a function of laser radiation frequency, I_0 is the laser intensity entering the sample, n is the gas concentration and L is the path length. $\kappa(\nu)$ is defined as the absorption coefficient of the gas at frequency ν. For laser diode based spectroscopic techniques where harmonic signals are produced, a modulation of the laser radiation is usually achieved by imposing a sinusoidal modulation of angular frequency ω, on the injection current of the device. The laser output frequency as a function of time is given by,

$$v(t) = <v> + a\cos(\omega t) \tag{2.18}$$

where $<v>$ is the average emission frequency from the laser, ω is the angular modulation frequency and a is the modulation amplitude. As the average emission frequency from the laser source is scanned across the gas absorption line of interest, it is assumed that the output power of the laser does not change such that equation 2.17 can be approximated and expressed as,

$$I(v) = I_0(v) \ (1-\kappa(v)nL) \tag{2.19}$$

By substitution of equation 2.18 into 2.19,

$$I(v) = I_0(v) \ (1-\kappa(<v> + a\cos(\omega t))nL) \tag{2.20}$$

The time dependent expression in equation 2.20, is an even function with time and can be expanded into a Fourier cosine series as,

$$\kappa(<v> + a\cos(\omega t)) = \sum_{n=0}^{\infty} H_n(<v>)\cos(n\omega t) \tag{2.21}$$

where $<v>$, for the duration of a modulation period is considered a constant. $H_n(<v>)$ is the nth Fourier component of the modulated absorption coefficient. Obviously, depending on the type of lock-in amplifier used, individual Fourier components can be selected to detect at the nth harmonic of the modulation frequency. In this instance the processed signals from the lock-in are proportional to,

$$I_0 H_n(<v>)L, \text{ for } n \geq 1 \tag{2.22}$$

and are strongly influenced by the absorption lineshape. If the effects of collisional broadening are the most dominant, then the absorption coefficient can be expressed as a Lorentzian function,

16

$$\kappa_L(\nu) = \cfrac{1}{1 + \left[\cfrac{\nu(t) - \nu_0}{\gamma_L}\right]^2} \tag{2.23}$$

where γ_L is the HWHM of the absorption line and at line centre $\kappa_L(\nu) = 1$. The definition of two dimensionless parameters are given by,

$$x = \frac{<\nu> - \nu_0}{\gamma_L} \tag{2.24}$$

and

$$m = \frac{a}{\gamma_L} \tag{2.25}$$

where m is define as the modulation index and thus the absorption coefficient becomes,

$$\kappa_L(x,m) = \frac{1}{1 + (x + m\cos(\omega t))^2} \tag{2.26}$$

Therefore, the 2nd Fourier coefficient (2nd harmonic) output from the lock-in amplifier for a Lorentzian absorption line can be expressed as,

$$H_2(x,m) = \frac{2}{\pi} \int_0^\infty \frac{\cos(2\theta)}{1 + (x + m\cos(\theta))^2} d\theta \tag{2.27}$$

Throughout this research, WMS was successfully implemented with a variety of semiconductor lasers. The frequency of the modulation was typically in the kilohertz region with the modulation index, $m = 2.2$ for $2f$ harmonic detection and 1.65 for $1f$ harmonic detection where maximum amplitude of the signal is obtained. The advantage of the technique in comparison to direct detection is demonstrated by the traces in figures 2.4 and 2.5. The absorption profile in figure 2.4 represents the direct detection of a water vapour absorption line in the 935nm region of the spectrum. The emission wavelength of an external cavity diode laser (ECDL) was tuned across the H_2O absorption line in a continuous manner by using a combination of injection current and piezo electric

transducer (PZT) voltage. Details of the wavelength tuning mechanism of the ECDL are given in more detail in chapter 4. As the laser wavelength is passed through the gas cell, the resulting decrease in the absorption signal was recorded with a photodiode. In figure 2.4, the effect of the decrease in output power of the laser, as the emission wavelength is tuned across the H_2O absorption line, is clearly observable with the sloping background on the recorded absorption signal.
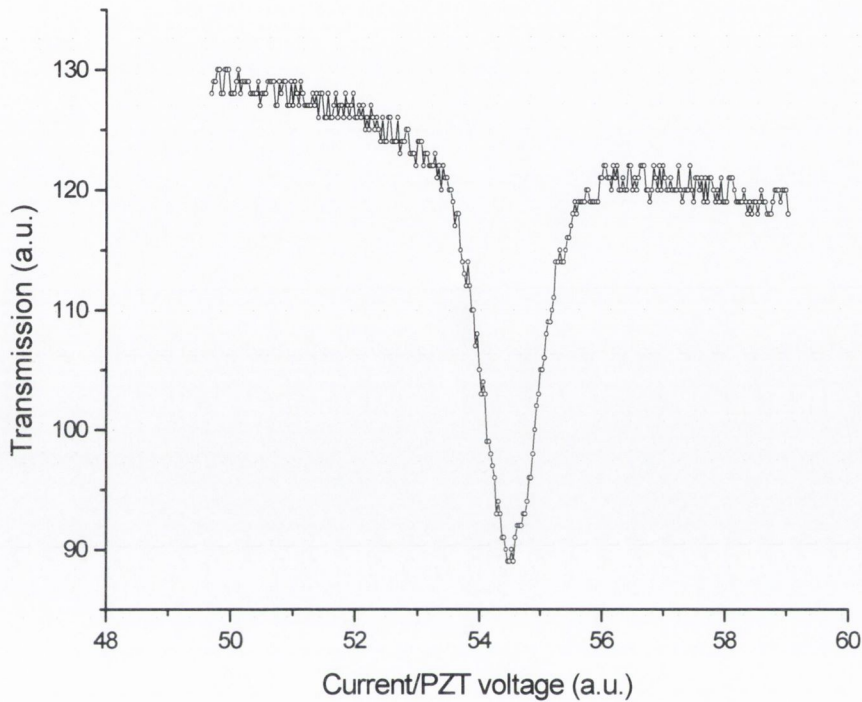
Figure 2.4. *Direct detection of a H_2O absorption line in the 935nm region of the spectrum.*

In comparison, when the WMS technique is implemented for detection of the identical water absorption line, with the PZT of the ECDL modulated at 14kHz, the change in the detected signal is significant. Figure 2.5 shows the *1f* and *2f* harmonic signals of the H_2O absorption line at 935.684nm with the sloping background removed. The zero-crossing point of the *1f* and the peak of the *2f* signals both represent the absorption line centre, which are commonly employed for frequency referencing and minimum concentration schemes, respectively. To demonstrate the effect of the modulation index on the detected absorption signals, a number of measurements of the *1f* harmonic and *2f* harmonic signals for increasing values of the modulation index, *m* were recorded.
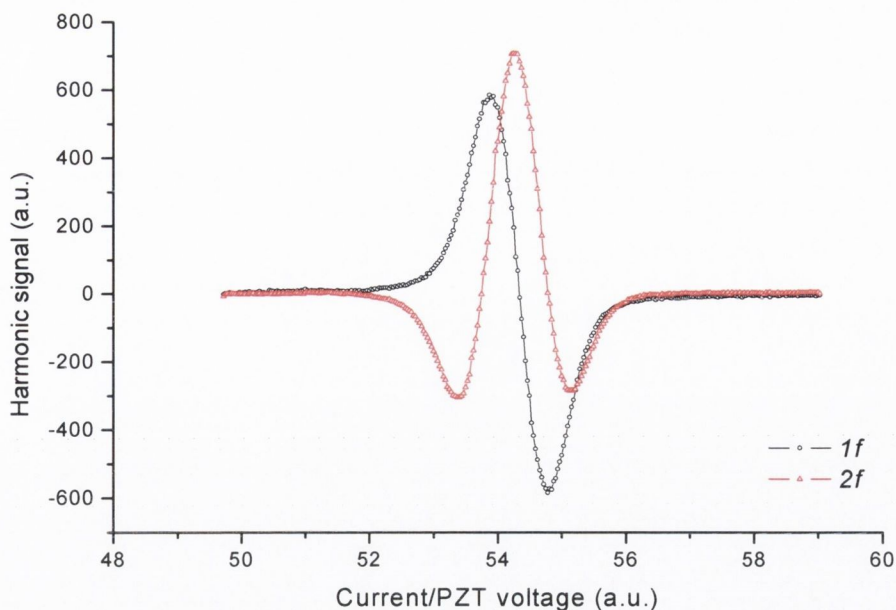
Figure 2.5. *Typical harmonic detection signals recorded with a lock-in amplifier showing the 1f and 2f harmonic detected traces with the sloping background conveniently removed.*

Figure 2.6 shows plots of the *1f* harmonic signal of a water vapour absorption line for various values of the modulation index. In addition to an increase in signal strength with increasing *m*, the lineshape profile broadens corresponding to a broadening of frequency. The maximum peak to peak value for the *1f* trace occurs when the modulation index is equal to 1.65.
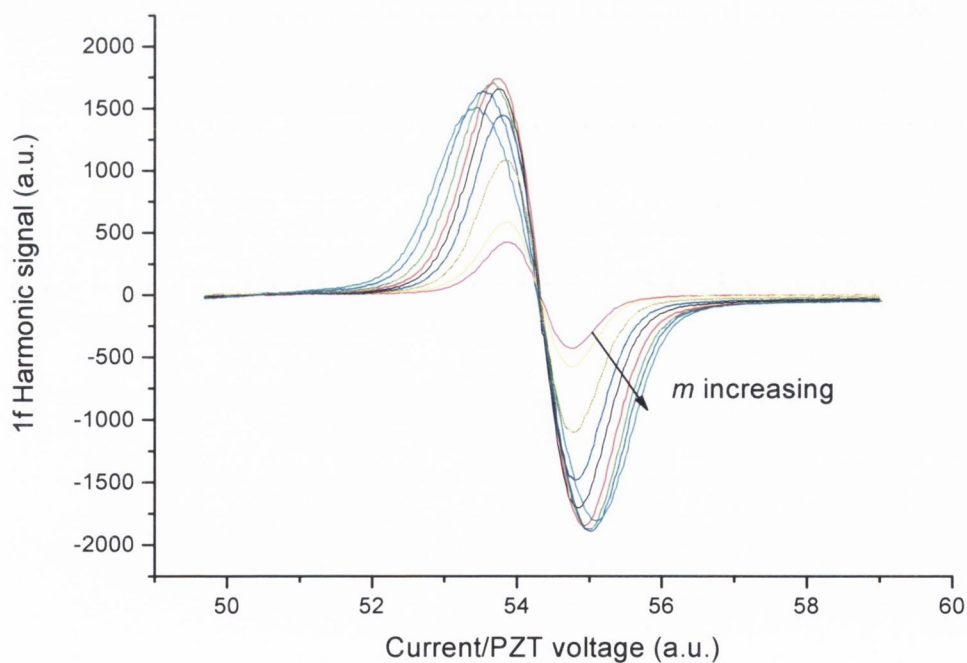
Figure 2.6. *1f harmonic detected signal measured as a function of the modulation index showing the change in peak to peak amplitude and broadening of the absorption line as m is increased.*

19

The same measurement was carried out for the *2f* harmonic signal as indicated in figure 2.7. Again, the modulation index is changed by increasing the amplitude of the modulation and for the case of the *2f* signal, a maximum amplitude is recorded for *m* equal to 2.2.
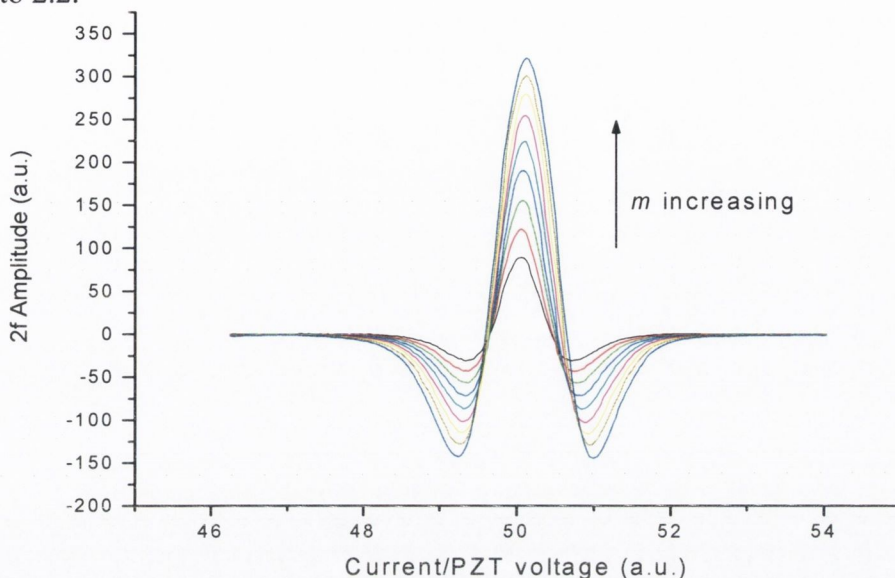
Figure 2.7. *2f harmonic detected signal of a H_2O absorption line at 935nm measured as a function of the modulation depth. The amplitude of the 2f signal increases as m is increased to a maximum value at m=2.2.*

Finally, the peak amplitudes of the *2f* traces as a function of modulation amplitude are shown in figure 2.8 demonstrating the initial increase and subsequent decrease in peak amplitude. The position on the graph where maximum *2f* signal occurs corresponds to *m* = 2.2, as expected [17].
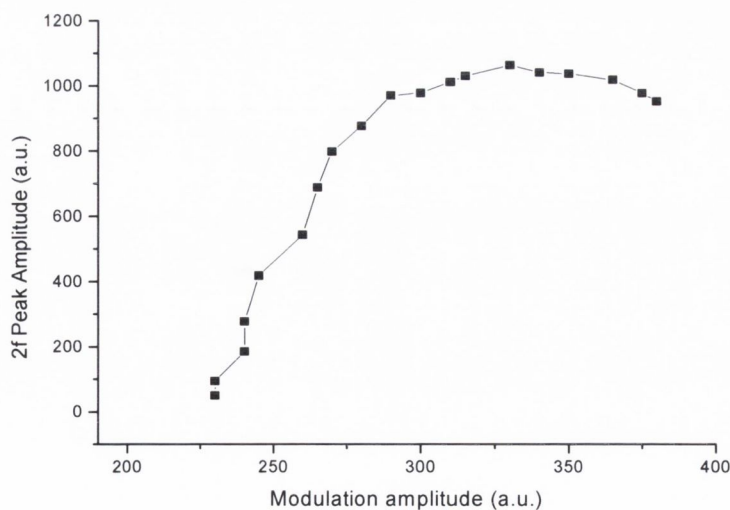
Figure 2.8. *2f harmonic peak amplitude of a H_2O absorption line at 935nm measured as a function of the modulation amplitude.*

To summarise, the WMS technique is an extremely powerful and beneficial technique for gas sensing applications using semiconductor diode lasers. The fact that modulation of the laser can be easily implemented by modulating the injection current to the laser, while the detection and processing of absorption signals is managed with a lock-in amplifier, generates an extremely effective technique to detect weakly absorbing gas species. The advantages of WMS are clearly evident with the removal of the sloping background present in direct detection and also the transfer of the detection to higher frequencies thus reducing any $1/f$ laser excess noise, which can reduce the accuracy of the detection process.

2.5.3 FMS

The primary difference between FMS and WMS is the frequency at which the diode laser radiation is modulated. FMS typically involves modulation frequencies set equal to or greater than the width of the absorption line. The main advantage of FMS over WMS is that the detected signal is shifted to higher frequencies where noise sources are reduced and also detector-limited sensitivities of the order 10^{-7} to 10^{-8} are possible [18]. A brief outline of the technique along with some experimental results is given here but a more detailed evaluation and assessment of the method can be found in [19]. The output of a laser diode can be modulated at some high frequency Ω, by using for instance, a phase modulator. The spectral output of the laser will consist of the carrier frequency ω_c, and sideband frequencies $\omega_c \pm \Omega$, as shown in figure 2.9.
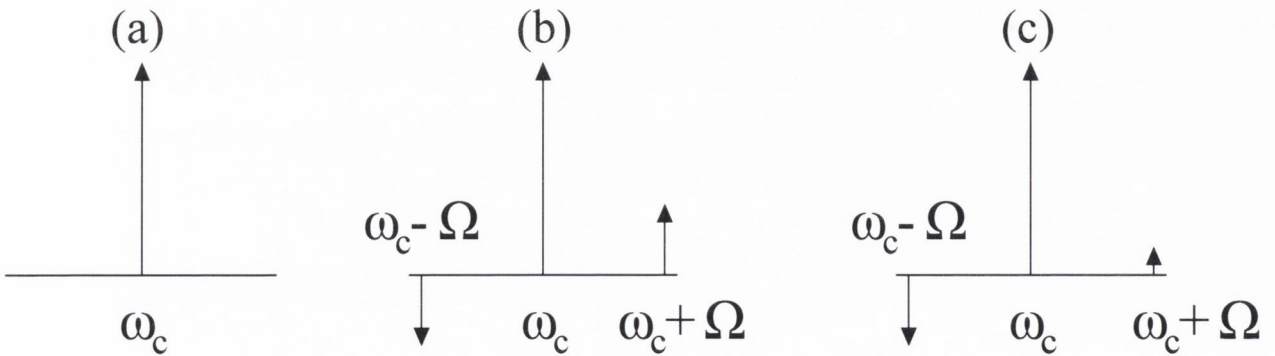
Figure 2.9. *Frequency and intensity profile of a diode laser beam (a) unmodulated, (b) modulated with no absorption and (c) modulated with absorption present with ω_c corresponding to the carrier frequency and Ω the sideband frequency respectively.*

When the emission frequency of the laser diode is passed through a particular absorbing species, the absorption will act on each of the sideband frequency components. This is illustrated by the reduction in the amplitude of the upper sideband ($\omega_c + \Omega$), as clearly indicted on the far right of figure 2.9. Typically, the modulation index is kept small so that the light spectrum consists of only the carrier frequency and one set of sidebands. The information of the absorption strength can then be extracted using phase sensitive detection techniques. FMS theory is written in terms of optical electric fields being transmitted through an absorptive and dispersive medium. In this way, phase information is retained in comparison to WMS where only intensities rather than electric fields representations are employed. For real systems, the intensity of the laser output fluctuates so that the electric field of a frequency modulated laser beam is given by,

$$E(t) = E_0[1 + M\sin(\omega_m t + \psi)]\exp[i\,\omega_0 t + i\beta\sin(\omega_m t)] \tag{2.28}$$

where M is the amplitude modulation index, ω_m is the modulation frequency, ω_0 is the optical carrier frequency, ψ is the phase difference between the amplitude and phase modulation and β is the frequency modulation index. Equation 2.28 can be rewritten, in terms of exponentials with the exponential frequency terms replaced with a summation over Bessel functions, as,

$$E(t) = E_0 \exp(i\,\omega_0 t) \sum_{l=-\infty}^{+\infty} r_l \exp(il\omega_m t) \tag{2.29}$$

$$\text{where } r_l = \sum_{k=-1}^{1} a_k J_{l-k}(\beta), \quad a_0 = 1, \quad \text{and} \quad a_{\pm 1} = \frac{\pm M}{2i}\exp(\pm i\psi) \tag{2.30}$$

where J_l is the lth order Bessel function. If this modulated electric field is passed through a medium with both absorption and dispersion effects, the transmitted intensity can be expressed as a sum of Fourier components at frequencies corresponding to multiples of the modulation frequency, ω_m. Analysis of the photocurrent using a lock-in amplifier at ω_m or some n ω_m harmonic, the resultant complex signal amplitude is given by,

$$I = 2I_0[Re(Z)\cos(\theta) - Im(Z)\sin(\theta)] \tag{2.31}$$

with,

$$Z = \sum_l r_l r_{l-n}^* \exp\{-1/2\alpha(\omega_0 + l\omega_m) - 1/2\alpha[\omega_0 + (l-n)\omega_m]\}$$
$$\exp\{-i\varphi(\omega_0 + l\omega_m) + i\varphi[\omega_0 + (l-n)\omega_m]\} \qquad (2.32)$$

where r^* is the complex conjugate of r. The detector phase angle θ relates the phase of the detected signal to that of the reference frequency in the lock-in amplifier so that the in-phase and quadrature components are 180^0 out of phase of each other. The in-phase component corresponds to pure absorption while the quadrature component corresponds to dispersion of the incident light. The trace in figure 2.10 represents the in-phase and quadrature signals of a detected water absorption line in the 935nm region of the spectrum. The emission wavelength of an ECDL was tuned linearly across the absorption line with the output fibre coupled to an external phase modulator. The output of the laser was thus modulated at 400MHz and the in-phase (I) and quadrature (Q) signals were processed with custom-made control electronics. The phase modulator consists of a low insertion loss, high electro-optic coefficient lithium niobate ($LiNbO_3$) crystal where the refractive index of the material is varied by applying an electric field [20].
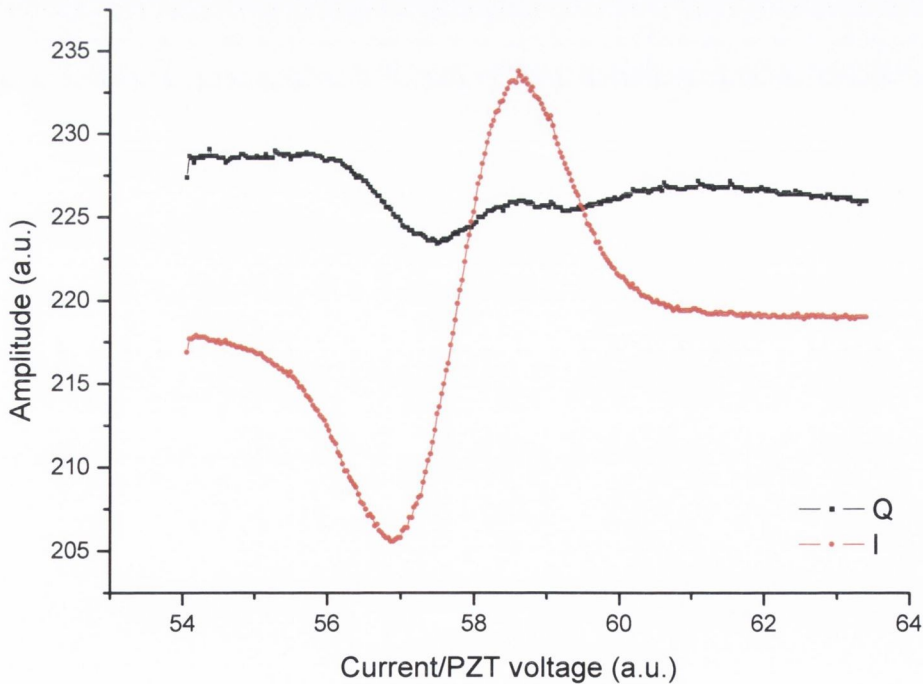
Figure 2.10. *FMS signal where the I and Q components are recorded as the emission wavelength of the laser is tuned across a H_2O absorption line.*

2.6 Summary

An outline of the main features of absorption spectroscopy has been presented. The basis for diode laser spectroscopy in the near infra-red region of the spectrum as a result of the vibrational overtone and combination band absorption profiles has been explained. The concept of linewidth of an absorption feature has been introduced with the most prominent broadening mechanisms, such as Doppler, collisional and a combination of the two examined in detail. A clear knowledge of these features is essential for accurate gas detection schemes. The concept of modulating the output beam of a laser diode in order to improve the sensitivity of the detection process is also discussed. The theory of both the WMS and FMS modulation techniques has been presented in addition to some experimental results involving H_2O vapour sensing in the 935nm region of the spectrum by employing both of these methods. In the succeeding chapters, the understanding and insight of the various broadening mechanisms, modulation techniques are demonstrated in experiments involving topics such as frequency referencing, frequency stabilization and noise measurements of laser sources. In particular, the majority of the experiments are concerned primarily with water vapour sensing at 935nm. Additionally, water vapour detection experiments are also carried out with a DFB laser emitting at 1.39µm. Further details of these measurements at 1.39µm are detailed in chapter 6.

2.7   References

[1]   P. R. Werle, "A review of recent advances in semiconductor laser based gas monitors," *Spectrochimica Acta Part A,* 54, pp. 197–236, 1998.

[2]   G. Wysocki, M. McCurdy, S. So, D. Weidmann, C. Roller, R. F. Curl, and F. K. Tittel, "Pulsed Quantum-Cascade Laser-Based Sensor for Trace-Gas Detection of Carbonyl Sulfide," *Appl. Opt.*, vol. 43, pp. 6040-6046, 2004.

[3]   Gmachl, C.; Capasso, F.; Kohler, R.; Tredicucci, A.; Hutchinson, A.L.; Sivco, D.L.; Baillargeon, J.N.; Cho, A.Y.; "Mid-infrared tunable quantum cascade lasers for gas-sensing applications", *Circuits and Devices Magazine, IEEE* vol. 16, pp. 10–18, 2000.

[4]   Colin N. Banwell, "Fundamentals of Molecular Spectroscopy", McGraw Hill Book Co Ltd; Third edition, 1983.

[5]   Gordon M. Barrow, "Introduction to Molecular Spectroscopy", McGraw Hill Text, 1962.

[6]   R.M. Measures, "Laser Remote Chemical Analysis", Wiley, New York, 1988.

[7]   B. H. Armstrong, "Spectrum Line Profiles: The Voigt Function." *J. Quant. Spectrosc. Radiat. Transfer,* vol. 7, pp. 61-88, 1967.

[8]   E. V. Browell, S. Ismail, and R. A. Ferrare "LASE Water Vapor, Aerosol, and Cloud Measurements During Recent Field Experiments", Tenth ARM Science Team Meeting Proceedings, San Antonio, Texas, March 13-17, 2000.

[9]   L.S. Rothmana, D. Jacquemarta, A. Barbeb, D. Chris Bennerc, M. Birkd, L.R.
        Browne, M.R. Carleerf, C. Chackerian Jr.g, K. Chancea, L.H. Couderth, V. Danai,
        V.M. Devic, J.-M. Flaudh, R.R. Gamachej, A. Goldmank, J.-M. Hartmannh, K.W.
        Jucksl, A.G. Makim, J.-Y. Mandini, S.T. Massien, J. Orphalh, A. Perrinh, C.P.
        Rinslando, M.A.H. Smitho, J. Tennysonp, R.N. Tolchenovp, R.A. Tothe, J. Vander
        Auweraf, P. Varanasiq, and G. Wagner, " The HITRAN 2004 molecular
        spectroscopic database," *Journal of Quantitative Spectroscopy & Radiative
        Transfer*, vol. 96, pp. 139–204, 2005.

[10]   D. S. Bomse, A. C. Stanton, and J. A. Silver, "Frequency modulation and
        wavelength modulation spectroscopies: comparison experimental methods using a
        lead-salt diode laser," *Appl. Opt.*, vol. 31, pp. 718-731, 1992.

[11]   Pawel Kluczynski, Jorgen Gustafsson, Asa M. Lindberg, Ove Axner, "Wavelength
        modulation absorption spectrometry-an extensive scrutiny of the generation of
        signals", *Spectrochimica Acta Part B 56*, pp. 1277-1354, 2001.

[12]   J. M. Supplee, E. A. Whittaker, and W. Lenth, "Theoretical description of
        frequency-modulation and wavelengthmodulation spectroscopy," *Appl. Opt.*, vol.
        33, pp. 6294–6302, 1994.

[13]   D. T. Cassidy and J. Reid, "Atmospheric pressure monitoring of trace gases using
        tunable diode lasers," *Appl. Opt.*, vol. 21, pp. 1186-1190, 1982.

[14]   D. M. Bruce and D. T. Cassidy, "Detection of oxygen using short external cavity
        GaAs semiconductor diode lasers," *Appl. Opt.*, vol. 29, pp. 1327-1332, 1990.

[15]   Grady J. Koch, "Automatic laser frequency locking to gas absorption lines", *Opt.
        Eng.*, vol. 42, pp. 1690-1693, 2003.

[16]   J Reid and D. Labrie, "Second-harmonic detection with tunable diode lasers —
        Comparison of experiment and theory", *Applied Physics B: Lasers and Optics*, vol.
        26, pp. 203 – 210, 1981.

[17] R.M. Measures, "Laser Remote Chemical Analysis", pages 214-220, Wiley, New York, 1988.

[18] C. B. Carlisle, D. E. Cooper, and H. Preier, "Quantum noise-limited FM spectroscopy with a lead-salt diode laser," *Appl. Opt.*, vol. 28, pp. 2567-2576, 1989.

[19] J. A. Silver, "Frequency-modulation spectroscopy for trace species detection: theory and comparison among experimental methods," *Appl. Opt.*, vol. 31, pp. 707-717, 1992.

[20] E. L. Wooten, K. M. Kissa, A. Yi-Yan, E. J. Murphy, D. A. Lafaw, P. F. Hallemeier, D. Maack, D. V. Attanasio, D. J. Fritz, G. J. McBrien, and D. E. Bossi, "A review of lithium niobate modulators for fiber-optic communications systems," *Selected Topics in Quantum Electronics, IEEE Journal of*, vol. 6, pp. 69-82, 2000.

Chapter 3

Semiconductor Diode Lasers

3.1 Introduction

The main objective of this chapter is to provide a general introduction to the field of semiconductor diode lasers for gas sensing applications, with specific detail on near infrared (NIR) lasers. Originally, it was the telecommunication industry that fuelled the research and advances in room temperature operating, wide-wavelength tuning range, low current threshold, and relatively low cost NIR semiconductor laser sources. As discussed in the previous chapter, the fact these devices can be easily modulated and applied to spectroscopic based detection schemes has lead to detailed and varied research to further improve laser sources, which in turn has lead to improved accuracy of gas detection techniques.

Semiconductor laser devices presently available on the market at the time of this work and their numerous applications will be discussed. In particular, we look at their relevance in terms of spectroscopic sensing applications and contrast the advantages and disadvantages of each. A more thorough description of the operating principles and design of an external cavity diode laser (ECDL) and a general introduction to a distributed feedback laser (DFB) is also presented. These devices were employed throughout the course of the work for this thesis. The spectral characterisation and investigation of both these types of diode laser with a view to operating them for gas sensing applications is detailed. In particular, sensing of H_2O vapour absorption lines in the 935nm region of the spectrum is examined. Characteristics such as single frequency emission, output power, continuous wavelength tunability, and spectral linewidth, all of which are critical for highly accurate gas detection systems, are investigated and described. The subject of external optical feedback in relation to spectral degradation of devices is also explored [1,2]. A series of measurements to investigate the effects of unwanted optical feedback are carried out on a slotted Fabry-Perot (SFP) laser. Also a measurement of the linewidth enhancement factor of the SFP device using the Hakki-Paoli method, is presented. To begin with, an introduction to a series of rate equations,

which describe the dynamics of a laser diode in operation, is presented. The interaction of charge carriers and photons in addition to some typical spectral light-current characteristics of a Fabry-Perot device are modelled. The aim of the rate equation simulation is to provide a basic understanding of the operation of semiconductor laser diodes, which are applied to gas sensing experiments throughout this thesis.

3.2 Coupled rate equations

One of the most informative methods to achieve a better understanding and knowledge of a laser diode operation involves a set of rate equations [3]. The operating dynamics of semiconductor lasers are well described by such equations that describe the interaction of photons and electrons inside the active region. The coupled equations illustrate a simple, yet very accurate mathematical description of the diode laser. By incorporating a simulated model of the laser dynamics a series of coupled first order differential equations were generated which, when solved, evaluate the interaction between the injected carriers and photons in the diode laser. The coupling of the different rate equations is caused by the carrier density dependence on the stimulated emission, the absorption and the refractive index in the active material. The carrier density rate equation takes the form of,

$$\frac{dN}{dt} = \frac{\eta_i I}{qV} - \frac{N}{\tau} - v_g gS \qquad (3.1)$$

where,

$$\frac{dN}{dt} = Generation\ terms - Recombination\ terms \qquad (3.2)$$

The generation term (optical pump) is modelled as a current flow and is given by,

$$Generation = \frac{\eta_i I}{qV} \qquad (3.3)$$

with, I = current

q = charge, V = volume of active region

η_i = internal quantum efficiency = 1

This electrical pump term is the source of carriers, and under equilibrium conditions, must balance the net rate of loss of the carriers caused by the different forms of recombination involved. The current increases the electron density in the active region but may be considerably less than the actual value for the current being driven into the contact. The reason for this loss is the lateral diffusion and spreading of the charge carriers. These losses, for simplicity have been placed into the non-radiative recombination term, which itself also leads to a loss of carriers without producing any photons.

The recombination term on the other hand is more complicated as several mechanisms have to be taken into account. These include, spontaneous emission (photon emission), stimulated absorption (photon absorption), stimulated emission (coherent photon emission) and finally, non-radiative absorption (energy/heat dissipation). So we can say that without a generation term, the carrier decay,

$$\frac{dN}{dt} = -\frac{N}{\tau} \tag{3.4}$$

where,

τ = carrier lifetime

Then the stimulated emission is given by,

$$R_{st} = v_g g S \tag{3.5}$$

where,

v_g = group velocity

g = gain

S = photon density

The expression for gain used in our model is given by the following,

$$g = g_0 \ln\left[\frac{N + N_s}{N_{tr} + N_s}\right] \tag{3.6}$$

30

Normally it is sufficient to use the two-parameter (N_{tr}, g_0) logarithmic functionality for the gain, with N_{tr} being the transparency carrier density at which the stimulated optical gain is cancelled by the stimulated optical absorption (the material is transparent for the light at that frequency, i.e. gain is equal to the loss), and g_0 is the gain coefficient, as it works reasonably well. However, for more linear gain curves the fit does not work as well so a third linearity parameter (N_s) is added to correct the problem. N_s is a constant to ensure the natural logarithm is finite at $N = 0$ such that the gain equals the un-pumped absorption. The equivalent equation for the rate of change of photons is considered next. The rate of change of photons within a laser cavity takes the form,

$$\frac{dS}{dt} = \Gamma v_g g S + \beta_{sp} B N^2 - \frac{S}{\tau_p} \tag{3.7}$$

where Γ = confinement factor

$\quad \beta_{sp}$ = spontaneous emission factor

$\quad B$ = bimolecular coefficient

In this instance, with regards to the photon density, the processes involved include stimulated and spontaneous emission (through which photons are created), absorption and mirror loss (through which photons are lost). The first term in the equation represents the stimulated emission and is multiplied by the confinement factor, which gives the percentage of total optical energy found in the active region. The second term represents the spontaneous emission and finally the losses, which are given by the photon density divided by the photon lifetime. An understanding of the dynamic response of a semiconductor laser is vital in particular in the area of optical fibre communication systems where the device current is modulated periodically and the laser output is in the form of pulses. When current is applied to the laser, stimulated emission can occur but the laser does not emit coherent light until the current exceeds a critical value. This value is known as the threshold current, I_{th}. As the current is increased to a level above I_{th}, a time interval passes, known as turn on delay, before the laser power starts to increase rapidly. Also, because of the non-linear nature of the interaction between the photon and carrier densities, the power does not increase linearly. The laser output oscillates

periodically for several nanoseconds before achieving its steady state value. These oscillations are commonly referred to as relaxation oscillations, and their frequency is governed by the non-linear dynamics of the photon-carrier interaction. The frequency of the relaxation oscillation is typically in the gigahertz range and increases with increasing injection current.

3.2.1 Simulated results

The rate equations are solved with the aid of a fourth order Runge-Kutta numerical technique used to solve differential equations [4]. The graph in figure 3.1 gives a clear and illustrative idea of how the carrier and photon densities interact and shows us how the two rate equations are coupled together. Some of the typical values for the parameters used in the simulation are also listed in figure 3.1. The photon density S is multiplied by 1000 here just to give a better pictorial contrasting view of how both N and S values are linked to each other. The device modelled for this simulation was a single mode Fabry-Perot laser diode emitting at 1550nm at room temperature.

Parameter	Value
Spon. emission factor, β	1e-4
Carrier lifetime (s)	1e-9
Cavity eff. Index	3.336
Bimolecular coeff. (m^3/s)	1e-16
Confinement factor	0.3
Cavity length (m)	300e-6
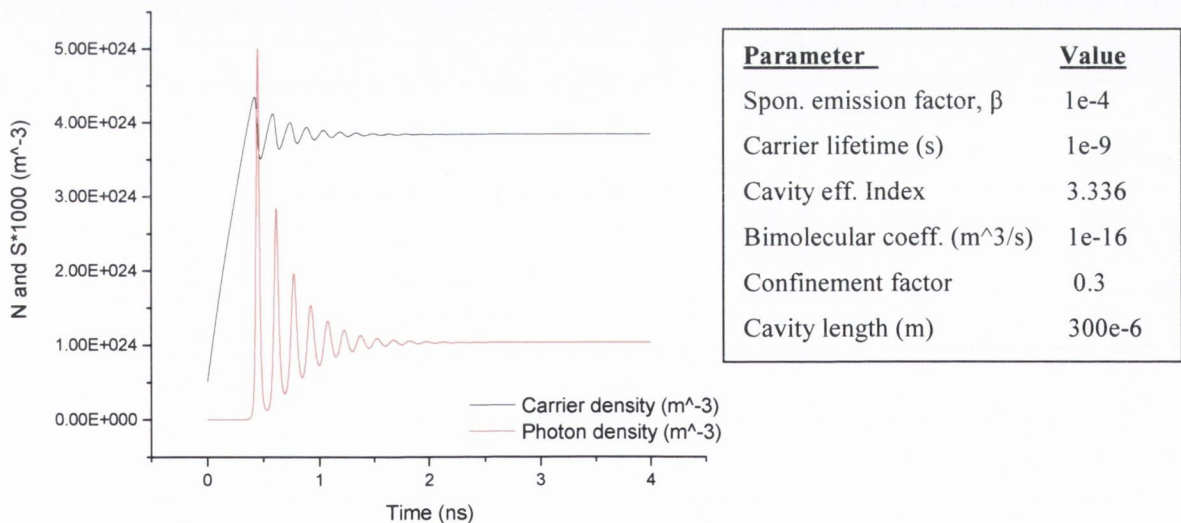
Figure 3.1. *Simulation of time evolution of carrier and photon densities demonstrating relaxation oscillations, along with some typical parameters.*

An initial value of $5 \times 10^{23} (m^{-3})$ is set for the carrier density N and S is set to zero, as there is no light output initially. Of course the advantage of the simulated model is that parameters can be constantly changed in order to investigate different scenarios. For the simulation in figure 3.1, the injection current density was set at 4000A/cm^2 and the time

range for the simulation is set from 0ns to 4ns. As shown in figure 3.1, the carrier density initially increases as the active region is filled. Of course, there is very little photon density present until the carrier density reaches its threshold value. At this point, stimulated recombination begins to limit a further increase in carrier density as the photon density starts to increase. This delay before the photon density "turns on" is called the turn-on delay of the laser. It is evident from figure 3.1 that the turn-on-delay of this particular laser simulation is approximately 0.5ns and about 2.5ns before the laser output power stabilises. A power output versus current curve, commonly referred to as a LI curve, is modelled using equation 3.8 and is illustrated in figure 3.2.

$$P = S.(hv).(V_p).(v_g) * \text{mirror loss} \tag{3.8}$$

with, S = photon density

hv = energy per photon

V_p = volume occupied by the photons, and v_g = group velocity

The numerically solved L-I curve is linear and the value for threshold current can be easily obtained. It is extremely beneficial for gas detection schemes if the laser source exhibits this behaviour. Otherwise, the accuracy and sensitivity of measurements are impaired if any sudden or discontinuous changes in output power occur.

Figure 3.2. *Plot of optical output power versus current for simulated behaviour of a Fabry-Perot device.*

3.3 Laser sources for gas sensing applications

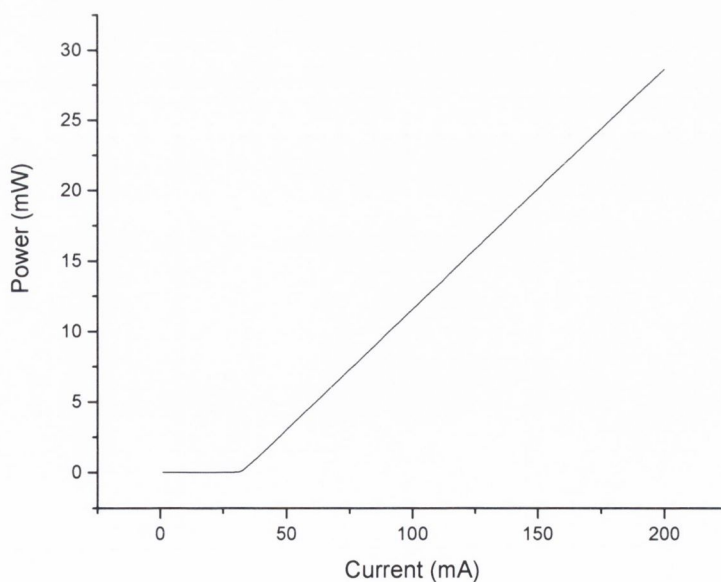In this section, a discussion of some of the most prominent laser diode sources presently available on the market for gas sensing applications is introduced. A brief description of some other common laser diodes and the design feature unique to all is also made. Some of the latest technology in terms of gas detection for both safety and defence scenarios with laser diode-based, high-resolution spectroscopic techniques, are also examined. Finally, a comparison is made between the various laser sources with particular reference to their spectral characteristics. The worldwide diode laser market was worth approximately $3.23 billion in 2005, which gives a tangible impression as to the importance of these devices [5]. Obviously, there are numerous different applications for these lasers not only in the gas detection/sensing field. For this discussion however, we will concentrate predominantly on this area and look at some of the devices and their designs, most commonly employed, and a sample of the more recent and promising innovations to date. An example of some of these laser diodes that are successfully applied to spectroscopic study include, external cavity diode lasers (ECDL), distributed feedback lasers (DFB), Fabry-Perot lasers (FP), slotted Fabry-Perot (SFP), distributed Bragg reflector (DBR), sampled-grating distributed Bragg reflector (SG-DBR), vertical cavity surface emtting lasers (VCSEL), and quantum cascade lasers (QC), to name but a few. The laser sources principally used throughout this research include an ECDL and DFB laser, which are described in more detail in section 3.4.

The simplest design for a laser diode, which is the basis for many other laser designs, is the Fabry-Perot resonator. Fabry-Perot lasers are constructed with a gain region and a pair of mirrors formed by simply cleaving the end facets of the device. Unfortunately, the only wavelength selectivity is from the wavelength dependence of the gain and the requirement for an integral number of wavelengths in a cavity round trip so that the device does not have single mode emission. The requirement for a laser diode to emit in only one mode is of paramount importance in many applications. Therefore, much research has been carried out to alter and invent new laser designs to achieve this single mode emission spectral characteristic. One outcome of this search for a single frequency device is the slotted or stabilised Fabry-Perot (SFP) laser diode [6,7]. In a SFP laser the mode selectivity is produced by introducing etched slots at precise longitudinal positions of the ridge waveguide, along the laser length. A schematic of a typical SFP laser diode

device is shown in figure 3.3. The device normally consists of a number of slots, which produce a refractive modulation of the cavity resonance spectrum by a change in the refractive index of the different sections causing reflection of the optical mode at these points. The slots introduce a perturbation along the cavity, which acts as a filter and thus a single longitudinal mode emission with a narrow linewidth may be achieved. One of the main advantages of this type of device is the reduced cost due to the design, processing and device fabrication yield. Consequently, this type of laser has been used for numerous telecommunications applications and has been utilized in certain gas sensing studies [8].
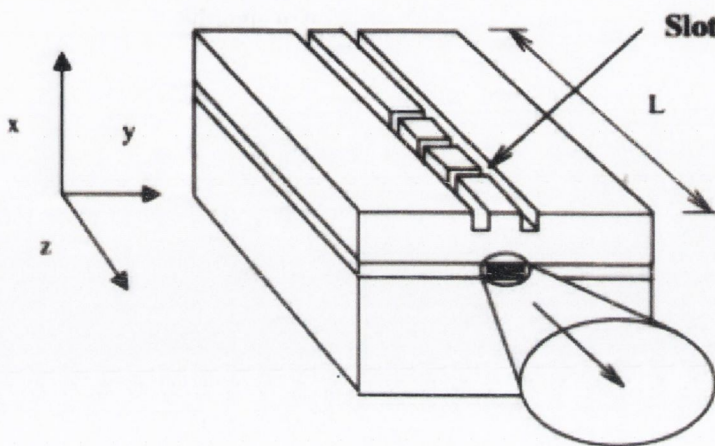
Figure 3.3. *Diagram of SFP device with three slots indicated in the ridge waveguide.*

In comparison, DFB and DBR laser diodes are expensive and more difficult to construct due to the re-processing and re-growth fabrication steps [9,10]. However, both of these devices show excellent spectral properties and have been the benchmark laser sources for both sensing and telecommunications systems [11,12]. DBR lasers were historically developed in parallel with DFB devices with the primary difference in the design of each being the location of the frequency selective grating section. For the DBR laser, it is located in a separate section from the active region of the laser diode while for the case of the DFB laser the feedback grating is, as the name implies, distributed throughout the laser structure, usually above or below the active region. The emission wavelength of these devices is controlled by temperature and injection current to the laser diode but the maximum wavelength tuning range is narrow and limited to only a few nanometres. In certain gas sensing systems where multi species identification and detection is required and for some telecommunication applications, such as wavelength-division multiplexing (WDM), where a wide wavelength tuning range of the laser source is favoured, the

overall wavelength tuning range of the DFB and DBR lasers are inadequate. A solution to this short wavelength tuning range was to design the so-called widely tuneable laser diode, where tens of nanometres tuning could be easily accomplished. An example of one such laser is a variation of the DBR structure and is termed, sampled grating DBR (SG-DBR) laser [13,14]. A typical structure for a SG-DBR laser diode has four sections consisting of a gain, phase, and two sampled grating mirror sections. The laser can operate at a particular single frequency when the reflection peaks for each end mirror coincide. The most important feature of the laser is its ability to tune the emission wavelength over very large ranges by modifying the injection current to the various sections of the laser [15]. There also exist many variations of the original four-sectioned structure where modulation components have also been incorporated into the laser diode design [16]. Further information on the design of the SG-DBR laser diode and other widely tuneable laser sources can be found in [17].

A vertical cavity surface emitting laser (VCSEL) is unique in comparison to the previously described laser devices in that the axis of the optical cavity is at right angles to the layered structure and light exits the laser from the top surface rather than the more standard edge emitting lasers. The major advantages of this type of laser include simpler device packaging and improved fibre coupling. Also, devices can be individually tested while still on a wafer before cleaving into individual die. The laser architecture consists of a pair of DBR mirrors positioned parallel to a wafer surface with an active region consisting of one or more quantum wells. Large wavelength tuning ranges of VCSELs of more than 30nm have been successfully achieved with various configurations of the original design [18,19]. Further information on VCSELs and their spectral characteristics and applications can be found in [20].

As discussed in chapter 2, the absorption lines probed with laser radiation in the near infrared region of the spectrum are rotational lines associated with overtone and combination bands of the fundamental vibrational absorption features. In order to effectively target these absorption lines in the near infrared spectrum a series of high sensitivity modulation spectroscopy techniques are required due to the weak absorption linestrengths of species at those wavelengths. The past few years have seen a development of a new breed of lasers called quantum-cascade (QC) lasers. With these devices it is now possible to create single frequency laser radiation that cover the mid-infrared region of the spectrum (~2.5μm - 20μm). This innovation has obviously immense significance for spectroscopic detection as the fundamental absorption spectra

of many molecules have much stronger absorption linestrengths in the mid-infra red of the spectrum [21]. Unlike other semiconductor laser sources, where the emitted wavelength is determined by the band gap of the material used to grow the device, the emitted wavelength of a QC laser is governed by the thickness of the constituent layers. The general idea of the device is to have intersubband-transitions of electrons inside a quantum-well structure where electrons are driven towards the active region by an applied electric field. When an electric current flows through a quantum-cascade laser, electrons cascade down an energy staircase emitting a photon at each step. The first QC lasers were operated in pulsed mode up to and above threshold but continuous wave operation required the device to be cryogenically cooled below room temperatures. However, after more than ten years of development devices have been shown to operate pulsed or CW up to and above room temperature [22-24]. The QC laser shows excellent properties including high power output, wide tuning range and ability to work at room temperature, which obviously make it ideal for many applications [25-27].

Finally, in recent times, the subject of security with regards to detection of harmful instruments and explosive materials has come to the forefront of scientific research. The latest innovations and progress made in Terahertz (THz = 10^{12} Hz) technology with the successful design and fabrication of both THz laser sources and detectors has fuelled a great deal of ground-breaking and exciting work. Its application in the area of medical imaging can be an advantage in comparison to current techniques like x-ray imaging for example. THz radiation can penetrate matter and reveals hidden objects, but in comparison to X-rays, THz radiation does not damage human tissue [28]. In addition, THz radiation is able to deliver information about the chemical composition of certain materials that exhibit unique spectral fingerprints in the terahertz range. This opens up completely new possibilities for the detection of illegal narcotics, explosives, concealed weapons and also manufacturing defects [29-31].

To summarize, a concise review of some of the latest diode laser technologies and their applications has been made. Depending on the relevant application and operational wavelength, whether it is for spectroscopic detection purposes or telecommunications applications, there is a variety of affordable, reliable, room temperature operating single frequency sources currently available. Some of the most popular laser diodes have been presented and the two lasers employed extensively in this work (ECDL and DFB laser) are now described in detail.

3.4 External cavity diode laser (ECDL) and distributed feedback laser (DFB) architecture

The main design features and theory of operation of both an ECDL and DFB laser are examined here. Special attention is paid to the components of the ECDL with particular emphasis on the Littrow configuration [32]. A concise assessment of the principle design features of a DFB laser diode is also made. Laser diodes can be divided into two classifications, monolithic and coupled cavity sources. The difference between the two is related to the location of the frequency selective element of each laser diode. In the case of the DFB laser, the frequency filter is incorporated within the laser cavity in the form of a distributed grating, whereas for an ECDL, the external grating governs the single frequency operation of the device. The principle function of the external grating is to increase the quality (Q) factor of the laser resonator and therefore reduce the spectral linewidth and stabilize the laser's emission wavelength. The Littrow configuration for a typical external cavity diode laser is depicted in figure 3.4. The general features of the ECDL used throughout this research include a diode laser with a dielectric anti-reflection (AR) coating on the front facet, a beam collimator, an external grating which provides the feedback to the laser, and a beam correctional mirror unique to this ECDL. The function of the beam correctional mirror (BCM) is to compensate for any movement of the output beam as the grating position is adjusted.
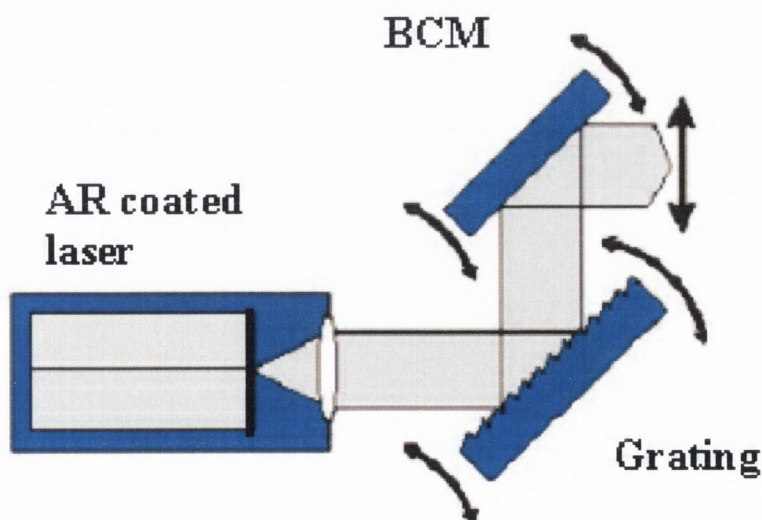

Figure 3.4 *Schematic of an external cavity diode laser in the Littrow configuration with external grating and beam correctional mirror (BCM) clearly indicated.*

The need for the front facet of the solitary laser to have an AR coating is paramount to the successful operation of an ECDL. The diode laser can only operate in the external cavity arrangement if the reflectance of diode laser's output facet is extremely low. Characteristics, such as increased tuning range, high output power, and a stable operating region of an ECDL can be dramatically improved, along with the laser lifetime, by introduction of an AR coated facet [33]. The requirement for strong external feedback is that the mirror losses of the diode laser cavity are much greater that that of the combined diode laser, grating filter and the coupling losses of the external cavity. Of course, most commercial available lasers have the option of AR coatings as it also serves to protect the front facet of a device from degradation due to high output power from the device. One of the most commonly utilized materials for anti-reflection coating of AlGaAs and InGaAsP facets is silicon monoxide. Temperature control of the entire ECDL set-up is achieved with a Peltier controller in combination with an AD590 temperature sensor located close to the diode laser.

Obviously, one of the most important elements in the ECDL design is the external grating that provides the feedback. The emitted laser light is spectrally filtered by an external grating and partially fed back into the laser diode. While the first order diffraction from the grating is reflected back into the laser diode, the zeroth order is coupled out. The wavelength is set by the grating, which diffracts the light with a certain wavelength directly toward the front facet. The exact emission wavelength of the ECDL is determined by the standing wave formed inside the cavity. Figure 3.5 shows a typical grating geometry, with grating period d, incident and diffracted angles α and β, as clearly indicated.
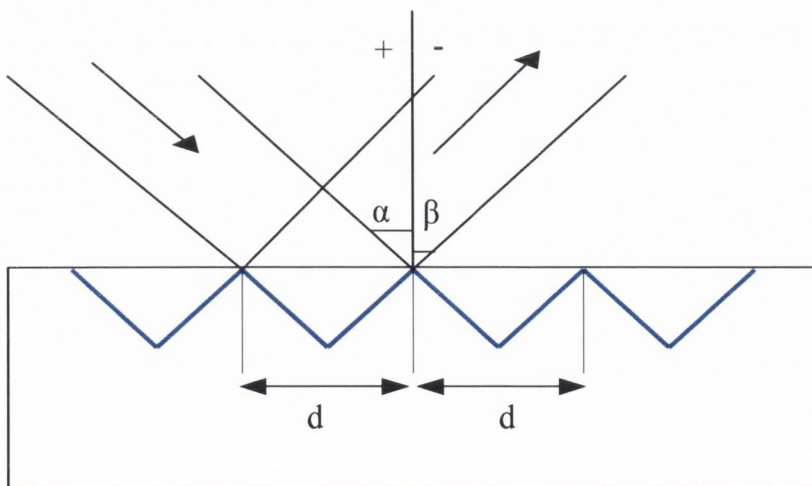

Figure 3.5 *Geometry of diffraction grating for plane waveforms.*

Diffraction gratings are the most commonly used wavelength filters for ECDLs. The formula for constructively diffracted orders of light reflected from a diffraction grating is,

$$n\lambda = d\sin\beta \qquad (3.9)$$

where d is the grating spacing between reflective surfaces, β is the angle of diffraction, λ is the wavelength of the incident light and n is an integer.

In order to achieve high resolution control of the grating position which is essential for accurate wavelength tuning of the laser, the external grating can be mounted on a piezoelectrical transducer (PZT). PZTs are solid-state actuators that convert electrical energy directly into mechanical energy with extremely high resolution. This allows the position of the grating to be finely and accurately tuned by application of a voltage to the PZT. Of course, the grating position can also be adjusted manually but this results in quite coarse tuning and should only be carried out when initially trying to operate the device at the desired wavelength. It is well known that the introduction of external optical feedback can strongly affect the properties of semiconductor diode lasers. It can cause variations in optical output power, spectral linewidth and laser threshold depending on the strength of the feedback [34]. Modelling the effects of the optical feedback by adding a time delayed feedback term to the standard laser rate equations is achieved by using the Lang Kobayashi equations [3]. For the case of an AR coated laser it is sufficient to treat only a single cavity round trip where multiple reflections are neglected.

The mechanism of mode selectivity in a coupled cavity laser such as an ECDL can be understood by referring to the three mirror model as indicated in figure 3.6(a). This figure is fundamental to the extended feedback model of a Fabry-Perot diode laser with external cavity. R_1 and R_2 correspond to the reflectivities of the end facets of the FP diode, and R_3 is the reflectivity of the external mirror as clearly indicated from the figure. L_d and L_{ext} are the laser cavity and external cavity lengths respectively.
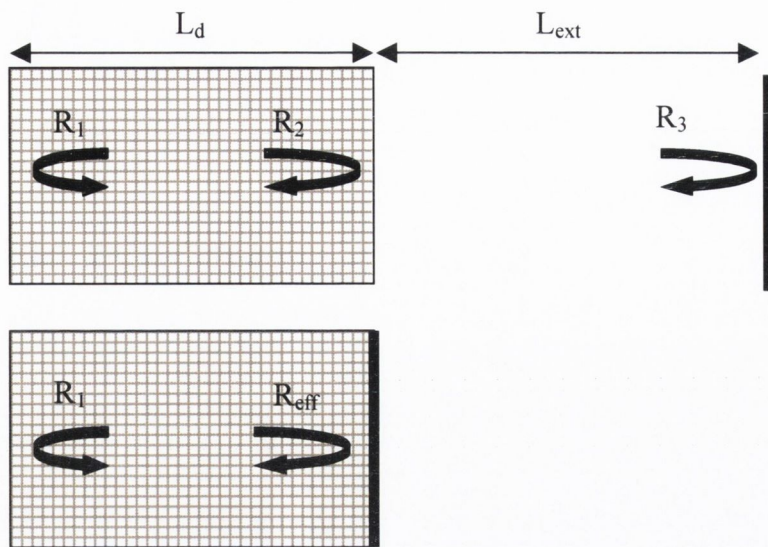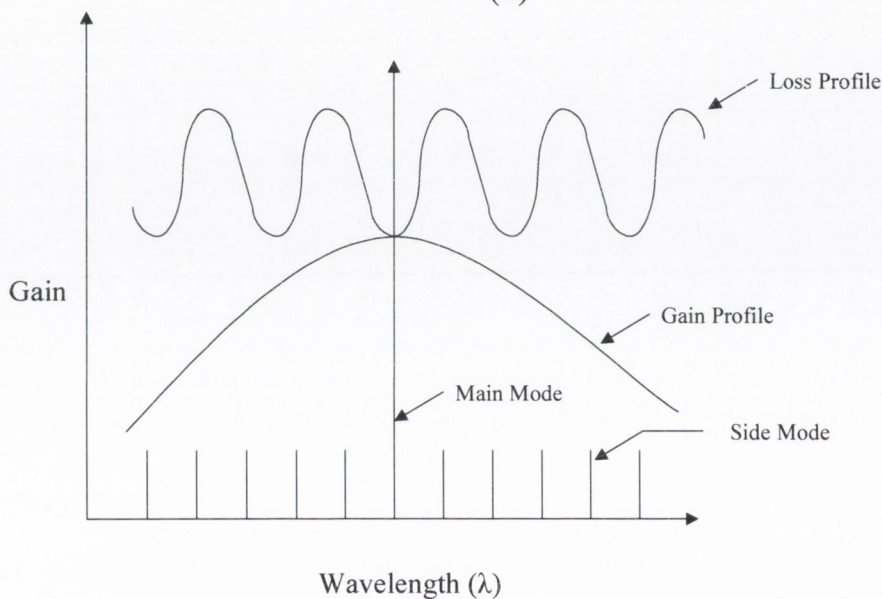
Figure 3.6. (a)*External cavity laser and the equivalent cavity with the effective mirror reflectivity R_{eff} that resembles the external section and* (b), *the net propagation gain and the net mirror loss as a function of wavelength.*

The reflection from the third mirror can be treated by combining it with the diode laser end facet, resulting in an effective mirror reflectivity, R_{eff} replacing the three mirror cavity to an equivalent two mirror cavity. The effect of the feedback from the external cavity can be modelled through an effective wavelength dependent reflectivity of the front facet from the external grating. As a result, the cavity loss is different for different FP modes of the laser cavity. In general the loss profile is periodic as shown in the figure

3.6(b). The mode selected by the couple cavity device is the FP mode that has the lowest cavity loss and is closest to the peak of the gain profile. Due to the periodic nature of the loss profile, other FP modes with relatively low cavity losses may also exist in the form of side modes whose power should be approximately 30dB below that of the main lasing mode.

External cavity lasers have very narrow spectral linewidths which make them appealing for many applications. The spectral linewidth of a diode laser is proportional to the spontaneous emission rate and inversely proportional to the number of photons in the laser cavity [35]. For most cases, the external cavity length L_{ext} is much longer than the original laser cavity length. The spontaneous emission rate is the number of photons emitted into the lasing mode per unit time. Because the mode spacing varies as $1/L_{ext}$, the spontaneous emission rate also varies as $1/L_{ext}$. The number of photons for a certain power level in comparison is proportional to L_{ext}. As a result of these relations, the linewidth of an external cavity diode laser is proportional to the inverse square of the external cavity length. This means that even for relatively short external cavities (in the centimetre range) for instance, linewidths of <300kHz have been recorded [36]. Not surprisingly, other arrangements exist for an external cavity laser, one of which is termed Littman-Metcalf [37]. For this design, the grating position is fixed and a rotating mirror can be turned to tune the wavelength. One of the major differences between the Littrow and Littman-Metcalf configuration is that the output power from the Littman-Metcalf is less due to a loss beam from reflections from the grating explained as follows. The beam emitted by the diode laser chip is collimated and then reaches the grating. The grating acts as a beam splitter with the zeroth order beam coupled out of the laser whereas the first order beam is coupled to the tuning mirror of the laser. There, it is coupled back to the grating which acts again as a beam splitter with the first order beam is coupled back into the laser. However, there appears again a zeroth order beam, which is coupled out of the laser, which results in light being lost and so the output power is reduced. Unfortunately, one of the main problems with external cavity arrangements is the mechanical and thermal stability of the system. In an effort to counteract this issue the use of micro-electromechanical structures (MEMS) have been successfully introduced into external cavity laser design as an alternative approach to act as actuator for the grating [38].

Distributed feedback lasers are one of the most important commercially available devices for both the research and industry markets. Its popularity is due to the excellent spectral

characteristics such as stable single frequency emission, very high SMSR, good wavelength tuning range and narrow linewidth making it especially suitable for telecommunications and gas sensing applications. The unique feature of DFB laser diodes, which separates them from other laser sources, is the introduction of a grating in the device structure. In comparison to a Fabry-Perot device where optical feedback for the laser resonator is provided by cleaving the end facets, a DFB laser diode has a grating introduced to one of the cladding layers. The optical feedback is obtained by the periodic variation of the effective refractive index of the corrugated optical waveguide, which as the name indicates, is distributed inside the laser cavity. The periodic index variation results in a wavelength selective feedback that is responsible for the devices exceptional single frequency emission properties. The key parameter for DFB laser operation is the coupling constant between the grating and the laser mode, κL, where κ is the coupling coefficient and L is the device length. This coupling is controlled by the spacing between the grating layer and the laser mode, as well as the grating corrugation function and index difference between the high and low index material consisting of the grating region. An example of a typical DFB structure is shown in figure 3.7.
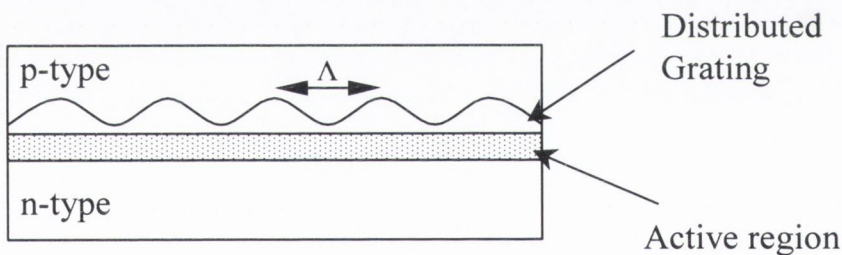
Figure 3.7. *Schematic illustration of a standard (DFB) semiconductor laser with the grating period Λ, shown.*

The maximum reflectivity of the grating occurs around the Bragg wavelength λ_B of the grating. The Bragg wavelength is given by,

$$\lambda_B = 2\Lambda n_e \tag{3.10}$$

where Λ is the grating period and n_e is the effective refractive index of the waveguide without any grating. For further information and more detailed analysis with regards to design, spectral characteristics and operation of external cavity diode lasers and distributed feedback laser diodes, the reader is referred to the following [39].

3.5   Spectral investigation of laser diodes for high resolution spectroscopy

In this section a number of fundamental experiments that help characterize a laser diode and determine its suitability to gas sensing applications, are presented. Of course, one of the most important attributes a laser diode can have for spectroscopic measurements is the ability to tune the emission wavelength of the device. This is especially important in the field of gas sensing where several absorption lines may need to be targeted, so continuous wavelength tuning of the device is essential. The output wavelength of a DFB laser, as already mentioned, can be tuned with injection current or temperature. Figure 3.8 shows the current induced temperature tuning behaviour of a DFB laser with injection current at 935nm. The maximum tuning range over the entire 30mA trace is 0.32nm, providing a tuning rate of 0.0104nm/mA with the laser showing excellent linear wavelength tuning behaviour.
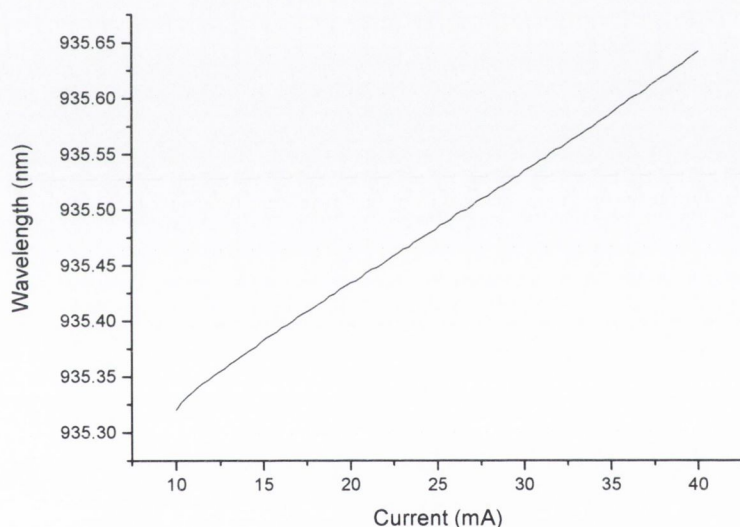
Figure 3.8. *Wavelength tuning characteristics of a DFB at 935nm with current, at 20^{0}C providing a tuning rate of 0.0104nm/mA.*

Obviously, continuous mode-hop free wavelength tuning is critical for a laser diode operating in a gas sensing system but it is generally not an issue for DFB laser technology. For example, when using the *2f* harmonic signal to detect an absorbing gas species as discussed in section 2.5, the resulting gas absorption profile can be corrupted if the wavelength tunes in a non-linear fashion. The wavelength tuning rate of the same device with temperature was measured to be 0.0597nm/^{0}C. The graph in figure 3.9 is a result of passing the output of the device through a 1 metre gas cell at 25mbar and detecting the resultant water vapour absorption lines in the 935nm region of the spectrum.

The trace shows the direct detection signal, measured with a photodiode, of the laser beam through a H_2O gas cell at a constant pressure and temperature. Due to the fact that the overall tuning range of the scan is approximately 1.2nm, it is clear to see that several absorption lines of varying linestrengths are detected.
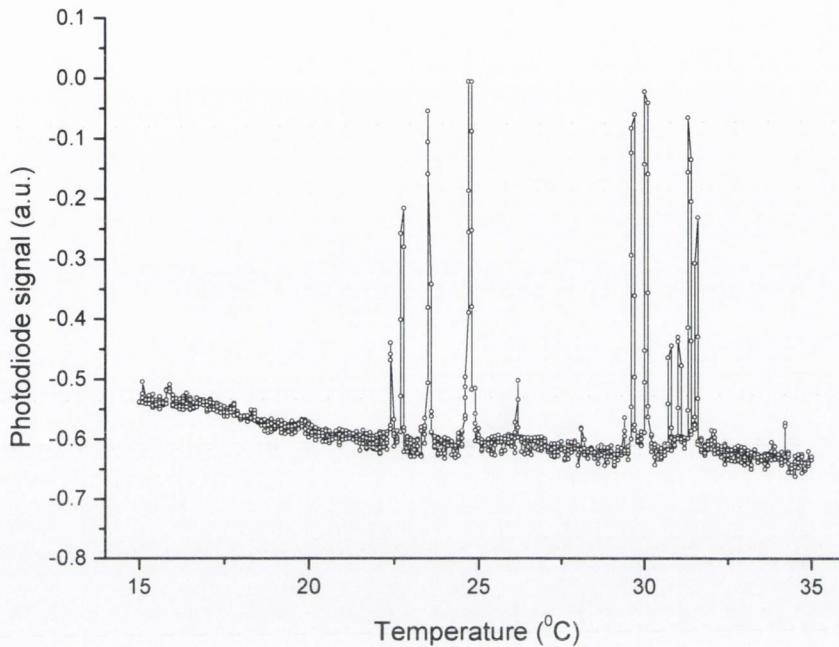
Figure 3.9. *Wavelength tuning of a DFB laser at 935nm with temperature at 30mA showing the direct detection of water absorption lines with obvious varying absorption strengths.*

Therefore, from an optimum operating procedure point of view with regards to gas detection schemes, it is more beneficial to tune the emission wavelength of a device with temperature in order to locate the absorption lines of interest. The improved wavelength resolution afforded with injection current tuning can then be applied to target one particular absorption line.

Knowledge of the SMSR (side mode suppression ratio) of a semiconductor diode laser is essential for device analysis as it gives vital information regarding the single frequency emission and spectral purity. The SMSR of a laser diode is defined as the ratio of the power in the central lasing mode to the power in the next most intense side mode measured in decibels (dB). The SMSR of a laser diode can be measured quite easily by fibre coupling the laser output and recording the resulting spectrum on an optical spectrum analyser (OSA). It is a simple method to determine if the laser under test is a single frequency laser, which is essential for gas sensing applications. Figure 3.10 shows an OSA trace over a narrow range of 6.5nm, depicting the SMSR of a DFB laser diode

emitting at 1.393μm with the main lasing mode and side modes clearly visible and SMSR >50dB.
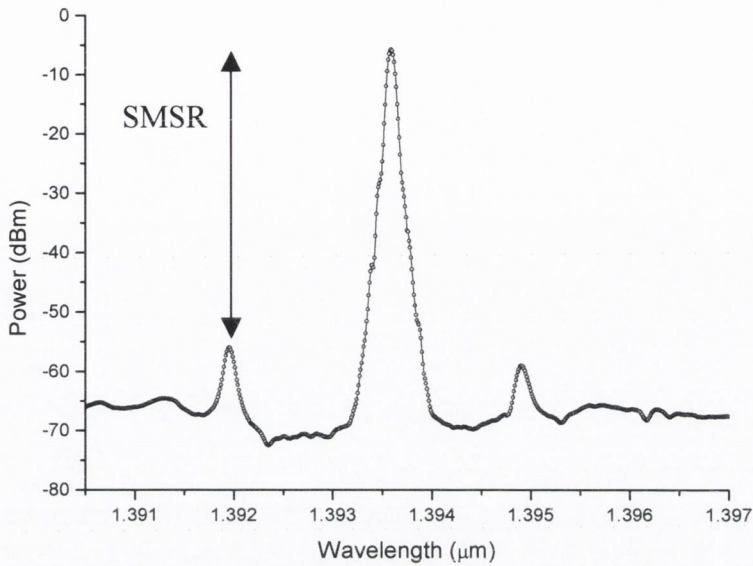
Figure 3.10. *Measured SMSR (>50dB) for a DFB diode laser emitting at 1.393μm with its temperature fixed to 20°C and the injection current set at 120mA.*

The output power from a diode laser can vary depending on the injection current and efficiency of the device. A laser diode with a large output power is desirable so that it can be used in a variety of experimental set-ups, involving both free-space and fibre coupled gas sensing arrangements. Obviously, most laser diodes are usually specified with a maximum output power value but for fibre-coupled schemes the maximum fibre coupled power is of principal importance.

Figure 3.11 shows the output power of an external cavity diode laser (ECDL) as a function of current and PZT voltage at constant temperature. The current to the ECDL was scanned from 70mA to 120mA and the PZT voltage over its entire 100V range (corresponding to a change in wavelength, 0.3nm < $\Delta\lambda$ < 0.5nm) showing a maximum output power of > 60mW. It should be noted that with fibre coupling of the ECDL the maximum output power recorded from the laser was significantly less than 60mW.
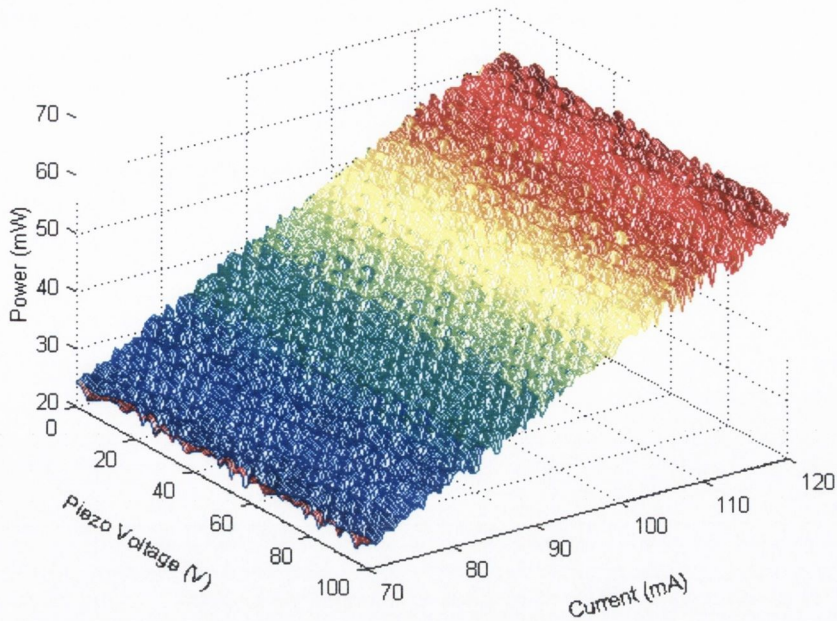
Figure 3.11. *Contour map of output power of ECL as a function of gain current and piezo voltage measured with a silicon photodiode Melles Griot universal power meter, at a constant temperature of 20C.*

Another very important spectral feature of a laser diode is the spectral linewidth. It is a measure of the temporal coherence or phase noise of the device and gives an indication of the minimum resolution available with the laser for gas sensing experiments. A typical linewidth of a Doppler broadened gas absorption line at low pressure can be several hundred MHz wide so it is critical that the laser has a spectral linewidth significantly less than this to target and accurately determine the spectral profile of the gas absorption line of interest. A more detailed discussion of this topic is given in section 4.3.

3.5.1 Optical isolation and spectral degradation of devices

The subject of isolation and spectral degradation of laser devices has been researched and studied in detail by many authors as it plays a significant role in the design and fabrication of laser diodes [40]. The issue of optical isolators, located internally within the packaging of devices, and some of the effects that can occur in the absence of isolation are discussed and presented. A series of experiments are described where a deliberate attempt is made to introduce external feedback to a slotted Fabry-Perot device chip and to observe the consequences in relation to spectral performance. Optical isolators are passive optical devices that allow light to be transmitted in only one direction. They are most often used to prevent light from reflecting back into the output

facet of the laser. Optical feedback decreases signal-to-noise ratio, SMSR and consequently degrades the resolution of a device resulting in less accurate detection limits for gas sensing and also higher bit-error rates in telecommunication applications. Ideally an isolator would pass all light in one direction and block all light in the reverse direction. Unfortunately, isolators introduce added expense and are typically large and even more costly for applications at wavelength regions not associated with telecommunications.

The experimental set-up for testing a single mode slotted Fabry Perot (SFP) laser diode to external feedback was to reflect the output beam back into the laser cavity with a 50% reflecting mirror placed about 10cm from the front facet of the laser. An output power versus current (LI) curve of the device was recorded for both experimental conditions where the laser was operated with and without optical feedback from the external mirror. The injection current to the SFP laser was scanned from 0mA to 120mA at a constant heatsink temperature of 20^0C and the change in output power was recorded with an optical power meter. Figure 3.12 shows the results for both cases where the presence of optical feedback to the device has the effect of modifying the output power of the laser in a non-linear manner. In figure 3.12 the effect of the feedback is clearly prominent and causes an undulation in the amplitude of the power output of the laser. The reduction in output power of the laser for the case with the optical feedback present is a result of the reflecting mirror.
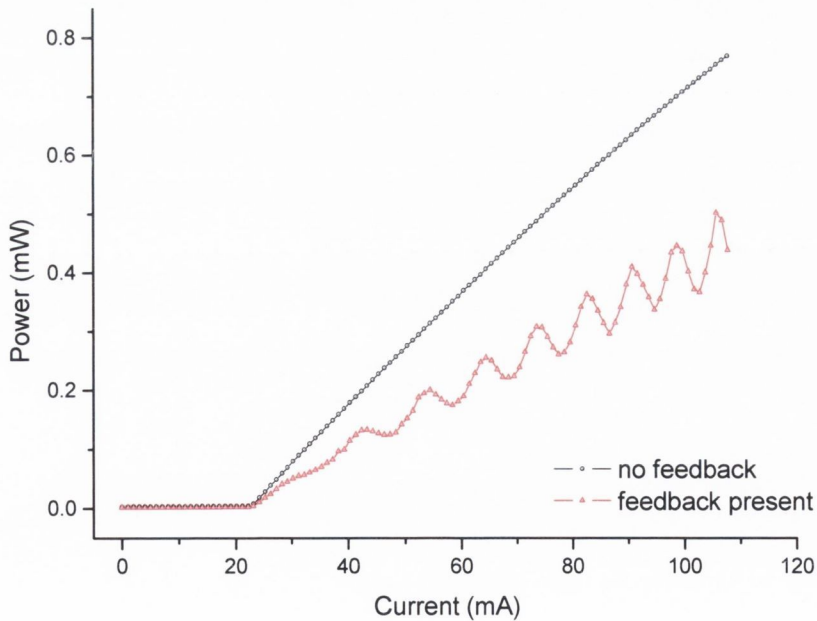

Figure 3.12. *LI curves for a slotted device measured at 20^0C showing the comparison between feedback present and without any external feedback to the laser.*

The peaks (valleys) in the output power occur when the feedback field subtracts from (adds to) the field within the laser cavity. For modulating the device as required for harmonic gas detection [41], this non-linear variation in output power caused by the optical feedback can produce false results. The effect of the external optical feedback on the spectral purity of the SFP laser diode was also tested by measuring the SMSR for both cases with and without the optical feedback from the external mirror. A laser with high SMSR is critical for gas sensing applications to ensure spectral purity so that the main spectral feature under test can be isolated from other absorption associated with other modes. Figure 3.13 shows a SMSR trace recorded with a spectrum analyser of the SFP at a constant current of 79.2mA at 20^{0}C showing a value >30dB.

By comparison, when the laser is subjected to optical feedback the effect has a negative impact on the single mode operation and SMSR of the device. Figure 3.14 shows the emergence of other side modes in the presence of the optical feedback with the main lasing mode centred at 1562.83nm while the presence of three enhanced side modes amplified by the induced feedback are clearly visible. As a result of the feedback, the SMSR has been reduced from 33.1dB to 25.6dB as shown in figure 3.14. It is clear from these series of simple measurements that the need for optical isolators in devices is critical, especially if the laser is employed in a field where single frequency emission, high SMSR and linear power change with current is necessary, as is the case for gas sensing application.
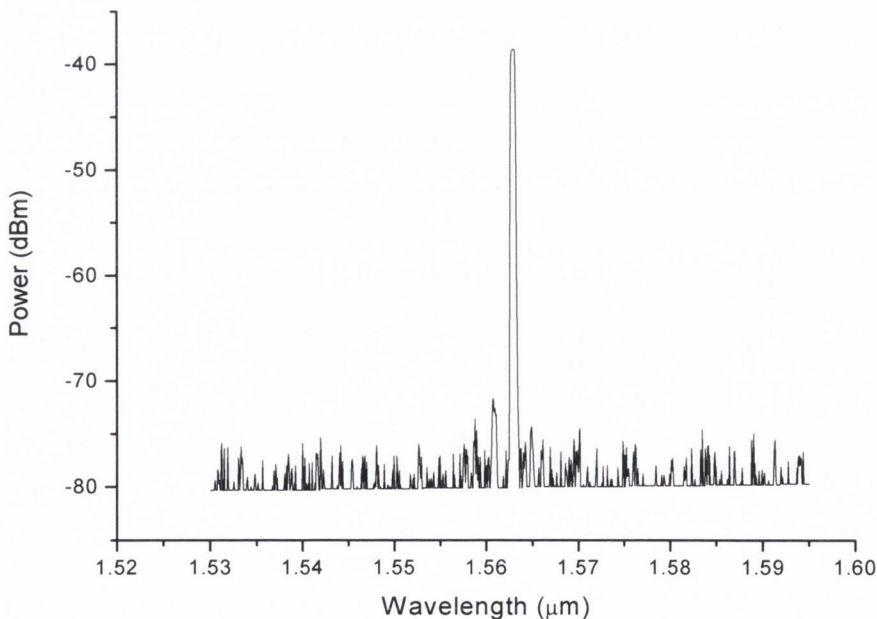
Figure 3.13. *Optical Spectrum with zero feedback present. The centre wavelength is 1562.83nm with SMSR >33dB at a drive current of 79.2mA at 20^{0}C.*
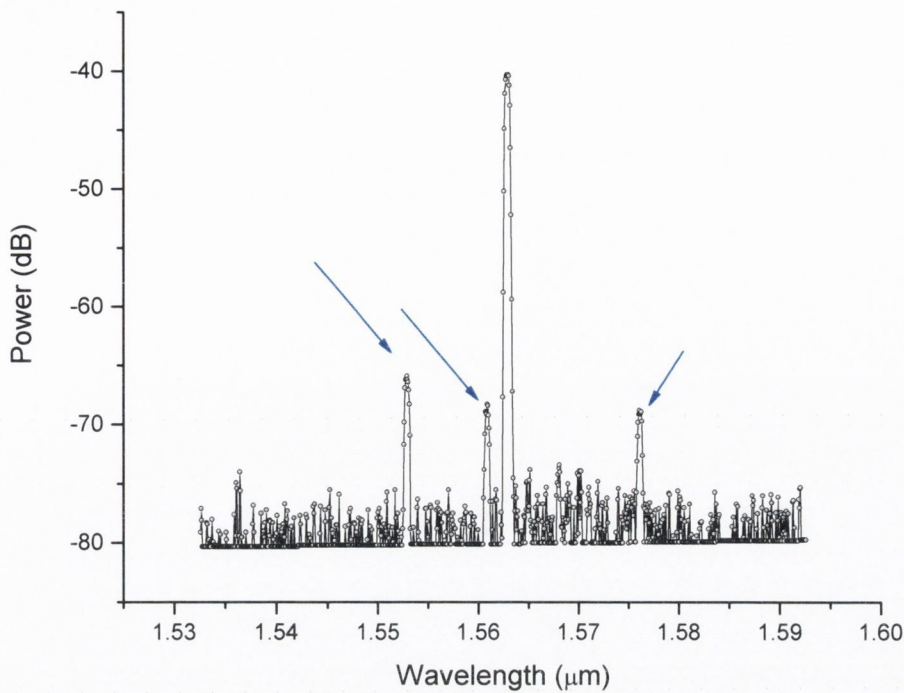
Figure 3.14. *Optical Spectrum of output emission from SFP device with feedback present measured with an Agilent (Model 86140B) OSA at a constant current of 79.2mA and temperature of 20⁰C.*

3.5.2 Linewidth enhancement factor

The linewidth enhancement factor, also known as the alpha parameter, has a fundamental influence on several aspects of diode laser characteristics and behaviour. For example, it has a significant influence on the spectral linewidth, mode stability, and sensitivity to optical feedback of diode laser sources. The observed origin of the linewidth enhancement factor lies in a discrepancy between actual measured and theoretical values for the spectral linewidth of a semiconductor diode laser. Schawlow and Townes had already calculated a fundamental limit for the linewidth before the first lasers were experimentally demonstrated [42]. While this limit was later shown to be closely approached by a number of solid state lasers, significantly higher linewidth values were measured for semiconductor lasers even when the influence of external noise sources was very low. It was then later found by C. Henry that the increased linewidths result from a coupling between intensity and phase noise, caused by a dependence of the refractive index on the carrier density in the semiconductor. Henry introduced the linewidth enhancement factor, α, to quantify this amplitude-phase coupling mechanism, and calculated that the linewidth should be increased by a factor $(1 + \alpha^2)$, which turned out to

be in reasonable agreement with experimental data [43]. The linewidth enhancement factor is defined as the ratio of the partial derivatives of the real and complex parts of the complex susceptibility, $\chi = \chi_r + i\chi_i$ with respect to the carrier density N,

$$\alpha = -\frac{\dfrac{\partial \chi_r}{\partial N}}{\dfrac{\partial \chi_i}{\partial N}} = -\frac{4\pi}{\lambda} \cdot \frac{dn}{dg} \qquad (3.11)$$

where dn and dg are the small index and optical gain variations that occur for a change in carrier density dN and λ is the wavelength. The linewidth enhancement factor of a slotted Fabry-Perot laser was measured using a technique commonly referred to as the "Hakki-Paoli method" [44]. This technique relies on the direct measurement of dn, the small change in refractive index and dg, the change in the modal gain, as the carrier density is varied by an unknown amount dN by changing the injection current to the laser below the threshold current limit in small increments. The resulting emission spectrum from the device, for each injection current value below threshold, is recorded with an optical spectrum analyser (OSA) with a resolution of ± 0.01nm, as shown in figure 3.15.
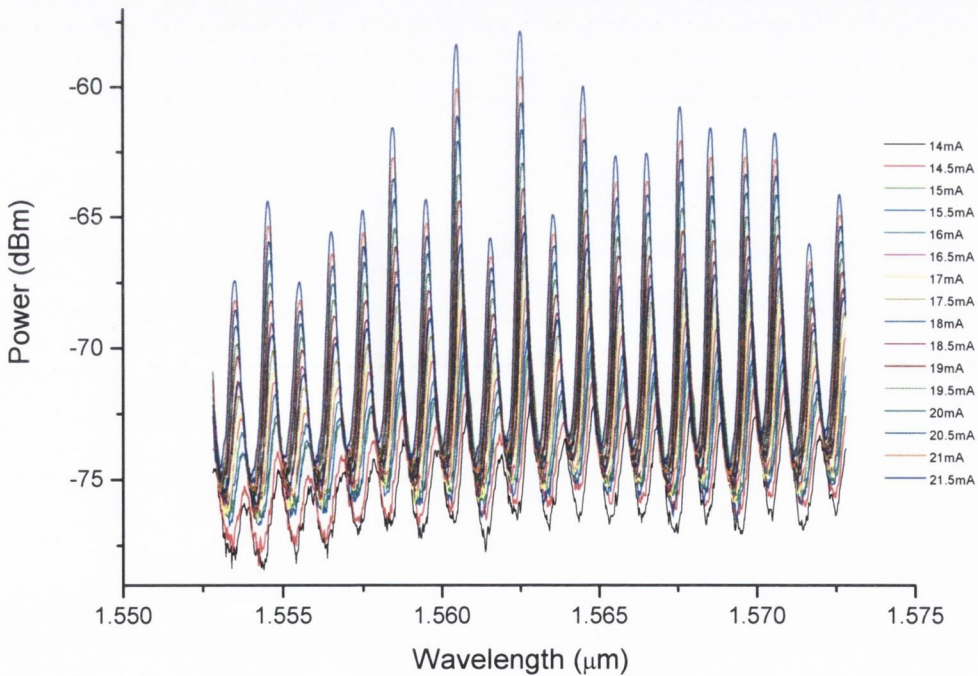
Figure 3.15. *Amplified spontaneous emission of the slotted device at various injection current values below threshold, at a constant heatsink temperature of 20^0C.*

51

For the SFP laser the current was varied from 14mA to 21.5mA in steps of 0.5mA at constant temperature of 20^0C. The change in refractive index dn is measured through the detection of the wavelength shift of the longitudinal Fabry-Perot mode resonance's, while dg is calculated using the Hakki-Paoli method by measuring the fringe contrast (peak to valley ratio) of the amplified spontaneous emission filtered by the Fabry-Perot cavity. The nett mode gain G_{nett}, of a particular lasing mode can be determined from the ratio of the peaks to the troughs in the output spectrum of the laser [45].

$$G_{nett} = \frac{1}{L} \ln \left(\frac{\sqrt{r_i} + 1}{\sqrt{r_i} - 1} \right) \qquad (3.12)$$

where L is the laser length which in this case was 300μm and r_i is depth of modulation calculated from ,

$$r_i = \frac{P_i + P_{i+1}}{2V_i} \qquad (3.13)$$

where P_i and V_i correspond to the peak and valley power respectively.

The change in refractive index dn, can be determined from the wavelength shift of the Fabry-Perot mode with change in injection current below threshold according to,

$$dn = (\lambda/2L\Delta\lambda)d\lambda \qquad (3.14)$$

where, $\Delta\lambda$ is the Fabry-Perot mode spacing, L is the cavity length, λ is the nominal wavelength and $d\lambda$ is the shift in wavelength with change of injection current. The laser mode spacing is given by,

$$d\lambda = \lambda^2/2N_eL \qquad (3.15)$$

where N_e is the effective index. Experimentally, the laser mode spacing is determined by recording the laser output on an OSA (Agilent, Model 86140B), with a resolution of $\pm$ 0.01nm, and then measuring the spacing between successive peaks, which in this case was measured to be 0.94nm as clearly shown in figure 3.16.
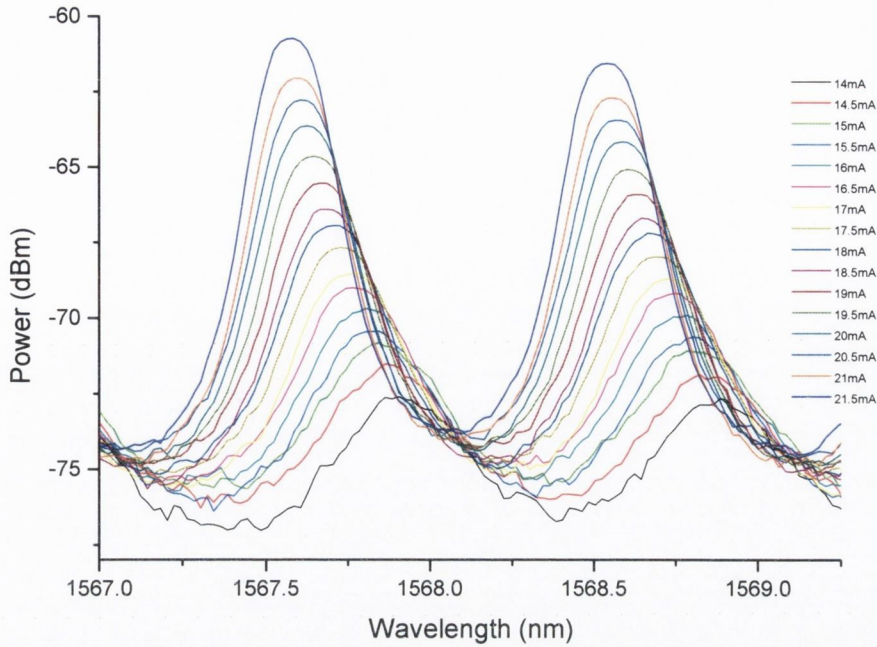
Figure 3.16. *Measurement of wavelength shift as the injection current is changed from 14mA to 21.5mA in steps of 0.5mA recorded with an OSA.*

Finally by substitution into equation 3.11 and cancellation of the carrier density terms, the linewidth enhancement factor is,

$$\alpha = \frac{2\pi}{\Delta\lambda} \cdot \frac{d\lambda}{dG_{nett}} \tag{3.16}$$

Then it is simply a matter of plotting the wavelength shift for each mode versus the corresponding nett mode gain as shown in figure 3.17, and substituting the slope of the graph in equation 3.16. For the SFP device emitting at 1560nm the α-parameter was measured to be α = 6.37.

$$\alpha = \frac{2\pi}{(0.96)}(0.974) = 6.37 \tag{3.17}$$

Values for the linewidth enhancement factor are typically between 3 and 7 but techniques that produce strain within laser structures have helped to reduce this value even further [46]. Obviously, a diode laser material system designed to have a low alpha parameter would be advantageous for lower sensitivity of the laser to external optical feedback.

However, a laser diode having a large alpha parameter could be extremely useful in the design of a widely tuneable laser diode where a large change in refractive index occurred for a relative small change in carrier density. Nonetheless, a laser diode with large alpha parameter has a negative effect on the spectral linewidth of the laser and results in a increased value.
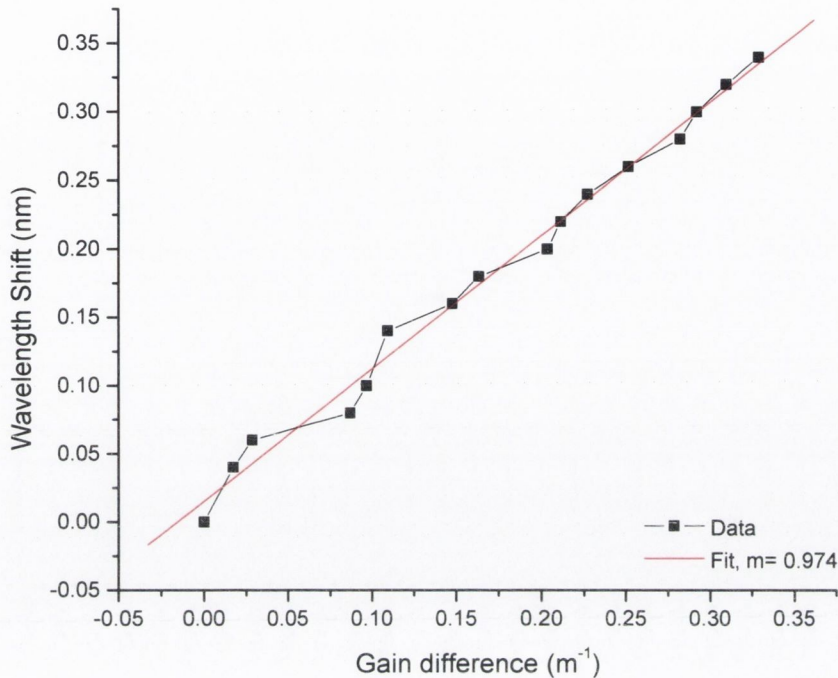
Figure 3.17. *Graph of wavelength shift versus modal gain.*

The Hakki-Paoli method, as already mentioned, is a below threshold current technique and it measures the material linewidth enhancement factor as a function of photon energy and injection current. Therefore, the ability to measure the α parameter above threshold does not exist with this measurement technique and so it's dependence on output power above threshold cannot be examined. Unfortunately, the technique cannot be successfully applied to devices with AR coated facets like DFB's for example due to the reduced fringe contrast, which makes the measurement of the *dg*, the optical modal gain change, unachievable. Recently, some research has been carried out to examine the effects of optical feedback on quantum dots semiconductor lasers (QDLs) of different device lengths and very low linewidth enhancement factors [47]. A lower linewidth enhancement factor for QD lasers results in a reduction of the spectral linewidth and also reduces the susceptibility of the devices to external optical feedback. Obviously, the ultimate goal is to fabricate a device where the need for an optical isolator is no longer necessary in the packaging of the laser [48].

3.6 Conclusions

Some of the most common and useful semiconductor diode lasers used in gas sensing and telecommunications applications have been reviewed. In particular, the design, operation and wavelength tuning operating procedure for both an ECDL and DFB laser have been outlined. The most recent innovations in laser design for example, quantum cascade lasers and the latest imaging techniques possible with these devices has brought about the extremely powerful, and informative technology of THz imaging. An examination of the laser sources with tests, such as LI curves, SMSR, output power and wavelength tuning range, have been described and experimentally carried out. These results can then help determine the suitability of devices for spectroscopic based gas sensing applications. Finally, an investigation of the sensitivity of a slotted Fabry-Perot device to unwanted external optical feedback was made in addition to a measurement of the linewidth enhancement factor of the laser, with a discussion of negating the use of optical isolators for all laser diodes.

3.7 References

[1]   K. Petermann, "Laser Diode Modulation and Noise", Kluwer, Dordrecht, 1991.

[2]   Lang, R. and Kobayashi, K. "External optical feedback effects on semiconductor injection-laser properties". *IEEE J. Quantum Electron.*, vol. 16, pp.347–355, 1980.

[3]   L. A. Coldren, S. W. Corzine, "Diode Lasers and Photonic Integrated Circuits", Wiley-Interscience; 1st edition, 1995.

[4]   William H. Press, Brian P. Flannery, Saul A. Teukolsky, William T. Vetterling. "Numerical Recipes in C." Cambridge, UK: Cambridge University Press, 1988. (See Sections 16.1 and 16.2.)

[5]   Steele, Robert V., " LASER MARKETPLACE 2006: Diode doldrums", *Laser Focus World*, Feb., 2006.

[6]   Corbett, B.; McDonald, D.; " Single longitudinal mode ridge waveguide 1.3µm Fabry-Perot laser by modal perturbation", *Electronics Letters,* vol. 31, pp. 2181 – 2182, 1995.

[7]   D. McDonald, B. Corbett; "Performance characteristics of quasi-single longitudinal-mode Fabry-Perot lasers", *Photonics Technology Letters, IEEE* vol. 8, pp. 1127 – 1129, 1996.

[8]   Weldon, V.; O'Gorman, J.; Perez-Camacho, J.J.; McDonald, D.; Hegarty, J.; Corbett,B.; "Methane sensing with a novel micromachined single-frequency Fabry-Perot laser diode emitting at 1331 nm", *Photonics Technology Letters, IEEE,* vol. 9, pp. 357 – 359, 1997.

[9]   Yi Luo; Weimin Si; Shengzhong Zhang; Di Chen; Jianhua Wang; "Fabrication of GaAlAs/GaAs gain-coupled distributed feedback lasers using the nature of MBE", *Photonics Technology Letters, IEEE* vol. 6, pp. 17 – 20, 1994.

[10] Hofmann, L.; Erbert, G.; Knauer, A.; Smirnitski, V.; Sebastian, J.; Klehr, A.; Weyers, M.; Stolz, W.; "MOVPE overgrowth of (InGa)P gratings for GaAs-based DBR laser Indium Phosphide and Related Materials," *Indium Phosphide and Related Materials*, Eleventh International Conference on, pp. 119 – 122, 1999.

[11] Takemoto, A.; Ohkura, Y.; Kawama, Y.; Nakajima, Y.; Kimura, T.; Yoshida, N.; Kakimoto, S.; Susaki, W.; "1.3-μm distributed feedback laser diode with a grating accurately controlled by a new fabrication technique" *Journal of Lightwave Technology*, vol. 7, pp. 2072 – 2077, 1989.

[12] Y.Suematsu, S.Arai, an/d F.Koyama "Dynamic-Single-mode Lasers," (Invited), *Optica Acta*, vol. 32, pp.1157-1173, 1985.

[13] Robbins, D.J.; Whitbread, N.D.; Williams, P.J.; Rawsthorne, J.R.;"Sampled grating DBR lasers for WDM systems" *Multiwavelength Optical Networks: Devices, Systems and Network Implementations IEE Colloquium on*, pp. 911 - 914, 1998.

[14] Larson, M.C.; Bai, M.; Bingo, D.; Ramdas, N.; Penniman, S.; Fish, G.A.; Coldren, L.A.;"Mode Control of Widely-Tunable SG-DBR Lasers" *Optical Communication*, ECOC, vol. 3, pp. 1-2, 2002.

[15] Liijeberg, T.; Tohmon, R.; Hall, E.; Abraham, P.; Focht, M.; Fish, G.A.; Larson, M.C.; Coldren, L.A.; "High-power, widely-tunable sampled grating DBR laser integrated with a semiconductor optical amplifier" Semiconductor Laser Conference, IEEE 18th International, pp.45 – 46, 2002.

[16] Akulova, Y.A.; Fish, G.A.; Ping-Chiek Koh; Schow, C.L.; Kozodoy, P.; Dahl, A.P.; Nakagawa, S.; Larson, M.C.; Mack, M.P.; Strand, T.A.; Coldren, C.W.; Hegblom, E.; Penniman, S.K.; Wipiejewski, T.; Coldren, L.A.; "Widely tunable electroabsorption-modulated sampled-grating DBR laser transmitter", *Journal of Quantum Electronics, IEEE*, vol. 8, pp. 1349 – 1357, 2002.

[17] Jens Buus, Markus-Christian Amann, Daniel J. Blumenthal, "Tunable Laser Diodes and Related Optical Sources", Wiley-IEEE Press; 2nd edition, 2005.

[18] Riemenschneider, F.; Maute, M.; Halbritter, H.; Boehm, G.; Amann, M. C.; Meissner, P., "Continuously tunable long-wavelength MEMS-VCSEL with over 40-nm tuning range" *Photonics Technology Letters, IEEE*, vol. 16, pp. 2212 – 2214, 2004.

[19] Li, M.Y.; Yuen, W.; Li, G.S.; Chang-Hasnain, C.J., " Record wide tunable top-emitting VCSELs for LAN applications", Lasers and Electro-Optics Society Annual Meeting, LEOS, 10th Annual Meeting. *Conference Proceedings, IEEE*, vol. 2, pp. 419 – 420, 1997.

[20] Carl W. Wilmsen, Henryk Temkin, Larry A. Coldren, P. L. Knight, A. Miller. "Vertical Cavity Surface Emitting Lasers" Cambridge University Press; New edition, 2001.

[21] Peter Werle, Franz Slemr, Karl Maurer, Robert Kormann, Robert Mucke, Bernd Janker, "Near- and mid-infrared laser-optical sensors for gas analysis", *Optics and Lasers in Engineering*, vol. 37, pp. 101-114, 2002.

[22] M. Beck and D. Hofstetter and T. Aellen and J. Faist and U. Oesterle and M. Ilegems and E. Gini and H. Melchior, "Continuous wave operation of a mid-infrared semiconductor laser at room temperature", *Science*, vol. 295, pp. 301-305, 2002.

[23] A. Evans and J.S. Yu and J. David and L. Doris and K. Mi and S. Slivken and M. Razeghi, "High-temperature, high-power, continuous-wave operation of buried heterostructure quantum-cascade lasers", *Appl. Phys. Lett.*, vol. 84, pp. 314-316, 2004.

[24] A. Evans and J.S. Yu and S. Slivken and M. Razeghi, "Continuous-wave operation of $l \sim 4.8$ μm quantum-cascade lasers at room temperature", *Appl. Phys. Lett.*, vol. 85, pp. 2166-2168, 2004.

[25] Troccoli, M.; Capasso, F.; Colombelli, R.; Gmachl, C.; Tennant, D.; Sivco, D.L.; Cho, A.Y.; Painter, O.J.; Srinivasan, K.; "Mid-IR quantum cascade lasers and amplifiers: recent developments and applications", *Lasers and Electro-Optics, CLEO/Pacific Rim. The 5th Pacific Rim Conference on*, vol. 1, pp. 15-19, 2003.

[26] Gmachl, C.; Paiella, R.; Tredicucci, A.; Hutchinson, A.L.; Sivco, D.L.; Baillargeon, J.N.; Cho, A.Y.; Liu, H.C.;"New frontiers in quantum cascade lasers and applications" *Selected Topics in Quantum Electronics, IEEE Journal of*, vol. 6, pp. 931 – 947, 2000.

[27] Gmachl, C.; Capasso, F.; Kohler, R.; Tredicucci, A.; Hutchinson, A.L.; Sivco, D.L.; Baillargeon, J.N.; Cho, A.Y.; "Mid-infrared tunable quantum cascade lasers for gas-sensing applications", *Circuits and Devices Magazine, IEEE*, vol.16, pp. 10 – 18, 2000.

[28] Dressel, M.; Gompf, B.; Mair, S.; "Near-field spectroscopy at THz frequencies - a new tool for solid state spectroscopy and biomedical imaging" *Infrared and Millimeter Waves, and 12th International Conference on Terahertz Electronics*, vol. 27, pp. 95 – 96, 2004.

[29] Miyamaru, F.; Otani, C.; Kawase, K.; "Terahertz imaging and sensing" *Lasers and Electro-Optics Society, LEOS, IEEE*, pp. 118 – 119, 2005.

[30] Ogawa, Y.; Kawase, K.; Yamashita, M.; Inoue, H.; "Non-destructive inspection techniques for illicit drugs using terahertz imaging", *Lasers and Electro-Optics, (CLEO). Conference*, vol. 1, pp. 3, 2004.

[31] Woolard, D.L.; Brown, R.; Pepper, M.; Kemp, M.; "Terahertz frequency sensing and imaging: a time of reckoning future applications?", *Proceedings of the IEEE*, vol. 93, pp. 1722 – 1743, 2005.

[32] C. J. Hawthorn, K. P. Weber, and R. E. Scholtena "Littrow configuration tunable external cavity diode laser with fixed direction output beam" *Review of Scientific Instruments*, vol. 72, no. 12, 2001.

[33] I. Ladany, M. Ettenberg, H. F. Lockwood, and H. Kressel, "Al$_2$O$_3$ half-wave films for long-life cw lasers", *Applied Physics Letters,* vol. 30, pp. 87-88, 1977.

[34] Tkach, R.; Chraplyvy, A.; "Regimes of feedback effects in 1.5-μm distributed feedback lasers", *Journal of Lightwave Technology,* vol. 4, pp. 1655 – 1661, 1986.

[35] G. Agrawal, "Line narrowing in a single-mode injection laser due to external optical feedback," *Quantum Electronics, IEEE Journal of,* vol. 20, pp. 468-471, 1984.

[36] D. McInerney, M. Lynch, J.F. Donegan, and V. Weldon, "Spectral linewidth and tuning requirements of sources for gas sensing in space-based applications at 935 nm", *IEE Proc., Optoelectronics,* vol. 153, pp. 33-39, 2006.

[37] M.G. Littman and H.J. Metcalf, "Spectrally narrow pulsed dye laser without beam expander (ET)," *Appl. Opt.* vol. 17, pp. 2224-2227, 1978.

[38] Uenishi, Y.; Honma, K.; Nagaoka, S. "Tunable laser diode using a nickel micromachined external mirror " *Electronics Letters,* vol. 32, pp. 1207-1208, 1996.

[39] Geert Morthier, Patrick Vankwikelberge, "Handbook of Distributed Feedback Laser Diodes" Artech House Publishers, 1997.

[40] Stubkjaer, K.; Small, M.;"Noise properties of semiconductor lasers due to optical feedback", *Journal of Quantum Electronics, IEEE,* vol. 20, pp. 472 – 478, 1984.

[41] Phelan, R.; Weldon, V.; Lynch, M.; Donegan, J.F.; "Simultaneous multigas detection with cascaded strongly gain coupled DFB laser by dual wavelength operation", *Electronics Letters,* vol. 38, pp. 31 – 32, 2002.

[42] A. L. Schawlow and C. H. Townes, "Infrared and optical masers", *Phys. Rev.* vol. 112, pp. 1490, 1958.

[43] C. Henry, "Theory of the linewidth of semiconductor lasers," *Quantum Electronics, IEEE Journal of,* vol. 18, pp. 259-264, 1982.

[44] B.W. Hakki and T.L. Paoli, "Gain spectra in GaAs double-heterostructure injection lasers," *J. Appl. Phys.,* vol. 46, pp. 1299–1306, 1975.

[45] Cassidy, D.T.: 'Technique for measurement of the gain spectra of semiconductor diode lasers', *J. Appl. Phys.,* vol. 56, pp. 3096–3099, 1984.

[46] H. D. Summers and I. H. White, "Measurement of the static and dynamic linewidth enhancement factor in strained 1.55μm InGaAsP lasers," *Electronics Letters*, vol. 30, pp. 1140-1141, 1994.

[47] Su, H., Zhang, L., Gray, A.L., Wang, R., Newell, T.C., and Malloy, K.J. "High external feedback resistance of laterally loss-coupled distributed feedback quantum dot semiconductor lasers", *Photonics Technol. Lett.,* vol. 15, pp. 1504–1506, 2003.

[48] O. Carroll, S.P.Hegarty, G. Huyet, B. Corbett, "Length dependence of feedback sensitivity of InAs/GaAs quantum dot lasers ", *Electron. Lett.,* vol. 41, pp. 416, 2005.

Chapter 4

Spectral Characteristics of Injection Seed Sources for Space-Based Gas Sensing Applications at 935nm

4.1 Introduction

4.1.1 Background

A single-frequency laser source with high output power, very low intensity noise and low phase noise is essential for successful coherent optical communication and precision spectroscopy. Such single-frequency, low-noise operation is significantly more difficult to achieve with high output power solid state lasers such as a Titanium:Sapphire (Ti:Al$_2$O$_3$), because these tend to be more susceptible to mechanical vibrations and are subject to significant thermal influences [1-3]. One method to overcome this problem is to employ a low noise semiconductor diode laser to act as a seed source for injection locking of the solid-state laser to a single emission frequency [4-8]. This chapter investigates the spectral characteristics of two semiconductor diode lasers and the suitability of these lasers to function as seed sources for a space-based gas sensing project. The overall objective of the study involved the stabilization of 4 laser frequencies to 4 specific predefined wavelengths. These wavelengths are associated with water absorption lines that occur in the 935-940nm region of the spectrum. A list of these H$_2$O absorption lines, with their wavelengths and line-strengths obtained from the Hitran database are summarised in table 4.1 below [9].

Water Absorption Lines	Wavelength vacuum (nm)	Line-strengths (cm/molecule)
Weak line	935.9065	4.15e^{-24}
Medium Strength line	935.56116	5.4e^{-23}
Strong line	935.68459	6.45e^{-22}
Off line	935.8564	6.0e^{-26}

Table 4.1. *Water absorption lines and corresponding line-strengths.*

The devices investigated are candidates for operation as injection seed lasers (ISL) for larger laser sources and are applied in a space-based water vapour sensing experiment. The experimental procedure involves locking the emission wavelength of one injection seed laser to the strongest water vapour absorption line using a reference gas cell and a wavelength modulation spectroscopy (WMS) technique [10]. This stabilized frequency is then used as a reference for three other lasers that are locked to three remaining absorption lines. Locking by means of gas absorption is the preferred technique since the absorption wavelength at a fixed temperature and pressure is constant. The stabilization technique for the three remaining lasers employs a Fabry-Perot interferometer to reference from the locked ISL.

This research is part of a larger study that examines atmospheric water vapour and aerosol distribution in the upper troposphere and lower troposphere in support of atmospheric modelling and chemistry studies. The parent project termed WALES (water vapour LIDAR (light detection and ranging) experiment in space) involves a differential absorption LIDAR (DIAL) instrument operating in the 935nm spectral range. The interest in the 935nm region of the spectrum is related to the presence of the 940nm H_2O absorption band as previously detailed in section 2.4. The DIAL technique compares the attenuation of two lasers pulses emitted at different wavelengths. The pulsed emission wavelength of the DIAL instrument at 935.684nm corresponds to the strongest water absorption line in table 4.1 and is indicated by λ_1 in figure 4.1. The dynamic range of the DIAL instrument is increased by using two other on-line wavelengths, λ_2, λ_3, of different absorption strengths and an individual weakly absorbing absorption line indicated by λ_4. The overall effect of the different water absorption linestrengths results in varied penetration depths of each wavelength as clearly indicated in figure 4.1 [11]. Considering typical water vapour profiles, the differing absorption linestrengths of the online wavelengths possess different penetration depths, thus allowing measurement at different altitudes. The strongly absorbing water vapour line is used for high altitude measurements with the more weakly absorbing lines can measure at lower altitudes. Sampling both strong and weak water vapour absorption lines at different wavelengths in the 935nm region can achieve a complete water vapour absorption profile across an entire altitude range. The importance of water in our everyday lives, without which the presence of life on earth would not exist, underlines the significance of this research. Further information on the WALES mission can be found in [12].
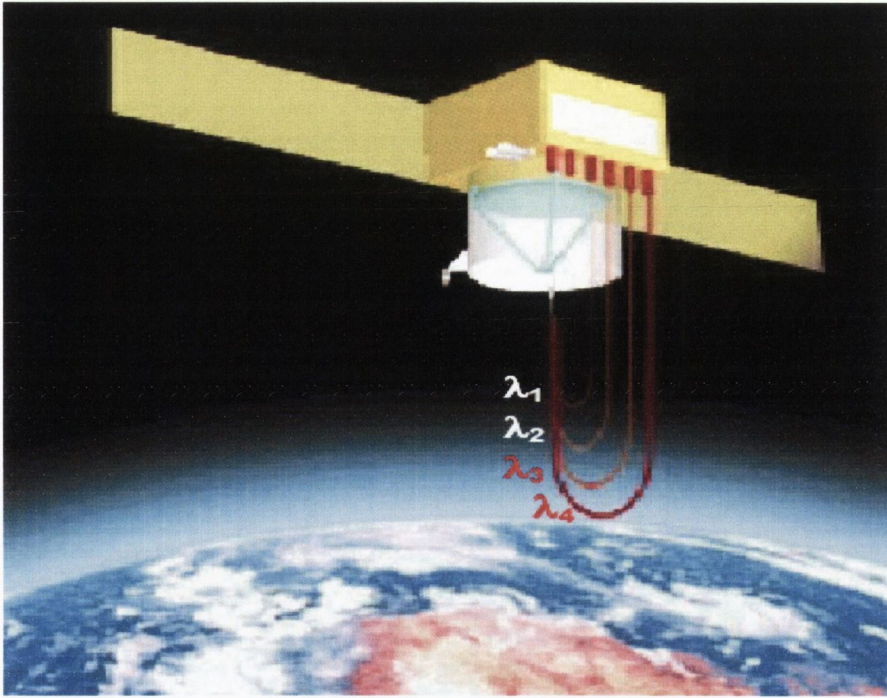
Figure 4.1. *Four pulses are transmitted at different wavelengths at three water absorption lines (strong, medium and weak) and an off-line wavelength. Backscattered light is detected at the four wavelengths.*

4.1.2 Candidate seed sources

The spectral characteristics of two different semiconductor diode lasers, which are to operate as the seed source for injection locking are explored in detail and compared. An external cavity diode laser (ECDL) supplied by Sacher Lasertechnik and operating in the Littrow configuration was the chosen technology for the ISL. At the time of this work it was the only laser to meet the required optical specifications of the project in terms of spectral linewidth and output power, at 935nm. Obvious advantages of the ECDL include narrow spectral linewidth, high output power, and wavelength tuning all of which are ideal for spectroscopic applications. However, ECDL's are not environmentally robust and are therefore unsuitable for space-based operation. This is due to thermal and mechanical instabilities of the device, but nevertheless are used here as a proof of principle approach. A distributed feedback (DFB) laser, supplied by Nanoplus, was also investigated as a possible alternative ISL. It should be noted that the preferred technology is a DFB laser but at the commencement of this work, these lasers were unable to meet all of the optical requirements, with regards to spectral linewidth and output power. One of the biggest problems in realising high quality single frequency lasers in the traditional and best understood material systems (GaAs/AlGaAs) for short wavelength lasers (<

1µm) is the oxidation in the Al of the AlGaAs overgrown layers during the grating writing process. This impairment has traditionally reduced the grating quality and the resultant control over the coupling ratio and the device. The coupling ratio is defined as the ratio of the optical power in the grating region to the total optical power of the DFB laser and is dependent on the quality of the grating. Recent results on new means of creating metal gratings on sides of the ridge waveguide, thus inducing complex coupling in the cavity, have shown good single mode yields and side mode suppression. This technique does not require the overgrown step required to date for the most widely used material system in this wavelength range. Other Al free material systems are available in the wavelength range but are still at an early stage for realizing single longitudinal mode laser sources [13]. Finally, care was taken in the ISL design set-up to ensure that the ECDL can be easily replaced by a DFB laser with only minimal changes. The overall system architecture would be left unaffected by the substitution of the laser source.

4.2 Device spectral characteristics

This research examines and compares the optical parameters of an ECDL and a DFB laser, both with single mode emission wavelengths at 935nm. Characteristics such as threshold current, wavelength tuning rate, maximum wavelength tuning range, side mode suppression ratio (SMSR), output power, and spectral linewidth are investigated. Knowledge of these characteristics is essential to ensure that the optimal operation of the devices is achieved. These characteristics concern accurate wavelength tuning and high spectral purity of the output emission so that highly accurate water vapour detection in the 935nm range can be easily obtained. Continuous wavelength tuning of the ECDL output is controlled by both injection current to the diode within the external cavity arrangement and a grating, which controls the frequency selective feedback from the external cavity.

To achieve high-resolution control of the grating position, which is essential for accurate wavelength tuning of the laser, the external grating is mounted on a piezoelectrical transducer (PZT). PZTs are solid-state actuators that convert electrical energy directly into mechanical energy by motion with extremely high resolution. This allows the position of the grating to be accurately tuned by application of a voltage over a maximum 100V range corresponding to a range of approximately $0.3nm < \Delta\lambda < 0.5nm$ [14].

Temperature stability of the laser is provided by a Peltier element in combination with a thermal sensor (AD590) mounted close the laser diode, which is connected to a suitable temperature controller, (ILX Lightwave, Model LDT 5910B). Varying the PZT voltage over the 0V to 100V range, the external grating can be precisely adjusted allowing the cavity length and therefore the emission wavelength to be accurately tuned.

The threshold current and slope efficiency of the two lasers are determined by measuring light-current (LI) curves. In the experimental set-up the heatsink temperature is kept constant at 20^0C and the output power of the lasers are measured using a Melles Griot universal power meter. For the ECDL, the PZT voltage to the grating was kept constant at 90V and the injection current to the laser was tuned from 0mA to a maximum of 120mA. The output power is recorded with a silicon photodiode in an integrating sphere arrangement. The resultant LI curve is shown in figure 4.2 where the maximum output-power of the ECDL is more than 60mW at 120mA. Due to the high divergence of the beam and fibre coupling losses, the maximum fibre coupled output power of the ECDL is significantly less. The laser threshold at this temperature of 20^0C is 43.8mA from the peak of the second derivative of the LI curve. The non-linearity of the trace in figure 4.2 is caused by mode hops due to the feedback from the external grating. The slope efficiency is calculated to be 0.2W/A above threshold.
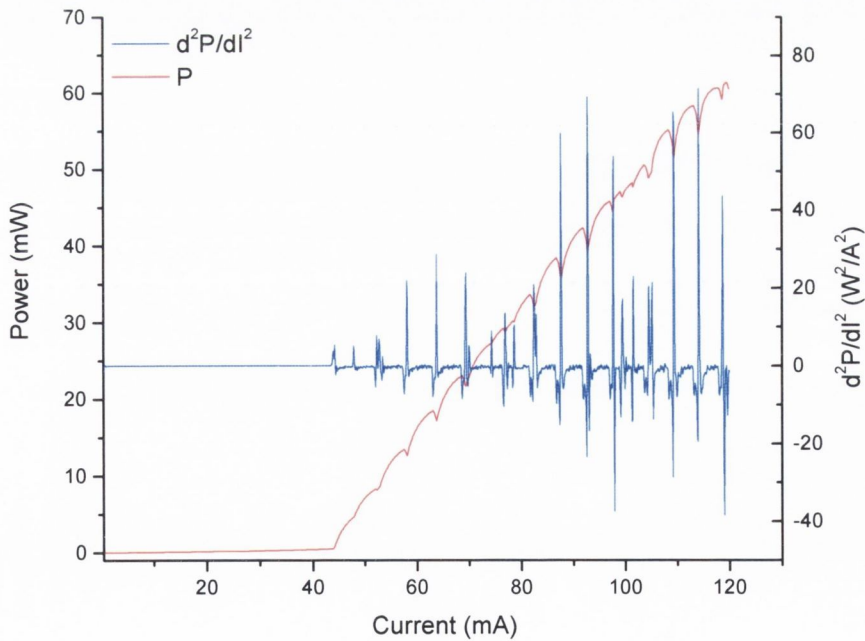

Figure 4.2. *LI curve and its 2nd derivative of the ECDL with current swept from 0mA to 120mA at a constant PZT voltage of 90V and temperature cooled to a constant 20^0C.*

With the injection current fixed at 90mA, the PZT voltage was also scanned and the output power recorded as shown in figure 4.3. The presence of a distinct peak output power value at the centre of each lasing mode in figure 4.3 is an extremely beneficial result for mode referencing of the ECDL and is described in more detail in Chapter 5.
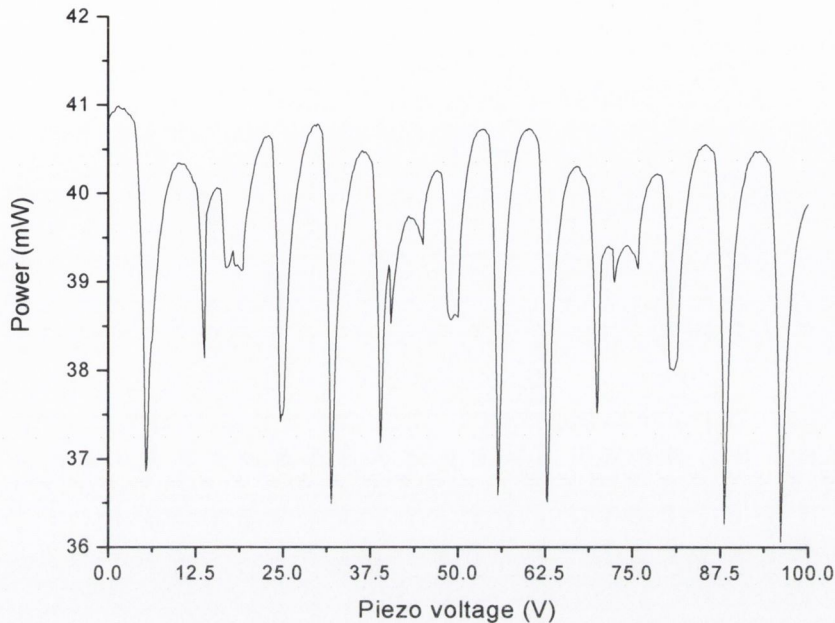

Figure 4.3. *Measured output power of ECDL with current kept constant at 90mA and PZT voltage swept from 0V to 100V at a constant of 20^0C.*

The DFB laser is fibre-coupled in a pigtailed style, FC/APC (fibre optic connector/angled physical contact) connection enabling it to be easily fixed to a copper mounting arrangement with a thermal sensor fixed close to the laser diode and electronically controlled with a temperature controller (ILX Lightwave, Model LDT 5910B). For the LI measurement of the DFB laser an ILX precision current source (ILX Lightwave, Model LDX 3207B) with a resolution of 0.05mA provides the injection current to the device. The fibre-coupled output power from the device was measured with an optical integrating sphere and a power meter. Figure 4.4 shows the emitted optical power as a function of injection current in the range 0mA to 40mA and shows excellent linearity. A value of 9.82mA is obtained for the threshold current while the slope efficiency in the range of 20mA to 40mA, is measured to be 0.283 W/A at 25^0C.
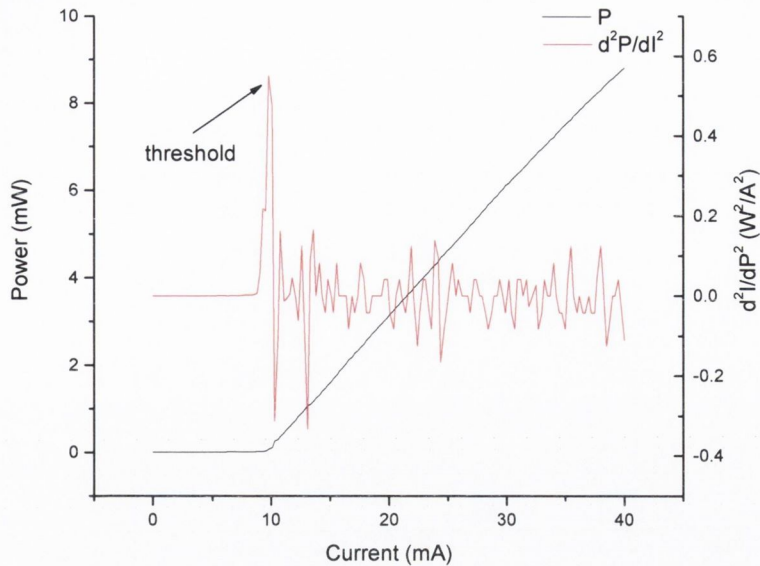
Figure 4.4. *LI curve and 2nd derivative of DFB at 935nm. The threshold current is calculated to be 9.81mA at $25^{0}C$.*

4.2.1 *Wavelength tuning operation and performance*

The significance of the wavelength tuning characteristics of a diode laser with respect to gas detection is critical. It can divulge the maximum wavelength tuning range of the device, which in turn can be used to determine if the laser is suitable or not for certain applications. The ECDL is classed as a widely tuneable laser source and due to its unique design it can provide a large wavelength tuning range. With the laser fixed at constant temperature, the wavelength can be varied with injection current but also by varying the voltage to the PZT [15]. Continuous wavelength tuning of the ECDL can only be achieved by simultaneous adjustment of the injection current and PZT voltage. From the trace in figure 4.5, it is possible to achieve quasi-continuous wavelength tuning over several nanometres, depending on which lasing mode the laser is scanned across [16]. However, the maximum continuous wavelength tuning for this particular device was measured to be 0.45nm. Figure 4.5 gives a clear indication of the tuning operation of the ECDL. This contour map of wavelength versus current and PZT voltage was recorded using the fast update mode operation of a multi wavelength meter (HP 86120B). Each point on the contour map is recorded approximately three times per second to a resolution of 0.01nm while the voltage is tuned over its full 100V range with the current scanned from 70mA to 120mA.
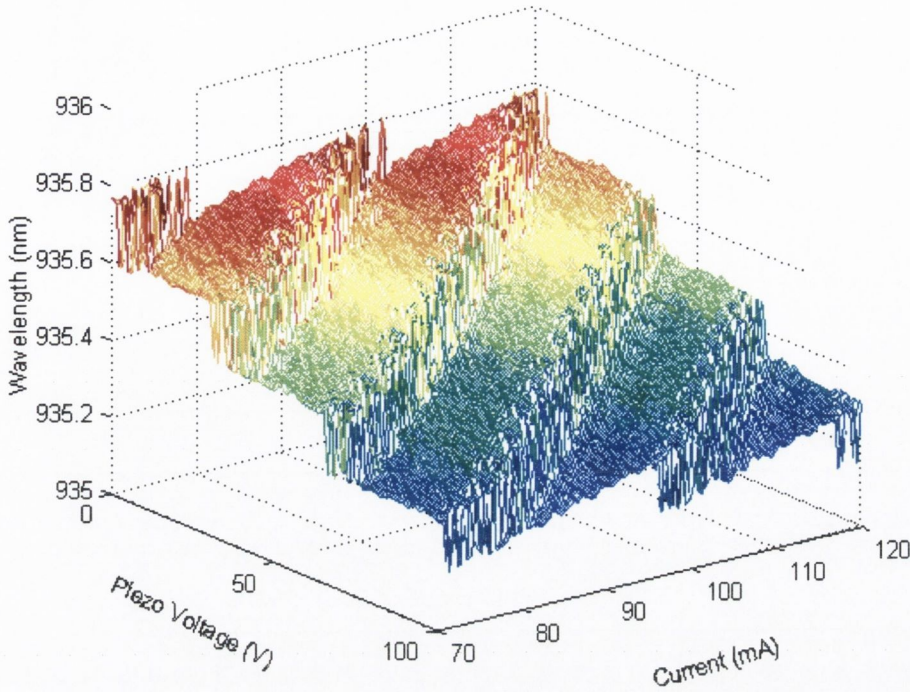
Figure 4.5. *Contour mode map of emission wavelength of ECDL as a function of current and PZT voltage at a constant temperature of 20^0C.*

The continuous tuning range may be extended by an increase in the current range to lower values less than 70mA. However, this would also result in a decrease in the output power. Single mode continuous wavelength tuning is only possible along certain positions of the lasing modes indicated by the flat, plateau regions in figure 4.5. In order to avoid any mode hops or experience any reduction in SMSR or output power, it is essential that the correct values for both the injection current and PZT voltage are applied. This ensures the tuning is fixed along the centre of the mode and away from the mode boundary positions. After recording the wavelength contour map and identifying the various lasing modes, a combination of current and voltage can be obtained to tune linearly across the mode and wavelength of interest. This is depicted in figure 4.6 where the dashed line indicates the ideal tuning position in the centre, for this particular lasing mode. In addition, this current/voltage simultaneous tuning combination can be achieved by making use of the internal monitor photodiode of the ECDL. By recording the output power of the laser instead of wavelength, the contour mode map can also be obtained. This method is quicker compared to the slow response of the wavemeter. This technique is described in more detail in section 4.3.3.
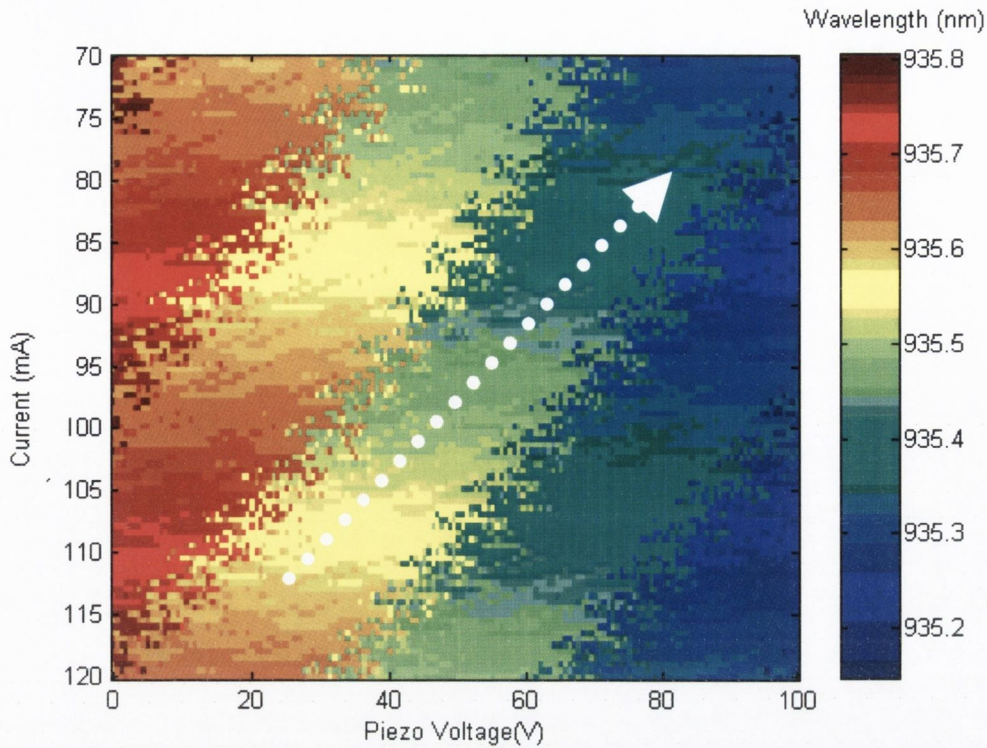
Figure 4.6. *Contour mode map of emission wavelength of ECDL with the white dashed arrow indicating the continuous wavelength tuning behaviour with an overall decrease in wavelength.*

The graph in figure 4.7 shows the results of the well-defined tuning contour path that provides a continuous wavelength range of the ECDL of 0.45nm, with simultaneous tuning of the current in the range from 70mA to 120mA and the PZT voltage over its full 100V range.

Figure 4.7. *Wavelength tuning behaviour of ECDL measured using a multi wavelength meter showing approximately 0.45nm of continuous tuning over the maximum PZT and 50mA current tuning range.*

The continuous wavelength tuning of the ECDL emission enables the targeting at 935nm or other water vapour absorption lines of interest. The wavelength of the ECDL can also be tuned by adjusting the external grating position or by independently changing the injection current to the diode. With the temperature of the ECDL fixed at 20^0C, the effect on the laser emission wavelength while varying 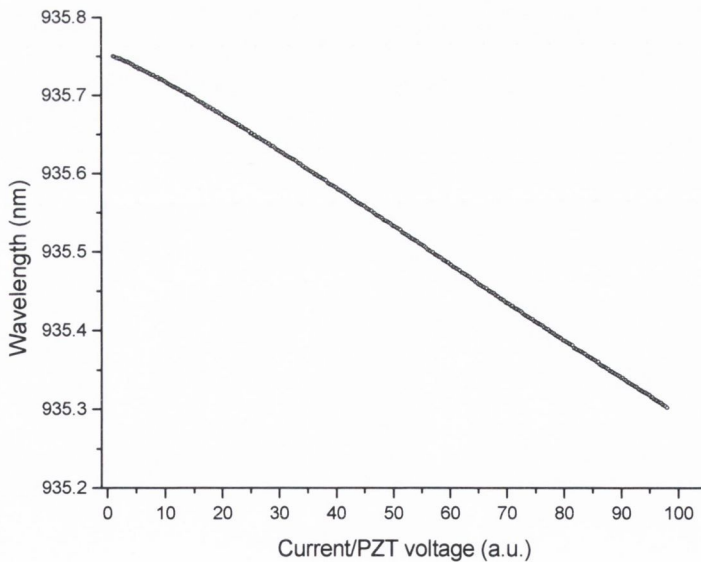both the injection current and PZT voltage independently is also explored. Figure 4.8 shows the wavelength tuning behaviour of the laser when the current is kept constant at 100mA and the PZT voltage is scanned from 0V to 75 V. If the grating is moved in the same direction as the optical output of the laser, as occurred in this case, the standing wave oscillating inside the cavity will be compressed, resulting in a continuous change in the wavelength. But as the wavelength changes, this compression also varies the diffraction angle from the grating. After a while, a mode with one more half-wave ($\lambda/2$) period inside the cavity will be pointing more directly toward the mirror, i.e. the mode will have lower losses, leading to an abrupt mode hop back in frequency clearly visible in the trace [17]. The larger shifts in wavelength are cavity mode hops as a result of mismatching between the laser cavity and the motion of the external grating to a lasing mode of lower loss.

Figure 4.9 shows the case where the PZT voltage is fixed and the injection current is scanned from 70mA to 120mA. For this situation, the increase in the current causes an increase in the optical cavity length of the diode laser with the PZT voltage fixed. This results in a mismatch in the overlap between the laser cavity modes and the grating feedback wavelength profile does not shift, which results in mode-hops and discontinuous wavelength tuning as clearly seen in the recorded trace. Both of these cases where the current and PZT voltage are tuned separately while the other is fixed, can be more easily understood by reviewing the trace in figure 4.6 which shows a plot of ECDL emission wavelength as a function of current and PZT voltage with the positions of the cavity mode hops easily observable. Obviously, this type of operation results in discontinuous wavelength tuning and is not useful in terms of gas sensing but it explains very clearly the intricacies of the design and operation of a typical ECDL.
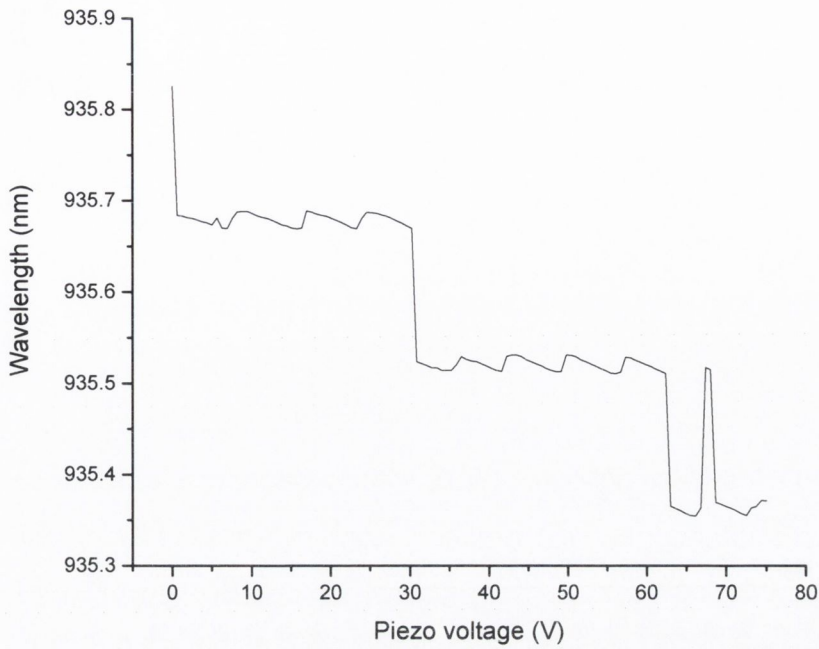
Figure 4.8. *PZT tuning as a function of wavelength of the ECDL with the current kept constant at 100mA and the diode heatsink temperature fixed at 20^0C.*
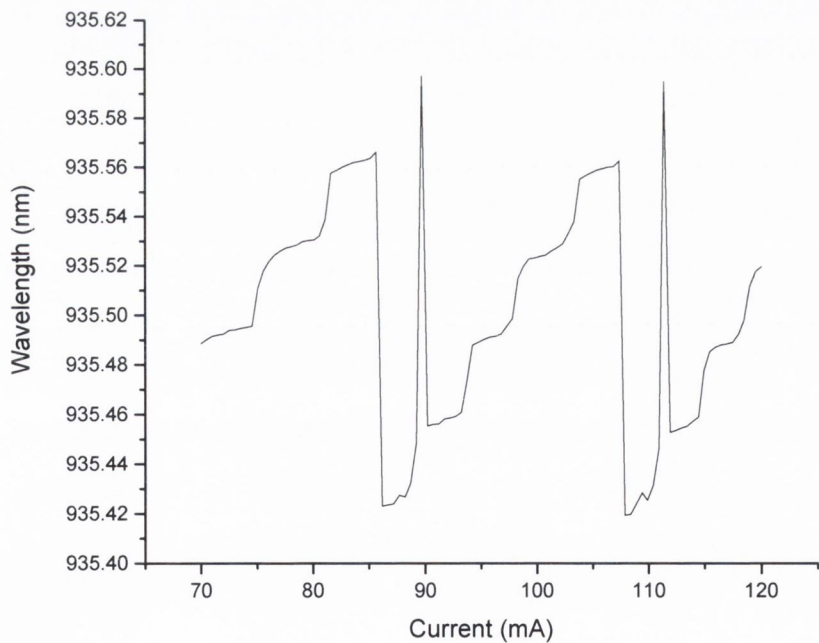

Figure 4.9. *Current tuning of the ECDL as a function of wavelength with the PZT voltage fixed at 50V and the diode heatsink temperature fixed at a temperature of 20^0C.*

By comparison, the wavelength tuning properties of the DFB laser diode emitting at 935nm are less complex. The emission wavelength of a DFB device can be tuned by either changing the temperature of the device directly using, for example, a Peltier thermoelectric device, or by changing the injection current to the laser. By increasing the laser mount temperature the refractive index in the tuning region is increased, thus the emission wavelength may be tuned in a linear fashion. Thermal tuning is based on the fact that the optical length of a diode laser varies with temperature of the laser chip. Increasing the laser mount temperature causes a narrowing of the energy band gap, with the optical spectrum shifting towards longer wavelengths. Thermal tuning is slow but extremely large mode-hop free tuning ranges over several nanometres can be achieved. Injection current tuning of the laser can cause a reduction in the refractive index and the emission is shifted to shorter wavelengths. Heat is also generated with carrier injection due to the nonzero resistance of the diode and so the overall effect is to increase the emission wavelength of the laser.

Typical tuning rates reported in the literature are $(\Delta\lambda/\Delta T) < 0.01$ nm/K and $(\Delta\lambda/\Delta I) < 0.001$ nm/mA for thermal and carrier density induced tuning respectively. However, in practice, current tuning rates show a wide variation since they are also highly dependent on the thermal resistance of the laser diode heat sink arrangement [18]. Figure 4.10 shows the measured emission wavelength dependence on temperature for the laser device in the range $14.5°C \leq T \leq 34.5°C$ at a constant drive current of 35mA. The greater wavelength tuning possible when the temperature of a DFB laser is varied can be very useful for identification purposes to locate the strongest absorbing gas lines in a wide range. To scan the gas absorption line in more detail, the DFB wavelength is varied by changing the current of the laser diode, which allows the molecular absorption line to be sampled with excellent spectroscopic resolution. Also shown in figure 4.10 is the emission wavelength dependence on drive current where the laser heat sink temperature, T, is held constant at three temperatures $T = 15°C$, $20°C$, and $25°C$. The emission wavelength tunes linearly with both temperature (T) and current, (I), at respective rates of $\Delta\lambda/\Delta T = 5.97 \times 10^{-2}$ nm/$°C$ and $\Delta\lambda/\Delta I = 1.05 \times 10^{-2}$ nm/mA. The maximum mode-hop free wavelength tuning possible with this temperature scan was 1.4nm and the maximum mode-hop free tuning with injection current was measured to be 0.32nm. The wavelength tuning procedure for the DFB is straightforward and far less complicated than the ECDL where a time consuming

contour mode map is initially required, to acquire the correct current/PZT combination for continuous wavelength tuning.
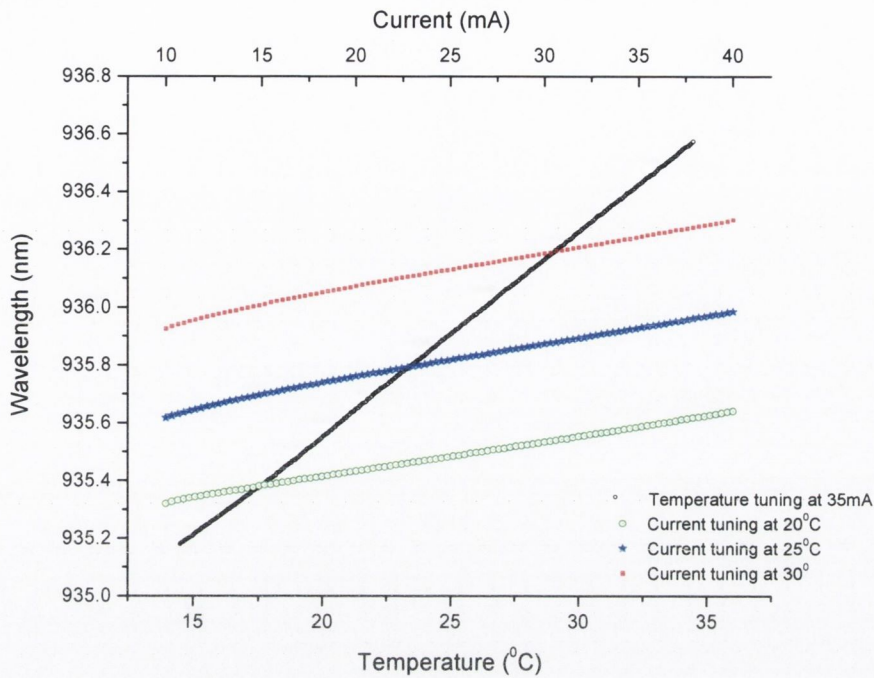
Figure 4.10. *Emission wavelength tuning behaviour of a DFB laser at 935nm as a function of temperature and current tuning.*

4.2.2 Spectral purity

For high performance gas sensing and optical telecommunications capabilities, it is necessary that all devices show dynamic single mode emission. The SMSR measurement is the quickest and easiest method to determine whether or not the laser emission is single mode. The SMSR of the ECDL was measured by viewing the fibre-coupled output from the device on an optical spectrum analyser (OSA, Agilient, Model 86140B) with a resolution of ±0.01nm. In particular, for spectroscopic gas sensing applications, a SMSR of >30dB is necessary in order to minimize mode partition noise and so prevent absorption signals associated with other modes interfering with the desired signal from the spectral absorption feature under investigation [19]. Mode partition noise in semiconductor lasers describes how the intensities of all longitudinal optical modes fluctuate [20]. It arises when the main and side lasing modes fluctuate in a certain way so that the overall intensity remains relatively constant. The SMSR of the ECDL emission depends greatly on the operational point of the device in terms of injection current and

PZT voltage. Therefore, it is vital that the laser tuning is maintained in a position away from any mode boundaries where the SMSR is drastically reduced. To get a better indication of how the SMSR of the ECDL output varies with current and PZT voltage, a contour plot of SMSR as a function of current and PZT voltage was recorded. Over the range of 80mA to 120mA for the injection current and 20V to 50V for the PZT voltage, the dominant lasing mode and the side modes are again mapped out for each operating point, measured using an OSA. Figure 4.11 shows the resulting plot with the ECDL having an overall SMSR, at the optimum operating points of the laser, of more than 40dB. The SMSR of the ECDL is clearly reduced significantly to < 8dB at the mode boundary positions.
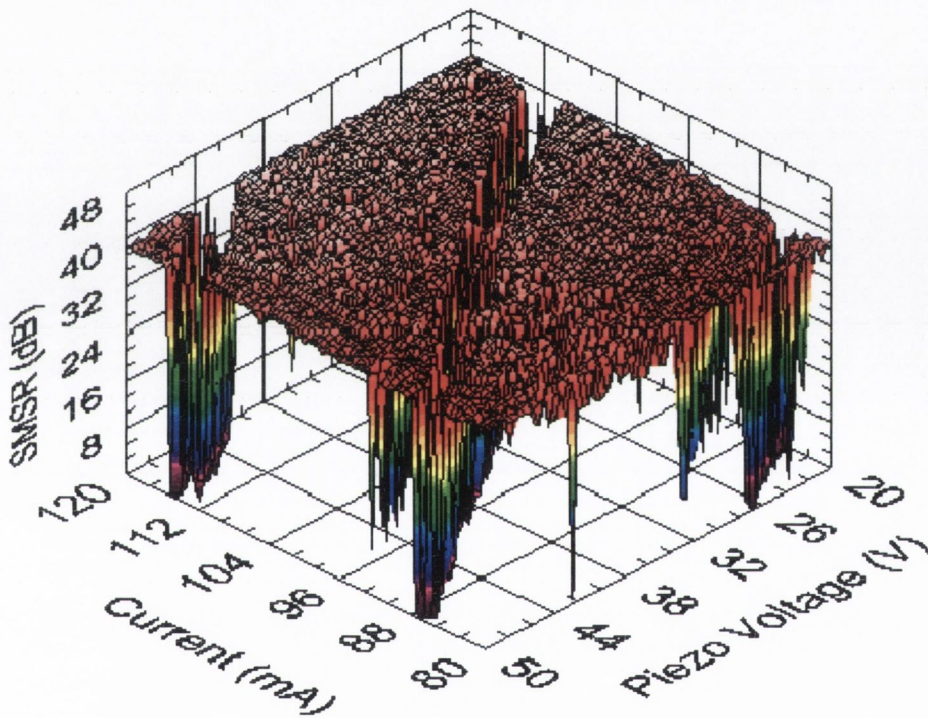
Figure 4.11. *Measurement of the SMSR of the ECDL emission as a function of current and PZT voltage, that controls the grating angle. The SMSR of the device is >40 dB at stable operating points and from the plot, clearly deteriorates at the mode boundaries.*

The SMSR of the DFB at 935nm was also recorded with an OSA, with figure 4.12 showing a typical spectrum of the device at a constant heatsink temperature of 23^0C, constant injection current of 35mA resulting in a SMSR value for the laser > 45dB.
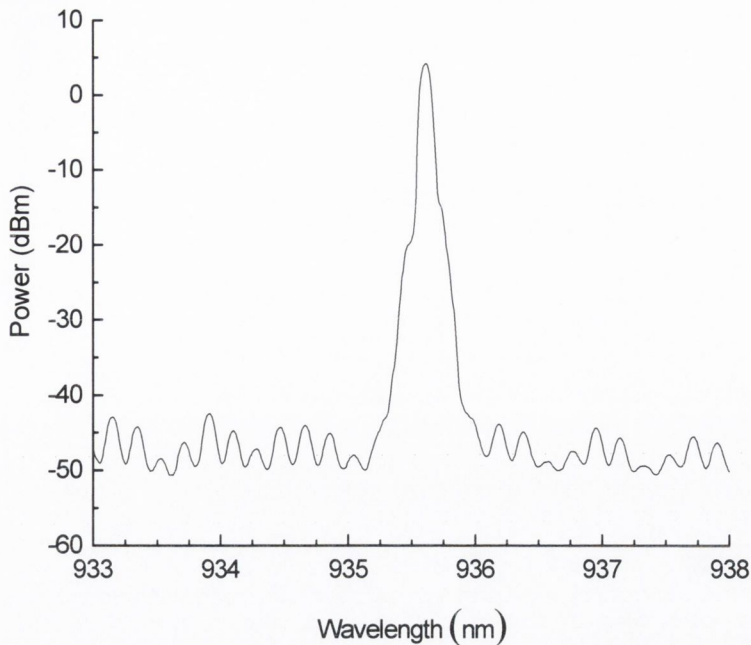
Figure 4.12. *SMSR >45dB for the DFB laser emitting at 935nm with its temperature fixed to 23°C and the injection current set at 35mA.*

Figure 4.13 shows emission spectra for various operating temperatures from 15^0C up to 30^0C at a constant drive current of 25mA and demonstrates the temperature tuning characteristics of the DFB laser diode. For all temperatures, single mode emission is observed with a side mode suppression ratio >35dB covering a wavelength tuning range of approximately 1nm.
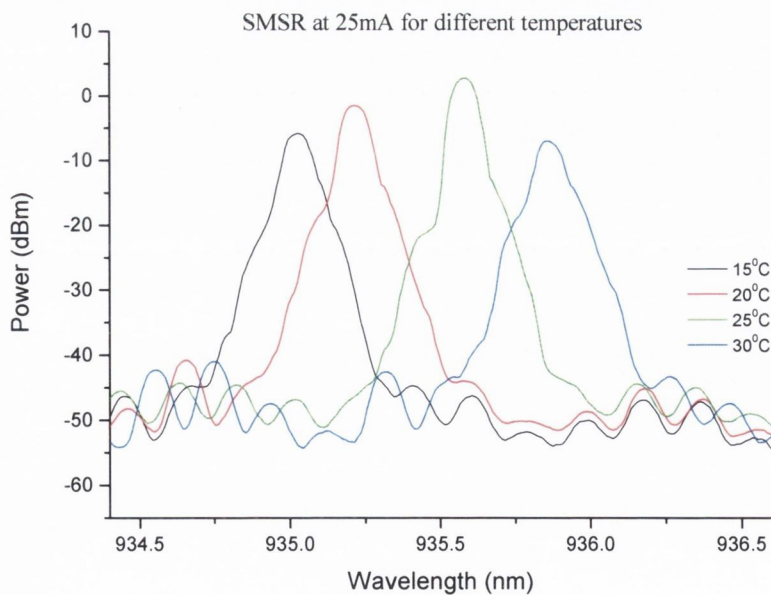
Figure 4.13. *Emission spectra of DFB laser at 935nm at a constant injection current of 25mA for various operating temperatures from 15^0C up to 30^0C.*

76

4.3 Spectral linewidth measurements

4.3.1 Laser spectral linewidth theory

The spectral linewidth of lasers is extremely important in the field of spectroscopic measurements as well as coherent optical communication systems and therefore has been studied in great detail by many authors [21-23]. Ideally, for a laser source applied to gas sensing it is necessary to have a device whose linewidth is much less than that of the target gas. A Doppler broadened gas linewidth can be typically 500MHz at room temperature, therefore it is essential for increased resolution that the target gas of interest is probed with a linewidth significantly less than 500MHz. In addition, since the spectral linewidth is a measure of noise of the laser output, a laser with a narrow linewidth can result in greater accuracy and higher signal to noise detection levels. The fundamental spectral emission linewidth of a laser is associated with fluctuations in the phase of the optical field. These fluctuations arise from carrier density oscillation, and spontaneous emission events of the gain medium into the cavity mode. In the optical field emitted from a laser, a stimulated emission event adds a photon to the field and the added photon has the same phase as the field already in the cavity. A spontaneous emission adds a photon whose phase is different to the phase of the field in the cavity. As a result of the addition of a spontaneous emission photon, the phase of the optical field changes with time and induces a phase change to the optical field. In addition to the spontaneous emission event, the amplitude of the optical field is also changed. By means of relaxation oscillations, the field decays to its steady state value but this causes an additional phase change. Because of the relaxation oscillations that occur after a spontaneous event, the carrier density will change because of the interaction between carriers and photons as described by the rate equation model in section 3.2. These carrier density fluctuations induce refractive index changes causing additional phase noise and a broader linewidth, defined by the linewidth enhancement factor, as described in section 3.5.2. As a result, the output of the laser is not perfectly monochromatic but exhibits some degree of phase noise defined by the spectral linewidth.

4.3.2 *Experimental*

Many methods exist for measuring the linewidth of laser devices depending on the particular device parameters. The use of a low noise current source to drive the laser under test can also help improve the accuracy of the measurement. The wavelengths of the ECDL and DFB devices under investigation here are in the 935nm range and therefore a delayed self-homodyne interferometric technique using kilometres of single mode optical fibre at 935nm was considered prohibitively expensive. Hence a short arm homodyne technique was employed for measurement of the ECDL linewidth. The linewidth of the DFB was also measured using a heterodyne technique with the ECDL employed as a local oscillator. In the former arrangement, the emitted optical field of the ECDL is mixed with a delayed version of itself. ECDL's have very narrow linewidths due the their unique architecture which employs an external cavity. The ECDL used in these measurements had an external cavity length of approximately 2cm. As explained in section 3.4, the effect of the external cavity narrows the linewidth so the delay in the short arm set-up is fixed to be shorter than the coherence length of the ECDL under test. Therefore, the two arms of the ECDL optical field mix coherently and a number of interference peaks appear in the detected power spectrum. The free spectral range of the peaks should correspond to the length of fibre used. For the linewidth measurement of the ECDL the output of the laser is split into two equal parts by means of a 50/50 coupler. One arm of the coupler is directed to 30m of fibre, which is much shorter than the coherence length of the laser. The other beam is passed through a polarization controlling stage. The polarization controller consists of three loops of fibre, which can be mechanically rotated. The two beams are then recombined with another 50/50 coupler and detected with an IR 1 GHz low noise photoreceiver (New Focus Model 1611). When the two coherent fields are combined at the detector, a frequency difference signal is detected which contains the combined FM field of the arm delayed by the 30m of fibre and the arm that passes through the polarization controller. The technique converts the combined optical power spectrum to an electrical spectrum, which is then displayed on an electrical spectrum analyser (Hewlett Packard, model 8563A). However, because this electrical spectrum contains the noise of the two combined signals, the −3dB FWHM centred at 0Hz is equal to twice the actual linewidth of the laser under test. The experimental set-up for the self-homodyne technique used for the measurement of the

spectral linewidth of the ECDL is shown in figure 4.14. For this particular measurement, the ECDL had a maximum fibre coupled output power >10mW at room temperature and an emission wavelength at 935nm.
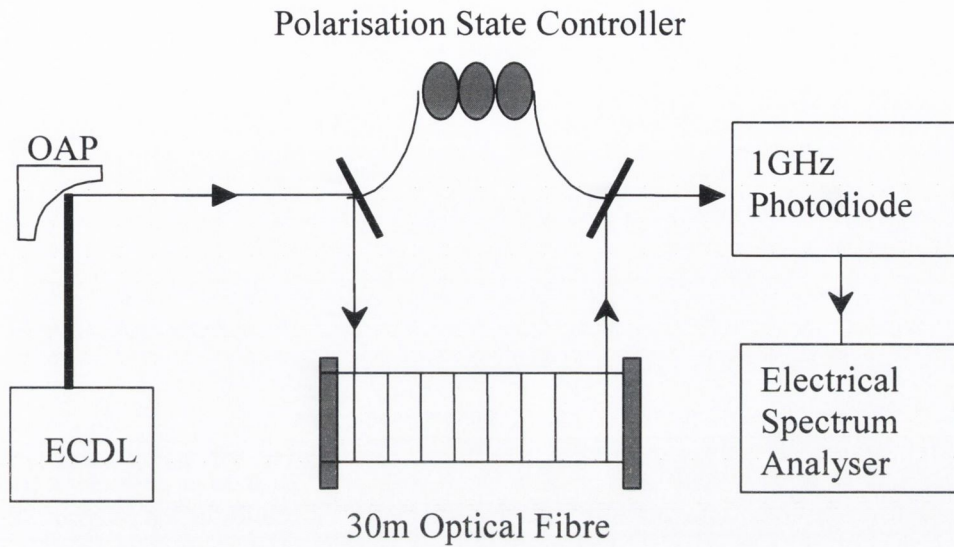

Figure 4.14. *Experimental set-up for ECDL spectral emission linewidth measurement using the short-arm method.*

The output of the ECDL is fibre-coupled via an integral collimator and a single mode fibre but unfortunately there was no optical isolator included in the device packaging. Therefore, the linewidth measurements, in the absence of an isolator, proved quite difficult since the short-arm measurement profile (Lorentzian envelope function with an underlying interference pattern) was very susceptible to masking by the effects of feedback to the laser. The source of the feedback most likely resulted from stray reflections from fibre ends or by spurious optical cavities. In practice, the profile was non-ideal. Despite careful set-up and repeated optimisation of the measurement system, the linewidth measurement results obtained under the conditions were considered unreliable. This was attributed to the feedback from the fibre coupling stage. In view of these results, it was decided to adopt a different approach and the measurements were repeated under different conditions. The emission from the ECDL was directly coupled out through free space, bypassing the collimator and fibre coupling. The linewidth measurements were then repeated. In this arrangement the free-space emission was directed to an off-axis parabolic (OAP) mirror to minimise feedback from refractive optical elements, before being coupled via an angle polished FC-APC fibre into the

Mach-Zender fibre interferometer. The geometry of this optical set-up was such that feedback to the ECDL was attenuated and its effects mitigated. Essentially non-optimum coupling to the interferometer with 10dB loss provided an effective 20dB isolation and decreased the sensitivity to back reflections from the first coupling stage. The resulting electrical spectrum of the linewidth measurement on the ECDL by the short arm homodyne method is displayed in figure 4.15.
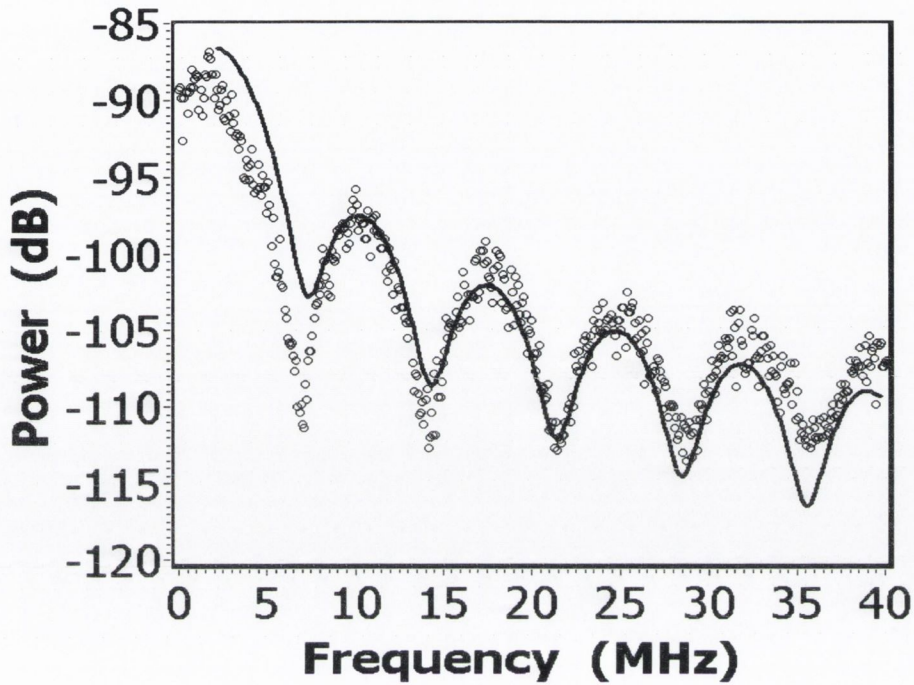
Figure 4.15. *The trace above shows the measured and fitted RF power (in dBm) in the range 0 to 40MHz giving a value of 230kHz for the linewidth of the ECDL.*

The resulting linewidth shape was fitted with the expression in equation 4.1 where a value of approximately 230kHz was obtained for the spectral linewidth of the ECDL [24].

$$G(v) = \frac{B\Delta v}{v^2 + \Delta v^2}\left\{1 - e^{-2\pi\tau\Delta v} \times (\cos(2\pi v\tau) + \sin(2\pi v\tau)/v)\right\} \qquad (4.1)$$

where, B is a scaling factor for the power level of the trace, τ is the delay time, v is the frequency and Δv is the half width at half maximum of the Lorentzian laser lineshape. The measured data in figure 4.15 does not exactly fit the ideal profile where a difference is observed in the envelope of the peaks. This difference is most likely caused by external feedback to the laser, which results in optical power fluctuations. With the short arm

method, the optical fields are mixing coherently and so the interference peaks are quite evident in the trace of the electrical spectrum.

The spectral linewidth of the DFB laser was also measured, with a heterodyne technique using the ECDL as a local oscillator (LO) since its linewidth was expected to be significantly less that that of the DFB device. The set-up for the heterodyne technique is shown in figure 4.16.
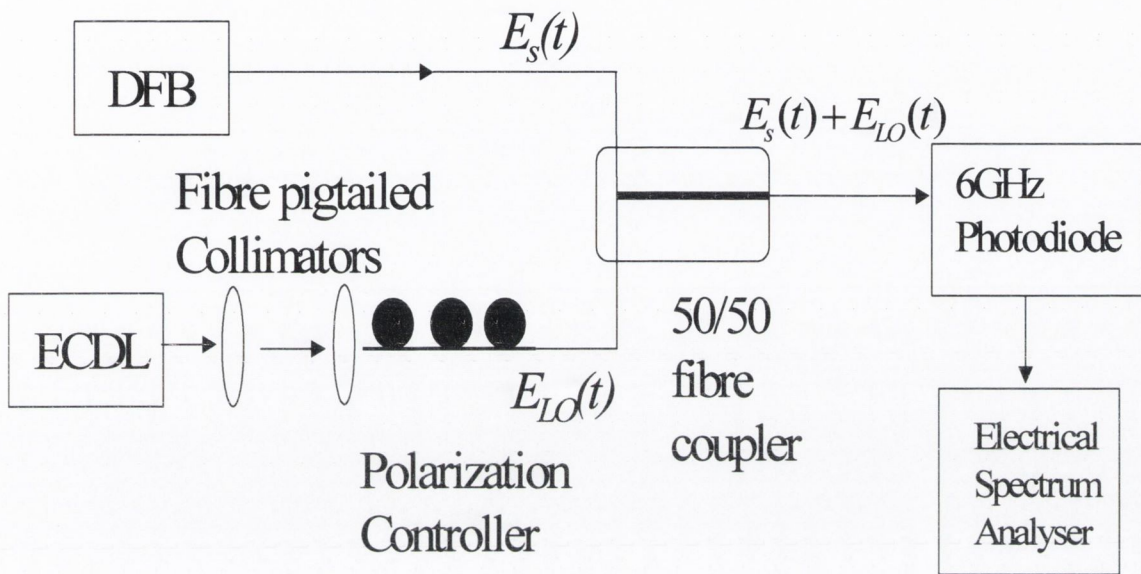
Figure 4.16. *Experimental set-up for DFB laser emission linewidth measurement.*

In this experiment, the ECDL output was directly fibre-coupled to a pair of free space collimators and by carefully adjusting the collimators, the feedback effects to the ECDL were attenuated and reduced allowing a more accurate evaluation of the spectral linewidth of the DFB. For this measurement technique, the emission wavelength of the ECDL is tuned to a frequency close to that of the laser under test and is fixed during the experiment. This creates a heterodyne beat tone between the LO and each of the frequency components in the signal spectrum as illustrated in figure 4.17. The emission wavelength of the ECDL was tuned to within approximately 4GHz of the frequency of DFB laser. This was achieved with careful adjustment of the ECDL operating parameters and employing a suitable large bandwidth photodetector, while monitoring the ECDL emission wavelength with a wavelength meter. For this measurement a 6GHz photodetector was employed which meant that matching the emission frequency of the two lasers was more easily achieved. For the heterodyne measurement, the frequency of

the local oscillator must be tuned close to the laser frequency under test so that the mixing product of the two lasers falls within the bandwidth of the detector. A summary of the theory behind the technique is given below and a more detailed description can be found in [25].

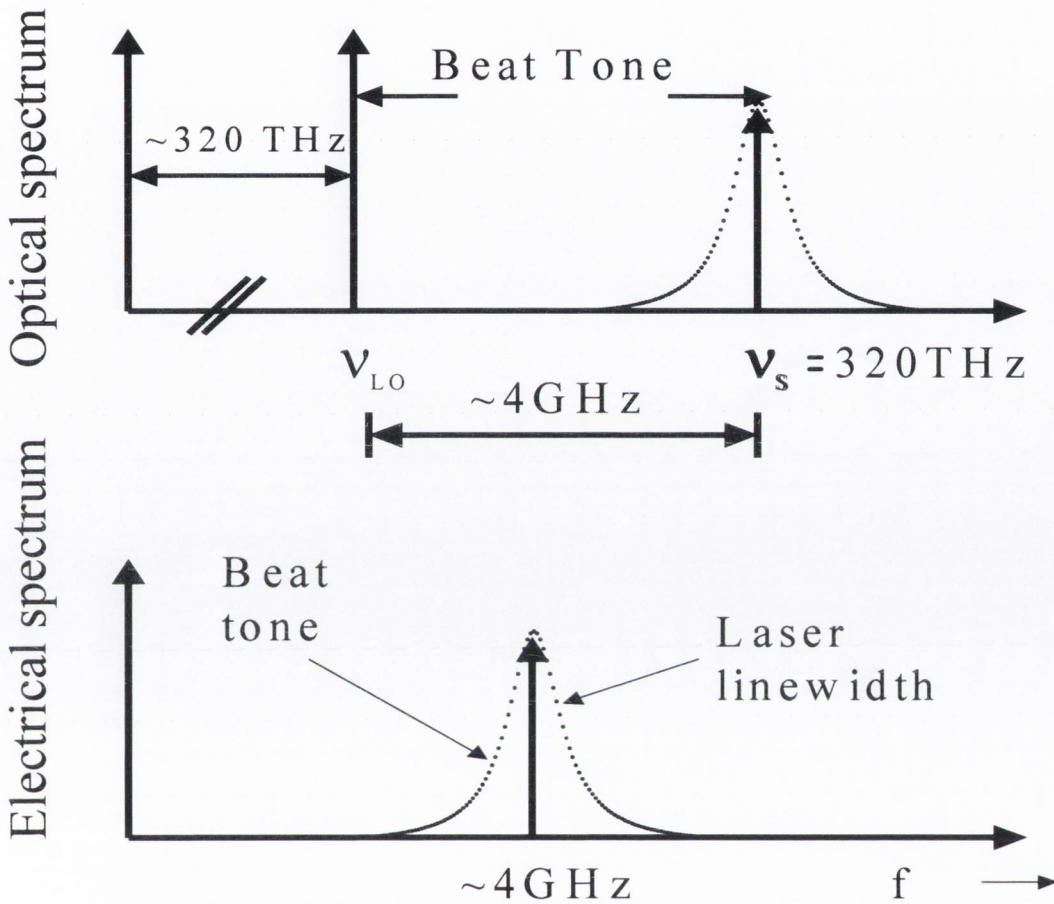Figure 4.17. *Illustration of heterodyne beat tone between the ECDL acting as the local oscillator and DFB laser diode.*

Consider the two optical fields of both LO and DFB devices incident on the photodetector, after passing through a 50/50 coupler,

$$E_s(t) = \sqrt{P_s(t)}e^{j(2\pi v_s t + \phi_s(t))} \tag{4.2}$$

$$E_{LO}(t) = \sqrt{P_{LO}(t)}e^{j(2\pi v_{LO} t + \phi_{LO}(t))} \tag{4.3}$$

where $P_s(t)$ and $P_{LO}(t)$ are the power variations as a function of time, v_s and v_{LO} are the optical frequency, and φ_s and φ_{LO} are the optical phase of the laser under test and the local oscillator respectively. The total field at the photodetector is thus given by Eq. (4.4),

$$E_T(t) = E_s(t) + E_{LO}(t) \tag{4.4}$$

Since we are detecting the amplitude and not the optical field, photodetection is quadratic with respect to the optical field so that,

$$P(t) = |E_T(t)|^2 \tag{4.5}$$

and the quadratic response, allows the detection of the interference between the two fields. The generated photocurrent, $i(t)$, in the detector is thus given by Eq. (4.6),

$$i(t) = R|E_T(t)|^2 \tag{4.6}$$

with the responsivity R of the detector given by

$$R = \eta_d q/hv \ [\text{A/W}] \tag{4.7}$$

where η_d is the quantum efficiency of the detector, q and hv are electronic charge and the photon energy respectively.

By substitution of Eq. (4.4) into Eq. (4.6), we get Eq. (4.8),

$$i(t) = R[P_s(t) + P_{LO} + 2\sqrt{P_s(t)P_{LO}}\cos(2\pi(f_{IF})t + \Delta\phi(t))] \tag{4.8}$$

with $f_{IF} = v_s - v_{LO}$ and $\Delta\varphi(t) = \varphi_s(t) - \varphi_{LO}(t)$

The first two terms in Eq. (4.8) correspond to the direct intensity detection, while the third term is the important heterodyne mixing term. Note, the dependence on the actual optical frequency is gone and only the difference remains (f_{IF}). It is important to note that

if either field were separately detected on the photodiode, the resulting photocurrent would follow only the power variations $P(t)$ and all phase information would be lost. A polarisation state controller is placed in the path of the ECDL (LO) in order to align the polarisation of the LO to that of the signal under test. Matching the polarisation of the two signals maximises the signal strength of the detected electrical field. The key requirement of this technique is to have a reference laser with a stable narrow (<1MHz) spectral linewidth. The reason for this is that the interference of the two optical fields is what is actually measured and so it is assumed that the linewidth of the LO is much less significant with respect to the laser under test. If this is the case, then the beat tone will be broadened primarily by the phase noise of the laser under study. It is also beneficial to have a wide bandwidth detector. A New Focus 6GHz photoreceiver (Model 1534-50) was used in the experiment allowing the tuning of the LO frequency to the DFB laser to be easily observed. A wavelength meter was also used, instead of an OSA, to add extra accuracy when matching the wavelength of the DFB under test and the ECDL. The overall accuracy of the technique can be improved by increasing the output power of the local oscillator because the strength of the detected power spectrum increases with local oscillator power, P_{LO}. The electrical spectrum of the detected signal contains information on the direct detection terms and products of optical mixing terms.

$$S_i(f) \approx R^2 \left\{ S_d(f) + 2[S_{LO}(v) \otimes S_s(-v)] \right\} \qquad (4.9)$$

The first term is just the direct detection term while the second term is the one of interest. It is the heterodyne mixing product that is the convolution of the local oscillator spectrum $S_{LO}(v)$ with the signal spectrum $S_s(v)$. The convolution originates from the multiplication of the time varying oscillator field with the signal field in the photodetector. Multiplication in the time-domain is equivalent to convolution in the frequency domain. Therefore the detected electrical spectrum will be given by Eq. (4.10),

$$S_i(f) \approx 2R^2 P_{LO} S_s(v - v_{LO}) \qquad (4.10)$$

For the DFB laser linewidth measurement, the ECDL output was directly fibre-coupled to a free space collimator. The FWHM and therefore the linewidth of the DFB laser, was calculated to be approximately 4.2MHz as shown in figure 4.18. This result is consistent

with the values specified by Nanoplus which state, that the linewidth of their 935nm DFB lasers are typically below 5MHz.
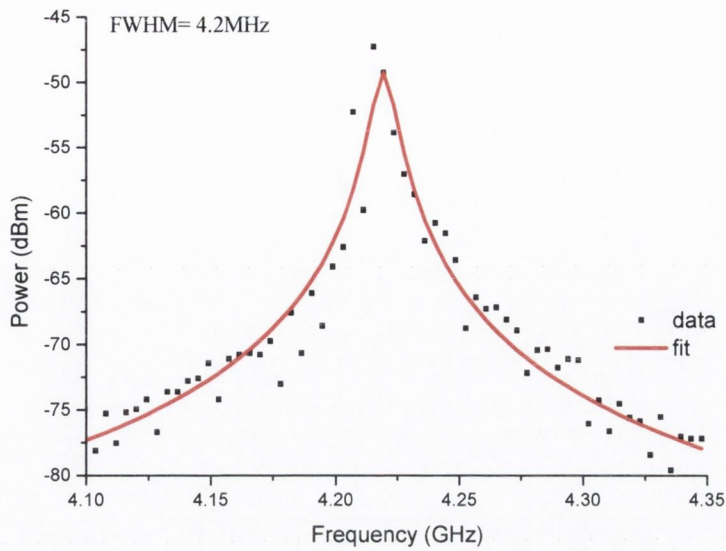

Figure 4.18. *DFB laser linewidth measurement with measured and Lorentzian fitted data giving a result of 4.2 MHz.*

4.3.3 Detrimental optical feedback, modulation considerations, and vacuum operation

The effect of optical feedback on the spectral characteristics of semiconductor lasers has attracted much study over the past twenty years [26]. Unwanted optical feedback can lead to the performance of the diode laser being degraded by destabilizing the laser output and can ultimately lead to a total failure, an effect known as coherence collapse [27]. This is especially the case for laser disc readers, optical fibre transmission and gas sensing applications. The system can often be degraded due to instabilities caused by even small amounts of unavoidable optical feedback from distant reflectors within the optical system [28, 29]. For example, optical reflections from the front surface of a fibre is about 4%, with approximately one tenth of this light being coupled back into the laser cavity. A similar situation can occur for a laser disc reader of a compact disc, where unwanted optical reflections from the disc can affect the operation of the device [30]. However, there is also a positive result from the optical feedback where it has been demonstrated that the chaotic output of semiconductor lasers with optical feedback can be successfully applied to optical encrypted communication systems [31-33]. Even very minute portions of the reflected light can destabilize the laser producing different kinds of regular

(periodic) or irregular (chaotic) oscillations of narrow or broad frequency bands thus limiting the range of applications of the whole device into which the laser is integrated. Careful isolation of the diode laser is thus necessary due to the unwanted feedback, resulting in an increase in the complexity and cost of such systems. The ECDL under test unfortunately did not have an optical isolator installed in the packaging of the device and this resulted in spurious behaviour on occasion in the laser output caused by unwanted optical feedback. The source of these unwanted reflections was most likely from alignment of the fibre output coupling stage of the laser. The effect of the external reflections was most easily and commonly observable in the recorded emission power planes using the internal monitor photodiode. Another method to extract information about the emission mode profile of the ECDL, in addition to recording the emission wavelength contour map, is to record the output power using the internal monitor photodiode of the device. With both the current and PZT voltage scanned over the appropriate ranges, the output power is recorded and a contour power plane is obtained as represented in figure 4.19(a). This result also gives a clear indication of the contrasting effect the unwanted feedback can have on the output power planes with figure 4.19(b) clearly demonstrating the negative impact the feedback can have on the power plane measurement. These measurements were taken by scanning the current and PZT voltage over a certain range and recording the corresponding output power using the internal monitor photodiode.
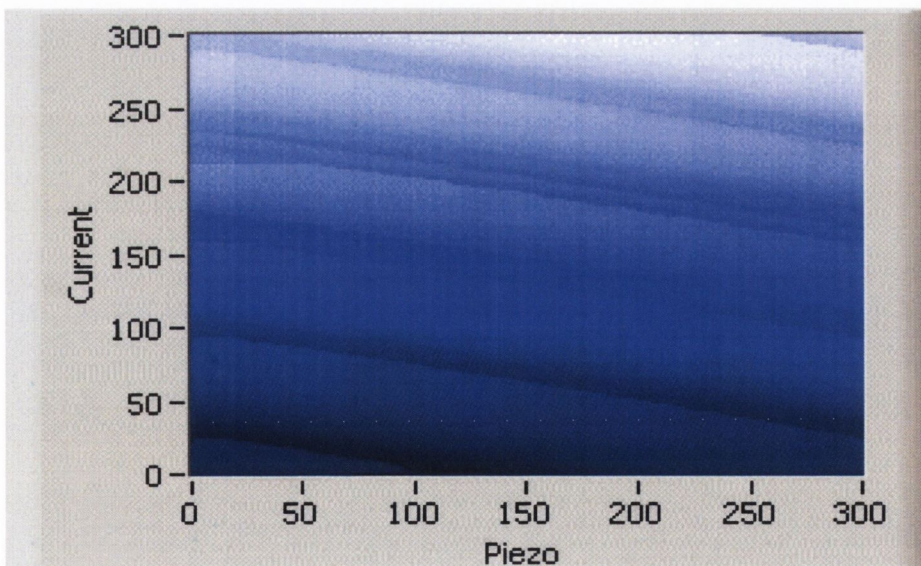

Figure 4.19(a). *Power planes of ECDL output emission recorded with an internal monitor photodiode for the case without any optical feedback.*
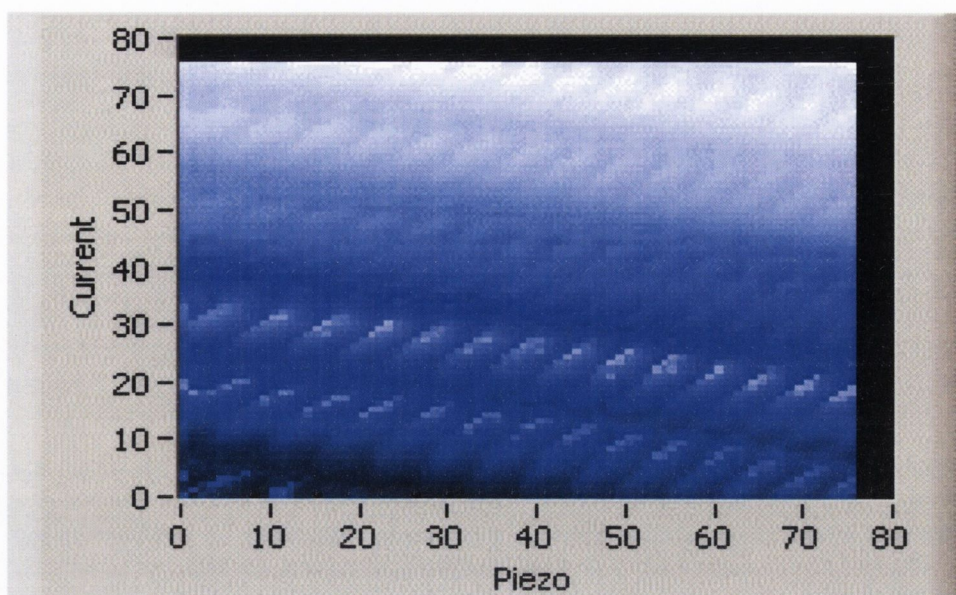
86

Figure 4.19(b). *Power plane of ECDL output emission recorded with an internal monitor photodiode with optical feedback effects clearly present.*

The graph in figure 4.20 demonstrates the effect of the feedback on the wavelength tuning and output power properties of the ECDL as it was tuned with a combination of current and PZT, along one of the lasing modes of the power plane of figure 4.19(b). It is clear from the trace that the output power recorded with the internal monitor photodiode, shows periodic fluctuations but more critical is that the wavelength tuning is no longer linear. For gas sensing systems, especially when the operating laser source has a widely tuneable wavelength range, an ideal situation exists if the output power remains constant while the wavelength is linearly tuned. Unfortunately, for the ECDL wavelength tuning operation, the output power actually decreases linearly with decreasing wavelength and so a periodic variation of the output power while tuning across an absorption line of a target gas can lead to unreliable results. This difficulty was observed on several occasions and is demonstrated in figure 4.21 where a H_2O vapour absorption line at 935.684nm was targeted using a WMS technique [10], described previously in chapter 2. The experimental set-up for the measurement involves modulating the voltage to the PZT with the laser output beam passed through a 1 metre long gas cell containing water vapour at a pressure of approximately 25mbar and fixed at room temperature. The ends of the cell were fitted with Brewster angled windows to eliminate the effect of interference fringes in the recoded data. The laser beam, after passing through the cell, is

then focussed onto a photodiode and the detected signal is fed to a lock-in amplifier to process the signals. The 2nd harmonic WMS profile (*2f* absorption signal) is acquired from the lock-in amplifier output and is generally preferred for gas identification purposes due to the peak of the *2f* signal at the absorption line centre. However, without an isolator in the ECDL set-up, the effect of the feedback on the detection measurement can be extreme and obviously can lead to inaccurate and unreliable readings.
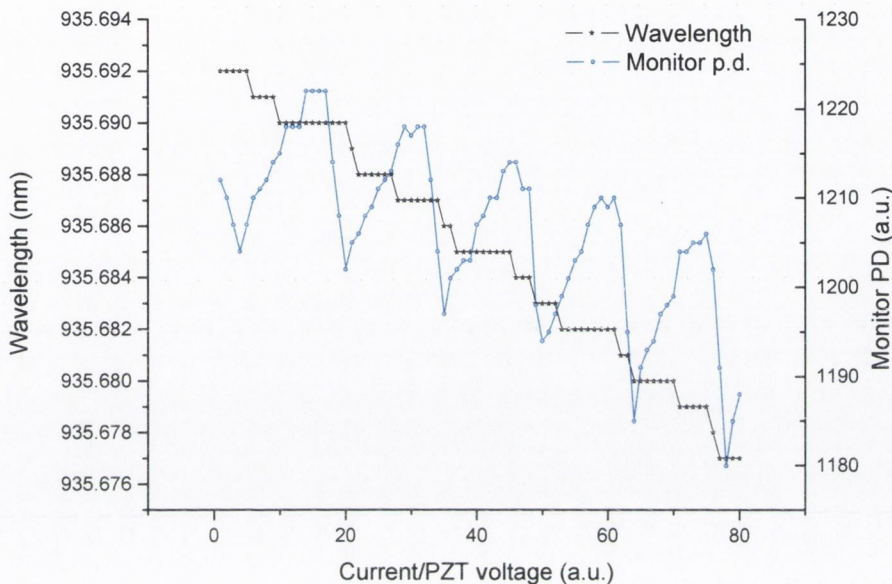
Figure 4.20. *Measured wavelength and output power of ECDL as scanned along one of the lasing modes in figure 4.19(b) with the effect of the optical feedback effects clearly present.*

The *2f* demodulated absorption signal in figure 4.21 is inaccurate and the signal displays the power fluctuation on either side of the H_2O absorption line. Furthermore, the interference present in the peak of the *2f* signal suggests that the detection of the absorption line centre is not precise which can ultimately lead to inaccuracies in the detection scheme. Also, this type of unreliable laser behaviour would lead to a total failure of a frequency stabilization laser system. However, it should be noted that the feedback problem for the ECDL was not a source of constant difficulty and with the appropriate measures taken, with regards to fibre coupling alignment and mechanical stability, the operation of the ECDL was satisfactory.
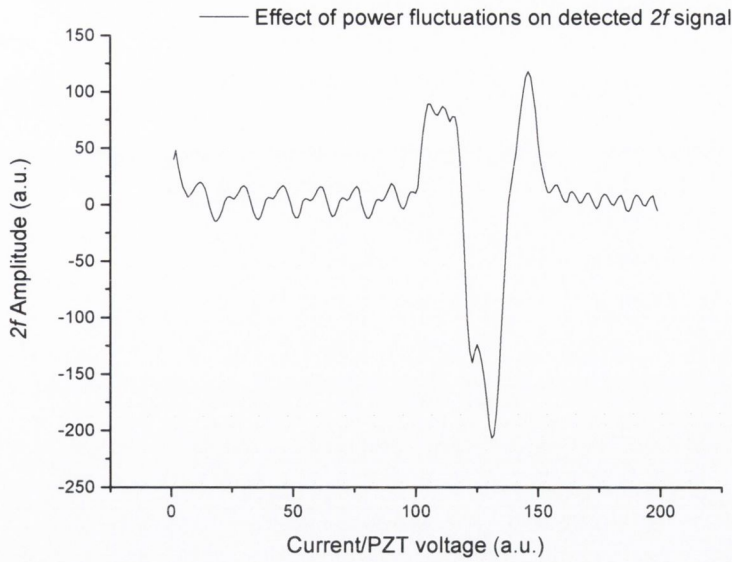
Figure 4.21. *Effects of power fluctuations on the wavelength tuning ability of the ECDL under modulation conditions caused by optical feedback.*

Figure 4.22 shows the improved performance of the ECDL where the effects of unwanted optical feedback have been isolated. In this instance the laser wavelength is scanned across a wide tuning range resulting in the direct detection of H_2O absorption lines and the corresponding *1f* harmonic WMS signals measured in the 935nm region. The continuous wavelength tuning range of approximately 0.45nm of the ECDL means that three lines were detected from this scan with the sloping background resulting from the decrease in output power of the device as the wavelength is tuned.
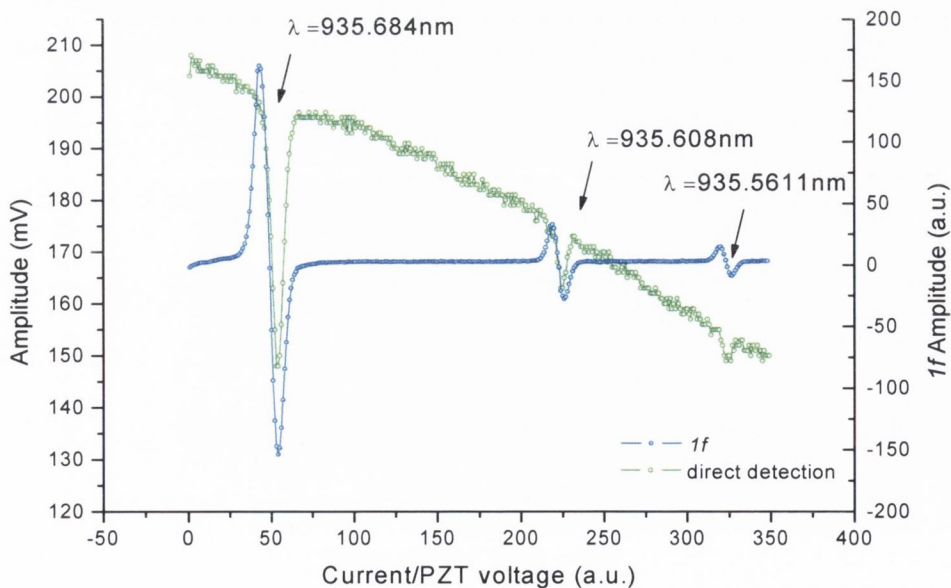
Figure 4.22. *Direct detection of absorption lines and the corresponding 1f demodulated WMS profile recorded with a lock in amplifier with the sloping background removed.*

The resulting *1f* harmonic WMS profiles recorded with a lock-in amplifier with the sloping background removed are also clearly observable. As the ECDL was a candidate for an ISL in a space environment, an experiment to investigate the spectral emission from the ECDL under near vacuum conditions (<1mbar) was also preformed. A custom-made vacuum chamber was constructed to house the laser with vacuum feed-throughs included in its design for the fibre optic output of the device and also for the electrical connections to the current source and temperature controller. A vacuum turbo pump was used to evacuate the chamber to less than 1mbar and was left operating for the test period of 60 minutes. Using the fibre-optic output coupled to an OSA, the wavelength and output power were then monitored every 5 minutes for the duration of the test with the ECDL fixed at a constant current of 90mA, PZT voltage of 50V and temperature of 22^0C. It is clear from the results shown in figure 4.23 that both the output power and emission wavelength of the device increase over the test period. The likely cause of the increase to both output power and wavelength is due to an increase in the ECDL temperature, as the generated heat could not dissipate within the vacuum.
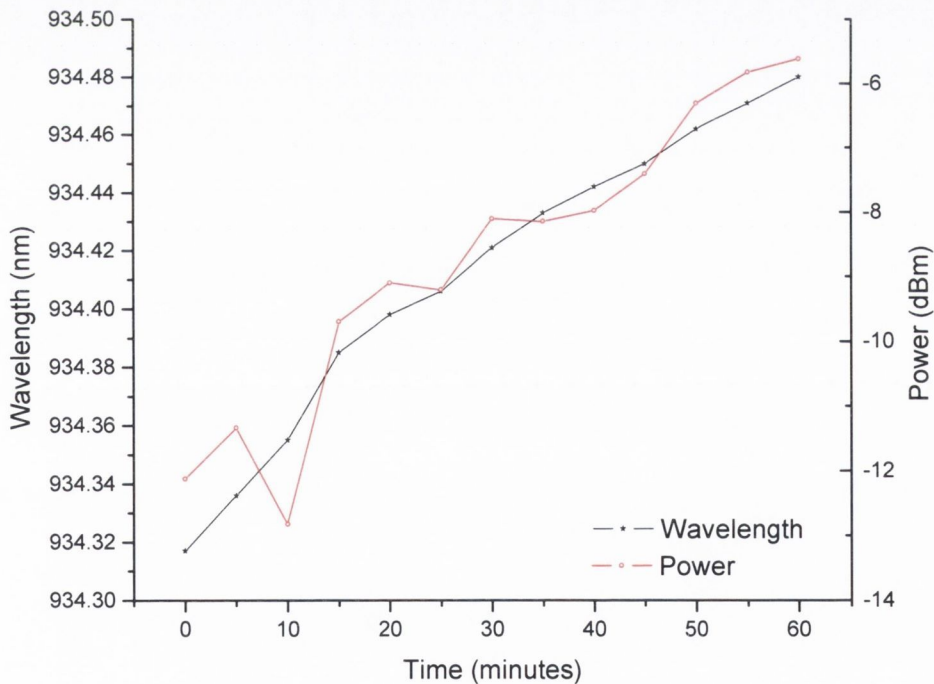

Figure 4.23. *Measured wavelength and output power of ECDL as a function of time while kept in a low pressure vacuum chamber at <1mbar for 60 minutes. The current was fixed at 90mA, PZT voltage at 50V and temperature at 22^0C.*

4.4 Conclusions

The spectral characteristics of two semiconductor diode lasers both with emission wavelengths at 935nm have been examined and the results compared to evaluate their suitability in operating as injection seed sources for a space-based water vapour sensing project. An ECDL operating in the Littrow architecture showed excellent wavelength tuning behaviour with a maximum, continuous, mode-hop free wavelength tuning range of 0.45nm and quasi-continuous wavelength tuning of over several nanometres. It showed SMSR > 40dB, output power > 60mW and the spectral linewidth of the device was measured to be less than 300kHz all of which suggest that it is an ideal candidate for water vapour spectroscopic studies. A DFB laser diode was also investigated as an alternative to the ECDL source and showed SMSR > 45dB, continuous wavelength tuning with both temperature (T) and injection current (I), at respective rates of $\Delta\lambda/\Delta T =$ 5.97×10^2 nm/°C and $\Delta\lambda/\Delta I = 1.05 \times 10^{-2}$ nm/mA, and a spectral linewidth of 4.2MHz.

The general operation of the two devices is however extremely contrasting in complexity. In order to operate the ECDL in continuous wavelength tuning mode, a contour mode map is initially measured to acquire the correct injection current/PZT voltage combination. However, over time the tuning behaviour of the ECDL can degrade due to its sensitivity to both temperature and mechanical instability. The DFB laser emission wavelength on the other hand can be rapidly tuned with a variation of either injection current or temperature and results in a larger continuous, linear wavelength tuning range.

The fact that neither of the lasers had an optical isolator in their design often led to a serious reduction in the device performance. This was especially the case for the ECDL possibly due to the higher output power of the device, causing some spurious reflections back into the cavity, which affected the initial spectral linewidth measurements and was also clearly demonstrated in figures 4.20 and 4.21. The problem with optical feedback can be avoided with careful adjustment of the fibre-coupling unit of the ECDL mounting. However, a more permanent and effective solution is needed if the device is to function long term, without any intervention, as would be the case for a space flight operation. This can be achieved with the installation of an appropriate internal optical isolator, before fibre-optic coupling. The ECDL emission wavelength can be tuned over a wide range (>10nm), which means many gas absorption lines can be targeted. The ECDL also showed good SMSR, high output power, and narrow spectral linewidth. However, the

sensitivity of the device to mechanical vibration eliminates it categorically as a viable injection seed laser diode source for a space-based gas sensing project. Nonetheless, the ECDL was implemented in a frequency stabilization scheme using a water vapour absorption line as a frequency reference and is described in detail in chapter 5.

To summarize, the excellent performance of the DFB laser with regards to continuous wavelength tuning, high output power and SMSR, and narrow spectral linewidth makes it an ideal laser source to probe H_2O vapour absorption lines at 935nm. Furthermore, the less complex design of the DFB laser in comparison to the ECDL makes it the obvious choice for the injection seed laser as it is far more suitable to space flight conditions with its inherent robustness. The ECDL is a superb laser source for use in gas sensing applications over a wide range of wavelengths with its excellent optical properties but is definitely more suitable in mechanically and thermally stable laboratory conditions.

4.5 References

[1]   J. C. Barnes, N. P. Barnes, L. G. Wang, and W. Edwards, "Injection seeding II: Ti:Al$_2$O$_3$ experiments," *IEEE J. Quantum Electron.* Vol. 29, pp. 2684–2692, 1993.

[2]   Y. K. Park, G. Guilliani, and R. L. Byer, "Stable single-axial mode operation of an unstable-resonator Nd:YAG oscillator by injection locking," *Opt. Lett.*, vol. 5, pp. 96–98, 1980.

[3]   R. L. Schmitt and L. A. Rahn, "Diode-laser-pumped Nd:YAG laser injection system," *Appl. Opt.* vol. 25, pp. 629–633, 1986.

[4]   R. Lang, "Injection locking properties of a semiconductor-laser," *IEEE J. Quantum Electron.*, vol. 18, pp. 976–983, 1982.

[5]   H. L. Stover and W. H. Steier, "Locking of laser oscillators by light injection," *Appl. Phys. Lett.*, vol. 8, pp. 91–93, 1966.

[6]   Barnes, N.P.; Barnes, J.C.; "Injection seeding. I. Theory" *Quantum Electronics, IEEE Journal of*, vol. 29, pp. 2670 – 2683, 1993.

[7]   Prasad, C.R.; Fromzel, V.A.; Smucz, J.S.; Hwang, I.H.; Hasselbrack, W.E.; "A diode-pumped Cr:LiSAF laser for UAV-based water vapor differential absorption lidar (DIAL)" *Geoscience and Remote Sensing Symposium, Proceedings IGARSS IEEE International*, vol. 4, pp. 1465 - 1467, 2000.

[8]   Kulatilaka, W.D.; Anderson, T.N.; Lucht, R.P.; "Development and application of an injection-seeded, nano-second, pulsed, optical parametric oscillator (OPO) for high resolution spectroscopy" *Lasers and Electro-Optics,(CLEO). Conference on*, vol. 3, pp.1975 – 1977, 2005.

[9]   L.S. Rothmana, D. Jacquemarta, A. Barbeb, D. Chris Bennerc, M. Birkd, L.R. Browne, M.R. Carleerf, C. Chackerian Jr.g, K. Chancea, L.H. Couderth, V. Danai, V.M. Devic, J.-M. Flaudh, R.R. Gamachej, A. Goldmank, J.-M. Hartmannh, K.W. Jucksl, A.G. Makim, J.-Y. Mandini, S.T. Massien, J. Orphalh, A. Perrinh, C.P. Rinslando, M.A.H. Smitho, J. Tennysonp, R.N. Tolchenovp, R.A. Tothe, J. Vander Auweraf, P. Varanasiq, and G. Wagner, " The HITRAN 2004 molecular spectroscopic database," *Journal of Quantitative Spectroscopy & Radiative Transfer*, vol. 96, pp. 139–204, 2005.

[10] D. S. Bomse, A. C. Stanton, and J. A. Silver, "Frequency-Modulation and Wavelength Modulation Spectroscopies - Comparison of Experimental Methods Using a Lead-Salt Diode-Laser," *Applied Optics*, vol. 31, pp. 718-731, 1992.

[11] http://esamultimedia.esa.int/docs/EEUCM/WALES_TPA.pdf

[12] http://esamultimedia.esa.int/docs/SP_1279_3_WALES.pdf

[13] M. Fischer, D. Gollub, M. Reinhardt, A. Forchel, "Advances in GaInNAs Edge Emitting Laser diodes," *8th Microoptics Conference* (MOC '01), Osaka, Japan, October 24-26, 2001 (Invited)

[14] M.W. Fleming and A. Mooradian, "Spectral characteristics of external-cavity controlled semiconductor lasers," *IEEE J. Quantum Electron.*, vol. 17, pp. 44-59, 1981.

[15] R. Wyatt and W. J. Delvin. "10kHz Linewidth 1.5μm InGaAsP External Cavity Laser with 55 nm Tuning Range." *Electronic Letters*, vol. 19, pp. 110-112, 1983.

[16] Cunyun Ye, *Tunable external cavity diode lasers*, chap. 4, World Scientific, 2004.

[17] L. Levin, "Mode-hop-free electro-optically tuned diode laser," *Opt. Lett.*, vol. 27, pp. 237–239, 2002.

[18] T.P. Lee, "Recent advances in long-wavelength semiconductor lasers for optical fiber communication", *IEEE Proc.*, vol. 79, pp. 253-276, 1991.

[19] P. Werle, "A review of recent advances in semiconductor laser based gas monitors," *Spectrochim. Acta Part A,* 54, pp. 197-236. 1998.

[20] Liou, K.-Y.; Ohtsu, M.; Burrus, C.A., Jr.; Koren, V.; Koch, T.L.; "Power partition fluctuations in two-mode-degenerate distributed-feedback lasers" *Journal of Lightwave Technology,* vol. 7, pp 632 – 639, 1989.

[21] C.H. Henry, "Phase noise in semiconductor lasers," *Journal of Lightwave Technology*, vol. 4, pp. 298-311, 1986.

[22] C.H. Henry, "Theory of the Linewidth of Semiconductor Lasers," *IEEE Journal of Quantum Electronics*, vol. 18, pp259-264, 1982.

[23] D.M Baney, W.V. Sorin, "Measurement of a modulated DFB laser spectrum using gated delayed self-homodyne technique", *Electron. Lett*. vol. 24, pp. 669-670, 1988.

[24] G. Genty, M. Kaivola, and H. Ludvigsen, "Measurement of linewidth variations within external cavity modes of a grating-cavity laser", *Opt. Commun.* Vol. 203, pp. 295-300, 2002.

[25] "Fiber Optic Test and Measurement" (Hewlett-Packard Professional Books (Paperback)) by Dennis Derickson.

[26] R. Lang and K. Kobayashi, "External optical feedback effects on semiconductor injection laser properties," *IEEE J. Quantum Electron.*, vol. 16, pp. 347–355, 1980.

[27] Lenstra, D.; Verbeek, B.; Den Boef, A.; "Coherence collapse in single-mode semiconductor lasers due to optical feedback" *IEEE J. Quantum Electron,* vol. 21, pp. 674 – 679, 1985.

[28] R. W. Tkach and A. R. Chraplyvy, "Regimes of feedback effects in 1.5 μm distributed feedback lasers," *J. Lightwave Technol.*, vol. 4, pp. 1655–1661, 1986.

[29] J. Mørk, B. Tromborg, and J. Mark, "Chaos in semiconductor lasers with optical feedback: Theory and experiment," *IEEE J. Quantum Electron.*, vol. 28, pp. 93–108, 1992.

[30] L.A Coldren and S.W Corzine, "Diode Lasers and Photonic Integrated Circuits", John Wiley and Sons (New York 1991) p246.

[31] Mirasso, C.R.; Colet, P.; Garcia-Fernandez, P.; "Synchronization of chaotic semiconductor lasers: application to encoded communications" *Photonic Tecchnology Letters IEEE*, vol. 8, pp. 299 – 301, 1996.

[32] S. Sivaprakasam, P. S. Spencer, P. Rees, and K. A. Shore, "Regimes of chaotic synchronization in external-cavity laser diodes," *Quantum Electronics, IEEE Journal of*, vol. 38, pp. 1155-1161, 2002.

[33] Sivaprakasam, S.; Shore, K.A.; "Message encoding and decoding using chaotic external-cavity diode lasers", *Quantum Electronics, IEEE Journal of*, vol. 36, pp. 35 – 39, 2000.

Chapter 5

Frequency Stabilization of an External Cavity Diode Laser with a Dual Feedback Locking Loop and Demonstration of a Novel Mode-Referencing Technique

5.1 Introduction

Frequency-stabilized lasers are widely-used sources for many applications ranging from high-resolution spectroscopy, optical network communication, and optical precision metrology. The high spectral resolution achievable with a narrow linewidth, single frequency-stabilized external cavity diode laser (ECDL) makes it an extremely attractive and powerful tool for gas sensing applications. Typically, for gas sensing a reference gas cell is used to lock the emission frequency of the laser to the centre of the gas absorption line thus ensuring high sensing accuracy [1]. In this chapter, a frequency stabilization technique with particular emphasis of the performance of an ECDL frequency locked to a H_2O absorption line at 935.684nm is presented. In addition to the ECDL operating as an injection seed laser, a mode-referencing technique as introduced in section 4.2, is explored as a means to improve the overall frequency locking system. Continuous tuning of the emission frequency of an ECDL is achieved with fine tuning of an external grating position and injection current combination, so that the desired gas absorption line which acts as a frequency reference, can be accurately sampled [2]. A predefined tuning contour path is fixed along the centre of a lasing mode to ensure continuous mode-hop free frequency tuning, optimum side mode suppression ratio (SMSR) and optimum output power. The typical size of a standard ECDL is larger than, for example, a hermetically sealed, butterfly packaged, distributed feedback (DFB) laser.

A consequence of the longer laser cavity that provides the narrow spectral linewidth is the difficulty in achieving rapid temperature stability of the long cavity, which in our case was approximately 2 cm long. The slow thermal response time of this particular laser is a problem when the need arises to switch wavelengths by changing the injection current to the laser by several milliamps in order to target and lock to other adjacent absorption

lines. As a solution to this problem, a dual feedback locking loop to overcome the long stabilization time and improve the overall performance and accuracy of a frequency stabilized ECDL is examined. In addition, a novel mode referencing technique is introduced which in conjunction with the dual feedback locking mechanism, enables the ECDL output to maintain its locked frequency even with a series of induced temperature increases to the laser and is described in more detail in section 5.4. The mode referencing technique was introduced because the recorded tuning contour plane, necessary to enable continuously tuning of the ECDL emission wavelength, does not remain constant. Gradually, the tuning contour plane drifts due to mechanical and thermal instabilities in the ECDL design. If the injection current/PZT voltage combination is fixed to a set-tuning path along the centre of a lasing mode and the tuning contour plane remains constant, then degradation of the laser output does not occur. However, if the tuning contour plane repositions due to aging effects or external influences, then the previously fixed tuning path combination of injection current and PZT voltage no longer operates in the optimum position. This can result in the laser operating in an unpredictable fashion with low SMSR, low output power and can lead to mode hops and ultimately in the loss of continuous wavelength tuning. Consequently, successful frequency stabilization of the device is not possible and will terminate due to mode hopping unless a mode referencing technique is implemented. The mode referencing technique developed during this work which in conjunction with the feedback locking mechanism, enables the device output to maintain its locked frequency. Even, in the presence of environmental and other effects which cause the operational characteristics of the laser to drift, successful frequency stabilization of the laser output is demonstrated.

5.2 Thermal stabilization time of ECDL

Frequency stabilization of the ECDL using a reference gas cell with current induced tuning of the device resulted in a very slow response time. The introduction of the dual feedback control approach for the frequency stabilization of the ECDL resolved the problem of the thermal stabilization time of the device which was particularly detrimental when large changes (>1mA) in the injection current were required. A simple method to quantify this time delay was performed by stepping the output frequency of the ECDL across a water vapour absorption line and measuring the resulting time response. A water

absorption line at 935.684nm was targeted using wavelength modulation spectroscopy (WMS) with the voltage to the PZT modulated at 14kHz. The resulting *1f* harmonic signal of the absorption line was recorded as the injection current to the device was switched [3]. Figure 5.1 shows the *1f* harmonic signal of the absorption line with the arrows indicating the positions on the *1f* trace between which the output frequency of the device was stepped. The procedure involved fixing the PZT voltage of the laser to a set point and then recording the response of the *1f* demodulated signal as the injection current to the device is stepped by an appropriate amount to the correct frequency positions, on either side of the absorption line centre. The injection current was set at 71.6mA for a period of 30 seconds and then was switched to 69.6mA again for 30s for a series of twenty scans with the resulting amplitude of the *1f* absorption signal recorded. From these measurements it is possible to observe the delay in the thermal settling time of the ECDL as clearly indicated in figure 5.2.
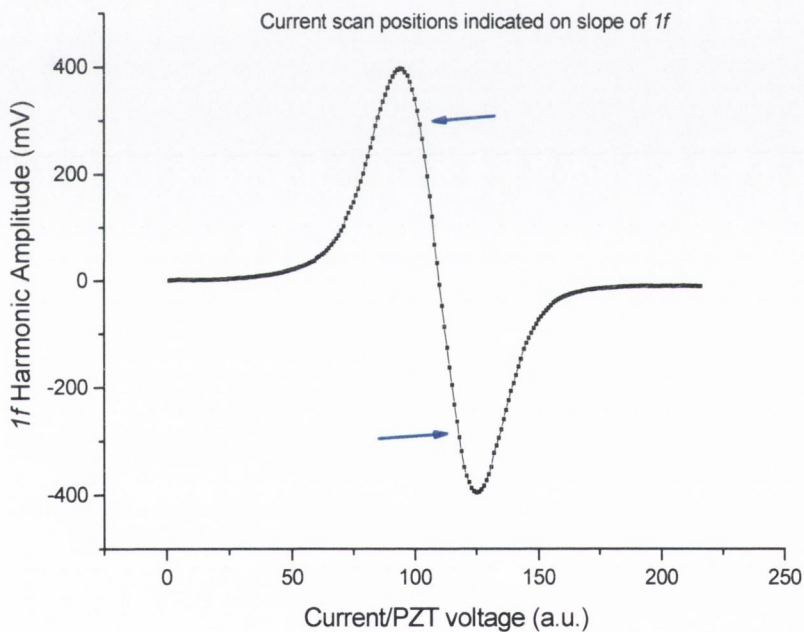
Figure 5.1. *1f demodulated signal of absorption line at 935.684nm with the positions indicated where the injection current to the ECDL was stepped from with the PZT voltage kept constant.*

20 scans were averaged for the *1f* demodulated response where the injection current was increased from 69.5mA to 71.5mA. An exponential profile was fitted to the *1f* signal response as shown in figure 5.3, and the ECDL thermal settling time was calculated to be approximately 1.6s.
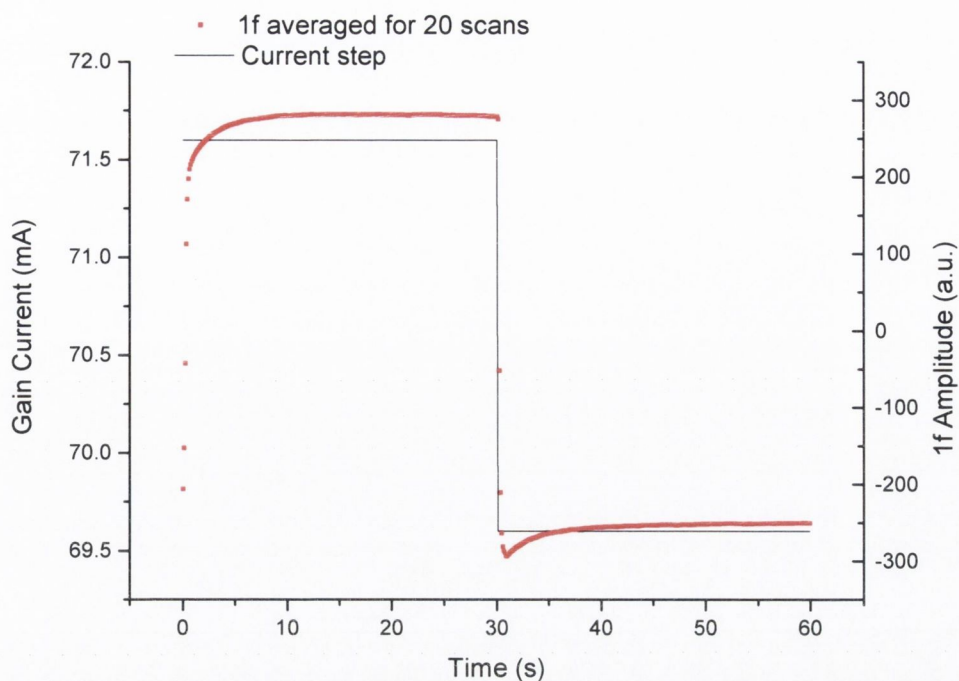
Figure 5.2. *Injection current values for each step and the 1f demodulated signal response averaged for 20 scans across the absorption line at 935.684nm.*

Figure 5.3. *Settling time of ECDL measured to be 1.6s from exponential fit to 1f demodulated response averaged for 20 scans across the H_2O absorption line.*

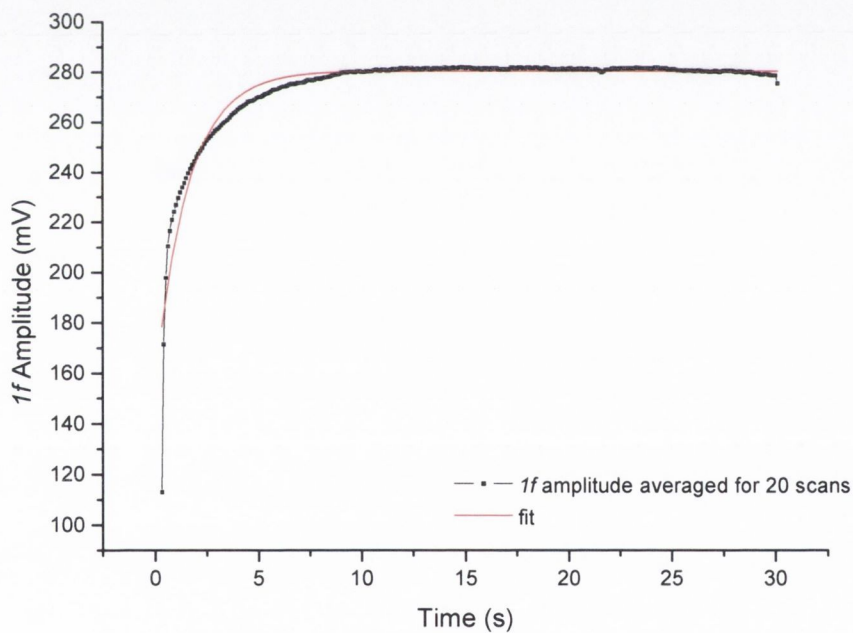Obviously, the long delay in thermal settling time of the device is not encouraging for a semiconductor laser working specifically in the area of gas sensing, telecommunications, or frequency referencing. Other widely tuneable lasers such as a SG-DBR device can also

be used for similar applications and they typically show very fast switching speeds (<1ms) and excellent thermal stability [4]. Even though the ECDL is classed as a widely tuneable device, this lasers ability to tune, rapidly switch and accurately frequency-stabilize to other wavelengths or absorption lines, is therefore seriously undermined. However, the fact that the ECDL has a PZT in place in the laser architecture can be used to an advantage. The limitations associated with the long thermal time constant with large changes in injection current to the laser can be overcome with the dual feedback control approach, as the PZT does not have any thermal interaction.

5.3 Frequency stabilization of an ECDL with a dual feedback loop

5.3.1 Introduction

In general, to lock the output emission frequency of a laser it is necessary to provide some form of reference frequency and a mechanism to tune and fix the laser at that frequency [5]. Many techniques exist and various frequency references have been explored but this work concentrates predominately on the detection and use of water vapour absorption lines in the 935nm region as frequency references. For example, fundamental references based on atomic or molecular absorption lines provide extremely high accuracy and are very stable under changing environmental conditions. In addition devices such as etalons and fibre Bragg gratings can also provide references at arbitrary wavelengths but their performance is degraded by the influence of temperature, pressure and strain and therefore need constant monitoring against a reference frequency [6]. Ultimately, the goal of this frequency stabilization work was to provide an ECDL with a stable frequency output so that the laser could function successfully as an injection seed laser (ISL), as discussed in section 4.1.1. Of course, depending on the wavelength of interest, other absorbing species in the near infra-red are also easily detected including CO_2, CH_4, and H_2S to name but a few [7]. An added advantage of using tuneable diode lasers is the fact that other absorption lines can also be targeted and used for frequency stabilization due to the wide wavelength tuning range of the device. With this Littrow configured ECDL the emission frequency is controlled with a combination of injection current and PZT voltage, and thus enabling a dual feedback approach for the emission frequency of the laser. As with any frequency stabilization procedure the main aim is to

reduce the error between the actual emission frequency of the laser and the reference frequency. Our feedback control can be described as a closed loop system where information regarding the difference between the laser output frequency and the reference frequency is constantly monitored in an effort to reduce the error signal by changing the injection current and PZT voltage to the laser. The feedback loop is implemented by a proportional controller and was designed ultimately to achieve optimum frequency locking accuracy of the output of the laser but also to implement rapid wavelength switching speed [8].

5.3.2 Dual feedback loop

The feedback loop for the control of the ECDL comprises two parts, a slow loop that tunes along the wavelength tuning contour with combination of injection current and grating adjustment, and a second faster loop that drives the grating only. Since the fast loop drives only the grating piezo actuator, and not the laser current, there is no thermal interaction present so that the fast loop can operate at shorter timescales (ms) in comparison to the slow loop. To demonstrate this scheme both parts of the feedback system were implemented as simple filtered proportional controllers, low pass for the slow branch and bandpass for the fast branch. For the slow branch, the low-pass filter cut-off and the proportional gain term are chosen to avoid any oscillatory behaviour in the laser output frequency and to obtain critically damped behaviour in the response to a step in laser current [8]. The high frequency side of the bandpass response of the fast branch was similarly determined while the low frequency side (within the slow loop response) ensures that the low frequency components are handled by the slow loop along the tuning contour. In order to gain a better understanding of the thermal stabilization time of the ECDL, which was critical for the slow loop operation, the tuning properties of the device were simulated and the slow loop performance was modelled under various conditions. The objective of the model was to try and obtain the optimum setting for the proportional gain term for the slow loop so that any oscillatory behaviour in the ECDL emission output could be successfully avoided while at the same time optimising the speed of the feedback control. The method to carry out this test involved stepping the emission wavelength output of the ECDL between two points around 935nm and then measuring the corresponding settling time and steady state error. This gave an indication

of how fast the feedback locking system was and how close the actual output frequency of the laser was to the reference frequency. Figure 5.4 shows a trace of the simulated results of a Labview program where the output wavelength of the ECDL is stepped between 935.63nm and 935.71nm with the corresponding current and PZT voltage values also clearly indicated. In the simulation a deliberate attempt was made to demonstrate the clearly visible oscillatory behaviour present in the ECDL output due to the proportional gain term being too large. Ideally, the optimum gain term determines the fastest response and accuracy of the feedback locking system without any oscillations in the output frequency.
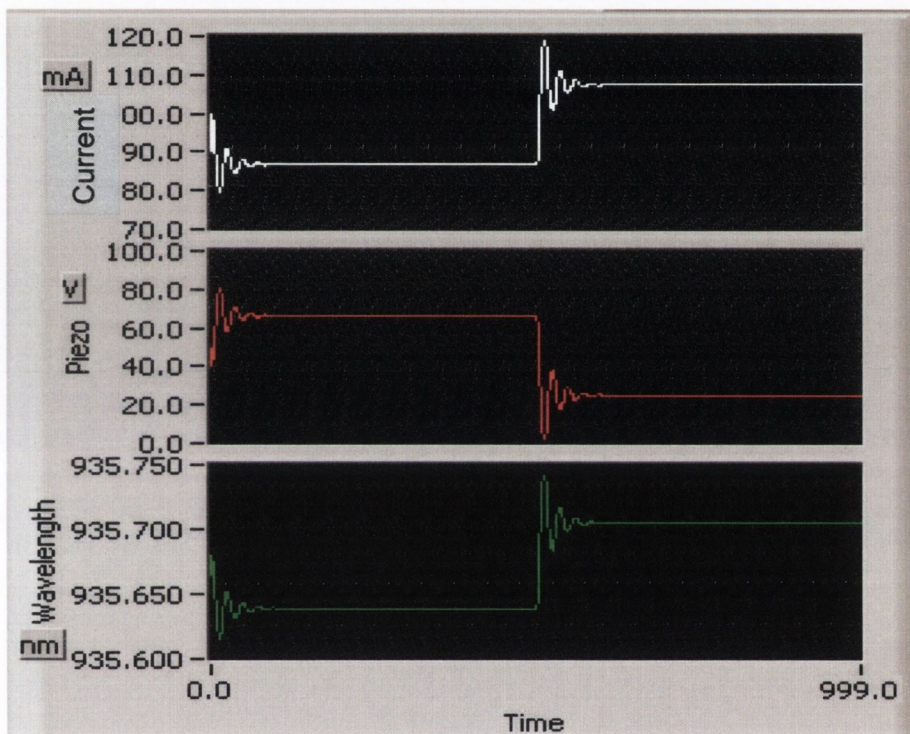
Figure 5.4. *Simulated data for the ECDL output wavelength stepped between 935.63nm and 935.71nm with the current, PZT voltage and wavelength also clearly indicated.*

5.3.3 Experimental

H_2O rotational absorption lines present in the 935 nm region of the spectrum were targeted to act as a frequency reference for the ECDL. WMS is used to lock the ECDL frequency to a H_2O absorption line that has a centre wavelength, of 935.684nm in vacuum and a linestrength of 6.45×10^{-22} (cm/molecule) [9]. Laser stabilization is based on comparing the emission frequency of the laser with that of a reference frequency, and then generating some

error signal that has a zero value at the desired locking frequency [10]. The configuration for the frequency stabilization of the ECDL along with the dual feedback loop scheme and the mode referencing step, which is described later, is shown in figure 5.5. Figure 5.6 shows the *1f* demodulated signal of the H_2O absorption line with its zero crossing point at the line centre, which is used to frequency lock the ECDL. As previously discussed, the ECDL emission wavelength at room temperature is single mode and the spectral linewidth of the device was measured to be < 300 kHz. The ECDL shows SMSR > 40dB, a maximum output power > 60 mW and approximately 0.45 nm continuous mode-hop free wavelength tuning over the full range of the injection current and PZT voltage [11].
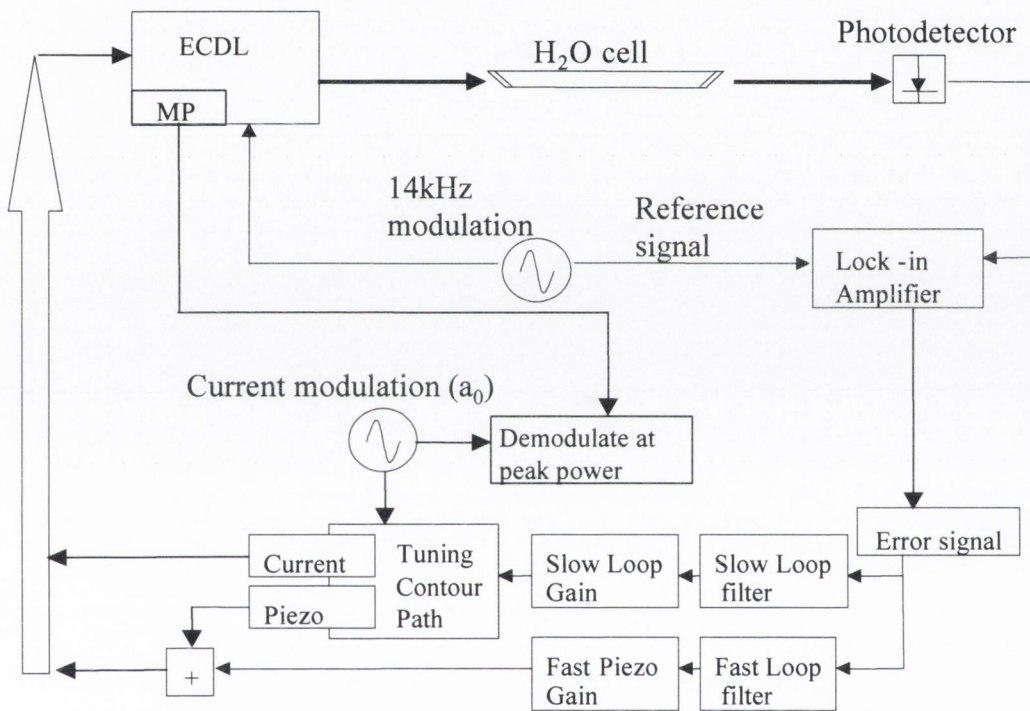
Figure 5.5. *Experimental set-up used for the frequency stabilization of the ECDL with the dual feedback locking loop and mode referencing steps illustrated. The modulation of the current term of the tuning contour path, along with the internal monitor photodiode (MP) of the ECDL are also included.*

The reference signal was obtained by passing the laser output through a 1 metre-long cell containing water vapour at a pressure of approximately 25 mbar, and detecting the resulting absorption signal with a photodetector. A WMS scheme was implemented with the PZT modulated at approximately 14 kHz and a lock-in amplifier (Signal Recovery, Model 7265) was used to process the detected signals [12]. Modulating the grating is preferred, as it will help reduce any amplitude-modulated component that is generally

present with injection current modulation, so it is acceptable to demodulate at the *1f* rather than the *3f* harmonic. To decrease the operational frequency drift of the laser, the temperature of the laser was kept constant at 20^0C and the signal from the photodiode, processed by the lock-in amplifier is then fed back to the PZT to correct any deviation in the output frequency of the laser form the reference. This operation formed the fast loop of the dual locking procedure.
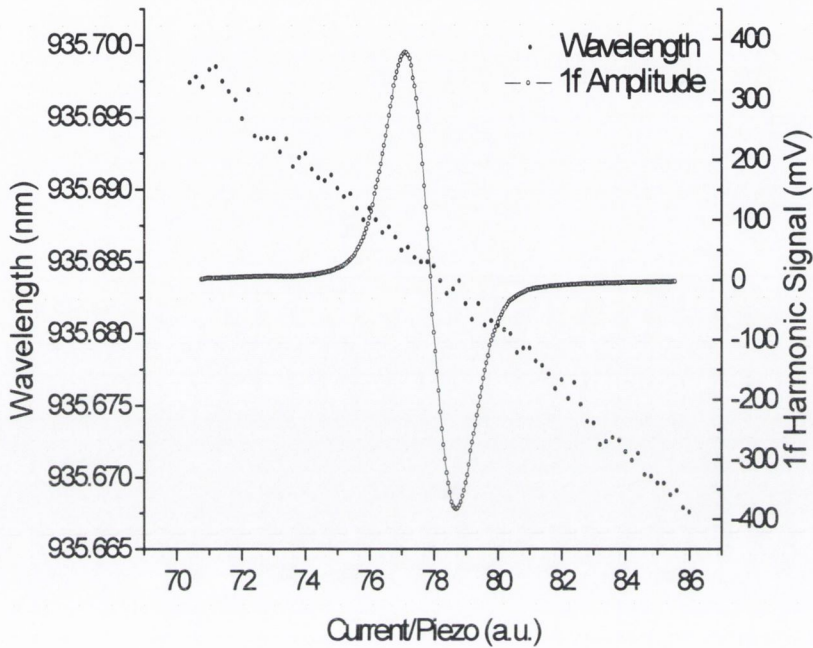
Figure 5.6. *Continuous wavelength tuning of the ECDL and the 1f harmonic signal of the absorption line at 935.684nm with the zero crossing at line centre, which is used to frequency lock the laser.*

To examine the dual feedback system in detail the frequency locking operation of each component of the dual loop was evaluated separately. The slow loop performance was demonstrated by locking the ECDL emission frequency for an extended period (hours). Figure 5.7 shows frequency locking of the laser output for approximately 11 hours. The accuracy of the locking, about the H_2O absorption line has a rms value measured to be 19.61MHz for the duration of the test. The response time of the slow feedback loop was also characterised.
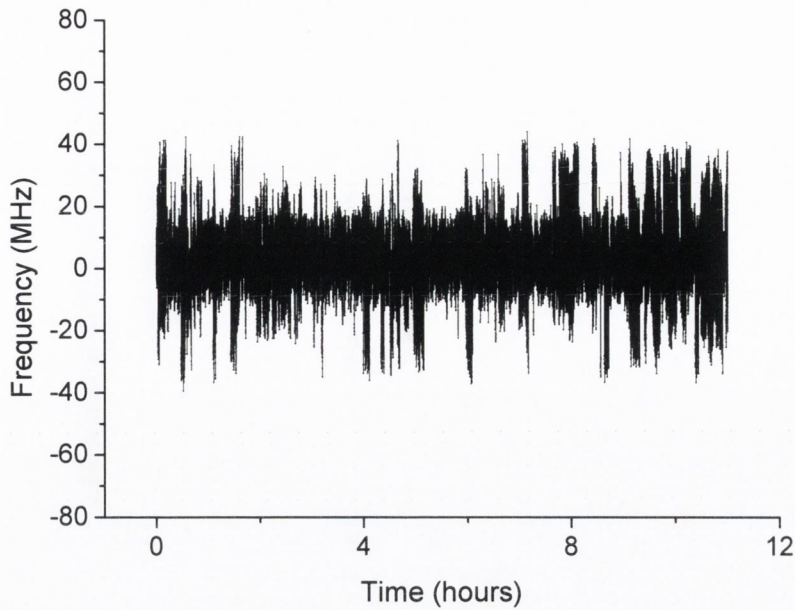
Figure 5.7. *Long term frequency stabilization of ECDL using the slow feedback loop. The 1f error signal was recorded for approximately 11 hours.*

This was achieved by firstly locking the emission frequency of the laser to a point on the slope of the *1f* demodulated signal and then stepping the feedback loop set point to the H_2O line centre and measuring the resulting settling time. The measurement was recorded with a digital oscilloscope and the slow loop response time calculated to be approximately 1s, as shown in figure 5.8.
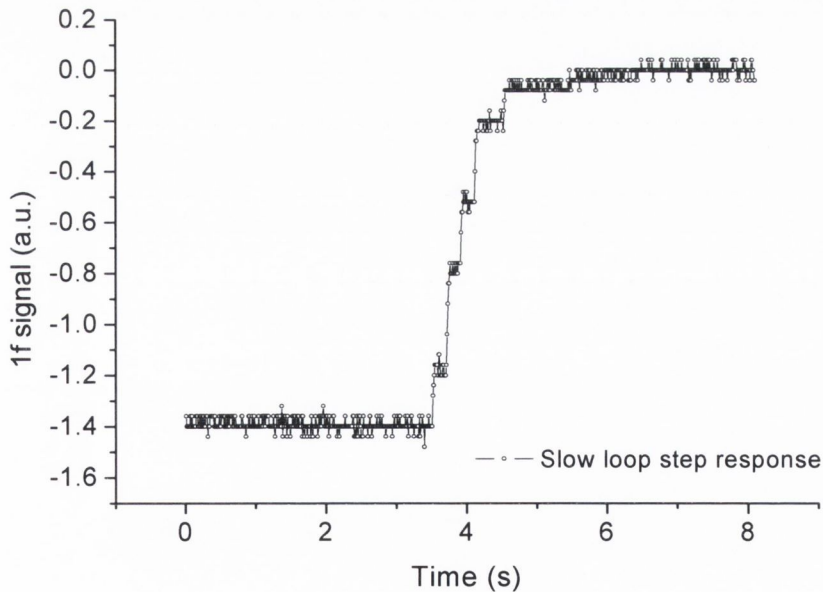
Figure 5.8. *Slow loop step response measurement determined to be 1.0s.*

The measurement was repeated for the fast loop with the emission frequency of the ECDL being switched over the same frequency range as the slow loop, the results of

106

which are shown in figure 5.9. The response time of the fast loop was measured to be less than 0.1s.
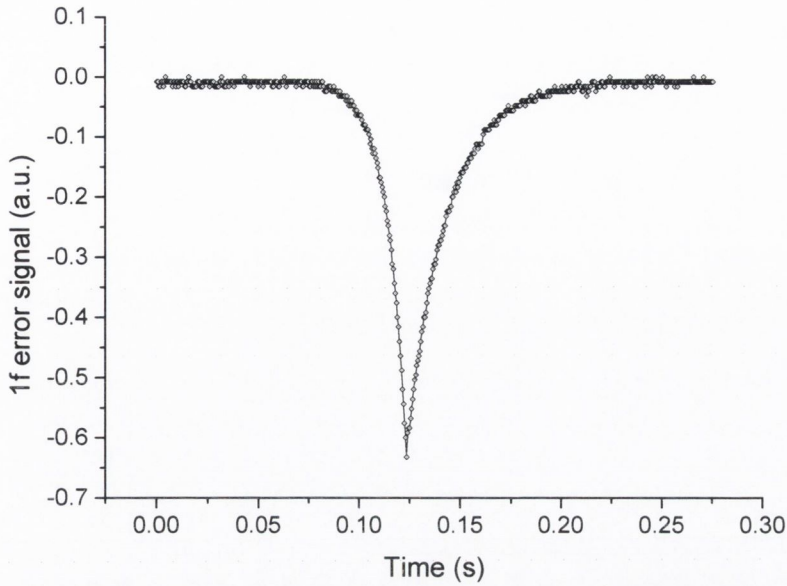
Figure 5.9. *Measured response time of the fast piezo loop as the frequency is stepped across the 1f slope.*

The accuracy of the dual loop was also tested by frequency locking the ECDL output for 4 minutes. A comparison of the two traces in figure 5.10 show the marked improvement in accuracy of the frequency locking system of the ECDL using the dual loop (Fig. 5.10a) in comparison to the slow loop alone (Fig. 5.10b). The accuracy of the ECDL emission frequency in this case is measured with a rms value of 1.69MHz.
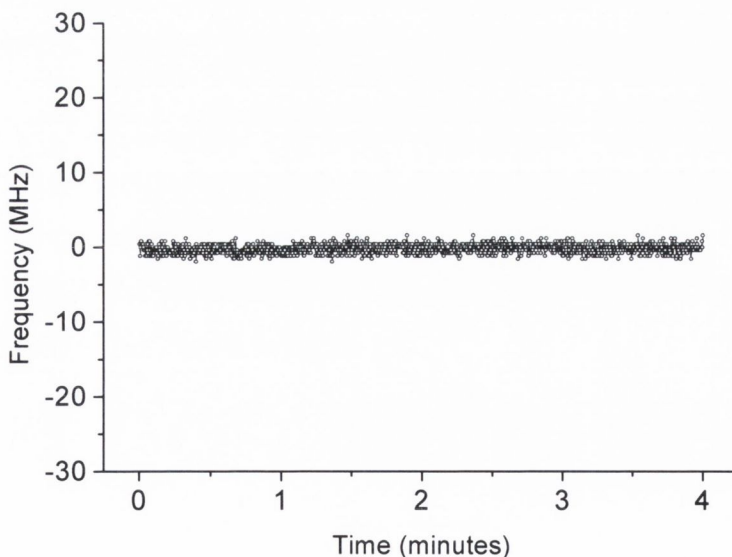
Figure 5.10a. *Measured frequency accuracy of dual feedback locking of ECDL with the frequency stabilized with rms value of to 1.69MHz.*

The noise on the locking frequency of the ECDL is also reduced by the increased bandwidth available with the dual feedback loop. Consequently, switching the ECDL output frequency to target other gas lines if required can be achieved rapidly and with greater overall accuracy.
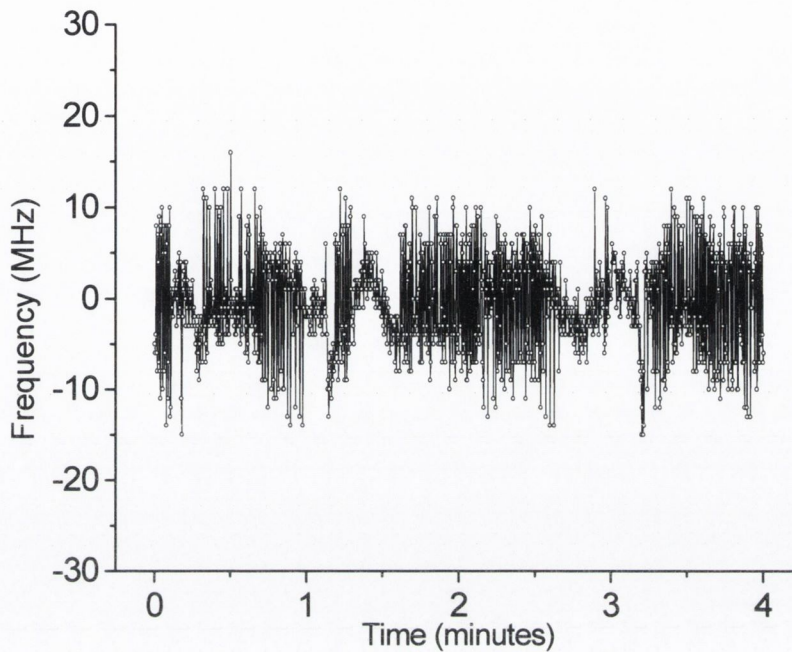
Figure 5.10b. *Measured frequency accuracy of ECDL emission with slow loop operation only.*

Frequency stabilization of external cavity diode lasers typically results in extremely stable and accurate values due to the improved resolution available with the narrow spectral linewidth of the laser. The value 1.69MHz frequency accuracy achieved by the Littrow configured ECDL in our experimental set-up compares well to other studies of suitable injection seed lasers for space-borne spectroscopic missions [13]. By comparison, an ECDL in the Littmann-Metcalf arrangement and operating at 852nm, tuned to the D_2 line of cesium atoms, frequency fluctuation of less than 0.8MHz using the third derivative signal have also been achieved [1]. In addition, absolute frequency stability better than 200kHz was achieved with an ECDL locked to an acetylene (C_2H_2) absorption line at 1.5μm [14].

5.4 Mode referencing

5.4.1 Introduction

The ability to stabilize the emission output of a diode laser to a reference frequency is of great importance for many applications ranging from optical telecommunications, injection locking of high power lasers, and spectroscopic based studies [15-17]. However, depending on the type of device involved, control of the frequency stabilizing mechanism may have varying degrees of complexity. For example, some widely tuneable sources with multi-section architecture, such as sampled-grating distributed Bragg reflector (SG-DBR) laser, require several current sources to drive the device and very precise manipulation of these is required to control and stabilize the output emission wavelength. [18]. This situation is similar to that pertaining to an external cavity diode laser where the emission wavelength is controlled by both injection current to the laser and a voltage to a piezo electric transducer (PZT) which controls the position of the external grating [19].

ECDL's have long been a source of great interest due to their wide wavelength tuning capability, high output power and of course the narrow linewidth available with an external cavity architecture [20,21]. In order to operate the ECDL such that the wavelength is tuned in a continuous, mode-hop free manner, which is essential for successful frequency stabilization, a tuning contour plane as is shown in figure 5.11 is first recorded. When the emission mode profile of the ECDL is obtained it is simply a matter of choosing the correct values of injection current and PZT voltage in a combination such that, when varied simultaneously, the laser wavelength tunes in a continuous linear fashion as indicated by the dashed arrow in figure 5.11. In general, for most widely tuneable laser diodes a similar situation occurs in that a mode profile of the output emission is first obtained so that correct operating currents can be chosen for continuous wavelength tuning of the device. Of course it is assumed that the mode profile initially recorded remains constant with time so that the device can operate in a continuous wavelength tuning mode, without fail. Unfortunately, this is not the case for some widely tuneable laser diodes [22-24] and for the ECDL used in this work, a shift in the tuning contour plane was observed over time caused by thermal or mechanical instabilities in the complex design of the laser [25].
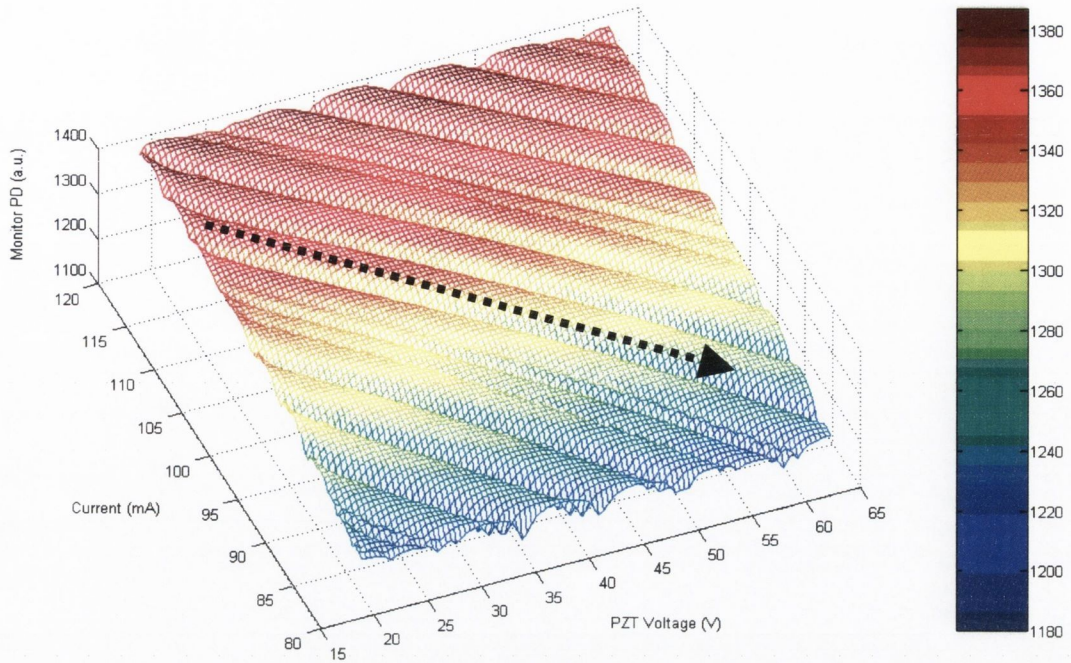
Figure 5.11. *Tuning contour plane of output power of ECDL recorded with the internal monitor photodiode, as a function of current and PZT voltage at a constant temperature of 20^0C with continuous wavelength tuning path clearly indicated with the dashed arrow.*

Obviously, this has a deleterious knock-on effect if the device is used in a frequency stabilization scheme, where a loss in continuous wavelength tuning ultimately leads to a complete failure in the frequency stabilization of the laser output. To counteract this problem, a mode referencing technique was implemented into the frequency stabilization scheme. Referencing (adjustment of operation parameters) of the ECDL while maintaining frequency lock ensures that the constant frequency emission remains on a characteristic line in the power plane equidistant from adjacent mode boundaries. A similar technique has been implemented for continual frequency control of a superstructure-grating DBR laser even with the onset of degradation in reflection properties of the DBRs due to long term aging or external effects [26]. With the mode-referencing step, it was possible to achieve in-situ monitoring of the position of the current/PZT voltage combination tuning path and compensate for any drift in the mode profile by locking the wavelength tuning path to the centre of the desired lasing mode. We demonstrate experimentally that it is possible to maintain frequency stabilization of an ECDL output to a H_2O absorption line with the inclusion of the mode referencing technique in the frequency locking system, while applying a series of induced temperature steps to the device heatsink.

110

5.4.2 Experimental

As previously discussed, the need for a mode referencing step to control the emission frequency of the stabilized ECDL source emerged as a direct result of problems faced due to thermal and mechanical instability of the device and a consequential change in the contour mode plane. The contour mode plane determines the values for the injection current/PZT voltage combination which provide the tuning path for continuous mode-hop free wavelength tuning. Initially, the mode referencing of the ECDL was accomplished by turning off the frequency locking procedure, fixing the PZT voltage, and then tuning the laser output with injection current only, across the lasing mode. The range of the current tuning was set large enough so that the mode boundaries on either side of the lasing mode were crossed. Then by differentiating the resulting power change across the mode boundaries, recorded with the internal monitor photodiode of the device, the centre of the lasing mode was acquired. The tuning path of the current/PZT voltage was then realigned onto the centre of the lasing mode, and the frequency locking subsequently switched back on. Obviously this worked well to reference the position of the lasing mode but the major disadvantage in this method is a loss in frequency stabilization of the ECDL output during the period the locking was switched off. In essence, with this method, the frequency locking has to be periodically turned off to determine if there is any drift in operational characteristics that need to be corrected to ensure continuation of the frequency locking. Our technique performs similarly, except that the wavelength remains constantly locked to the desired set point throughout the mode referencing and the frequency stabilization scheme remains in constant operation also. The main function of the mode referencing procedure is to align the wavelength tuning path to the centre of the lasing mode of interest so as to avoid any mode hops or reduced SMSR near the mode boundary positions. In our case this is achieved by firstly locking the ECDL output to the absorption line of interest and then as the frequency stabilization is in operation, a small modulation is applied to the current of the wavelength tuning path. The tuning contour path is determined by a 2nd order polynomial fit, which selects the best fit of values of injection current/PZT voltage combination so that a well defined wavelength tuning contour path is achieved. The modulation of the current is indicated in figure 5.12 and is in the perpendicular direction to the dotted line, which indicates the injection current/PZT voltage combination that determines the wavelength tuning path.
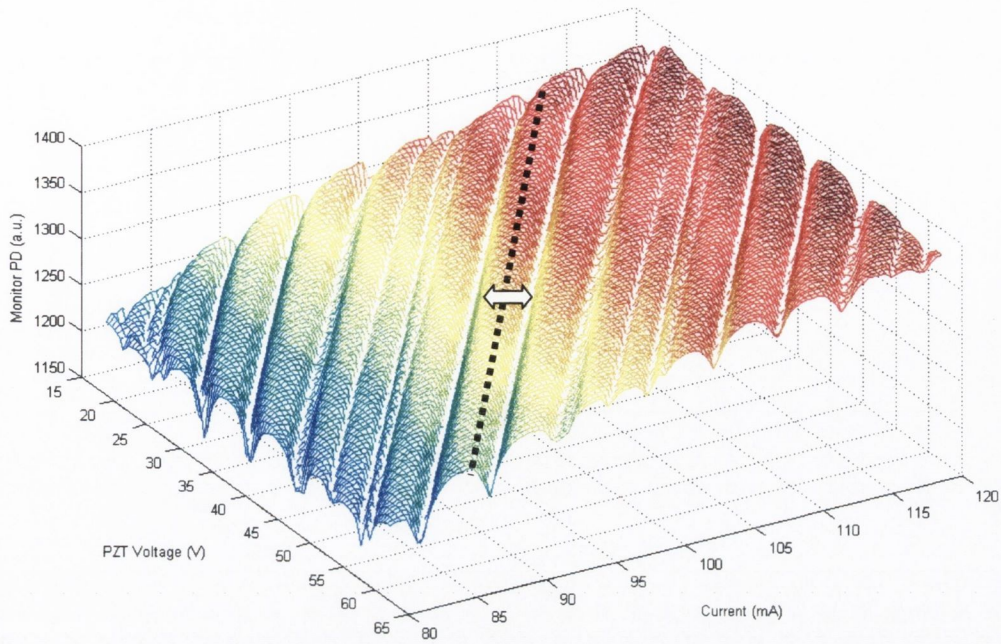
Figure 5.12 *Mode profile of ECDL emission measured with the internal monitor photodiode at 24^0C from 80mA to 120mA and 18V to 62V as the current and PZT voltage are scanned.*

The arrow in figure 5.12 represents the modulation of the a_0 term which is in the perpendicular direction to the wavelength tuning path. A detailed scan of the variation in output power of the ECDL, measured with the internal monitor photodiode across the mode, is shown in figure 5.13. With this change in power, it was possible to set the amplitude of the modulation on the a_0 term large enough so that a value for peak power, corresponding to the centre of the lasing mode, was measurable. Then it was simply a matter of setting up another feedback loop so that the wavelength tuning path could be locked to the peak power of the lasing mode and hence, locked to the centre of the lasing mode. As the modulation on the a_0 term of the polynomial is perpendicular to the direction of continuous wavelength tuning, the locking frequency is maintained at the desired wavelength.
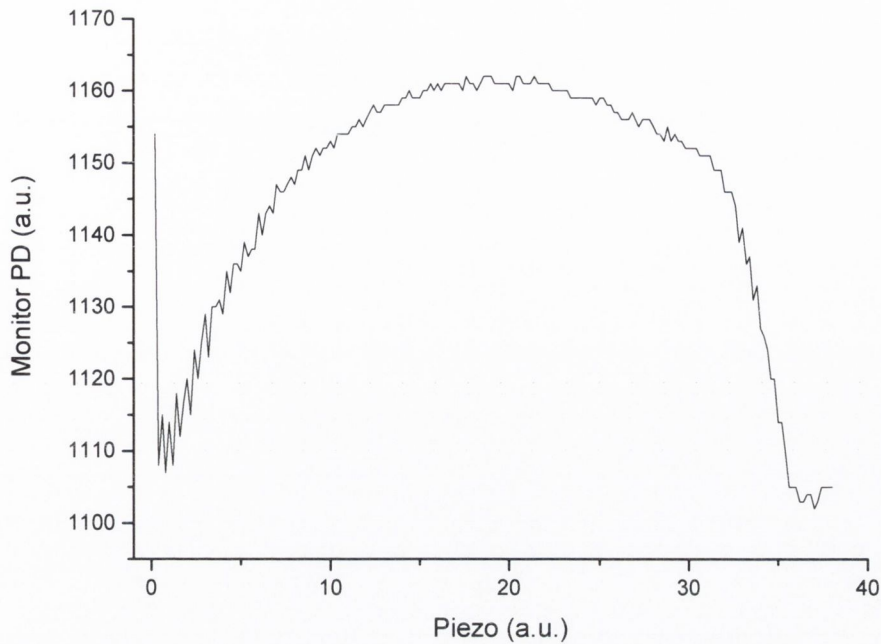
Figure 5.13. *Recorded monitor photodiode showing the variation of the output power across a particular lasing mode. The current is kept constant and the PZT voltage is varied at a constant temperature of 24^0C.*

The experimental set-up for the mode referencing is similar to that of the dual feedback locking loop operation except for the addition of another feedback locking loop element where the output power of the ECDL is recorded with the internal monitor photodiode as shown in figure 5.5. The basis upon which the emission wavelength of the ECDL can be maintained at the same value throughout the mode referencing operation is explained clearly with reference to figure 5.14. The graph shows the recorded photodiode power of the detected laser radiation, as a function of injection current and PZT voltage over a certain range, after passing through a 1 meter gas cell containing water vapour at 25mbar. From the trace, the positions of various water absorption lines are easily observable and it is noted that the absorption is constant across the different modes. This implies that the wavelength, in the perpendicular direction to the wavelength tuning path, is constant so that the ECDL output can remain frequency stabilized to the desired wavelength (in our case, H_2O line at 935.684nm) throughout the mode referencing operation.

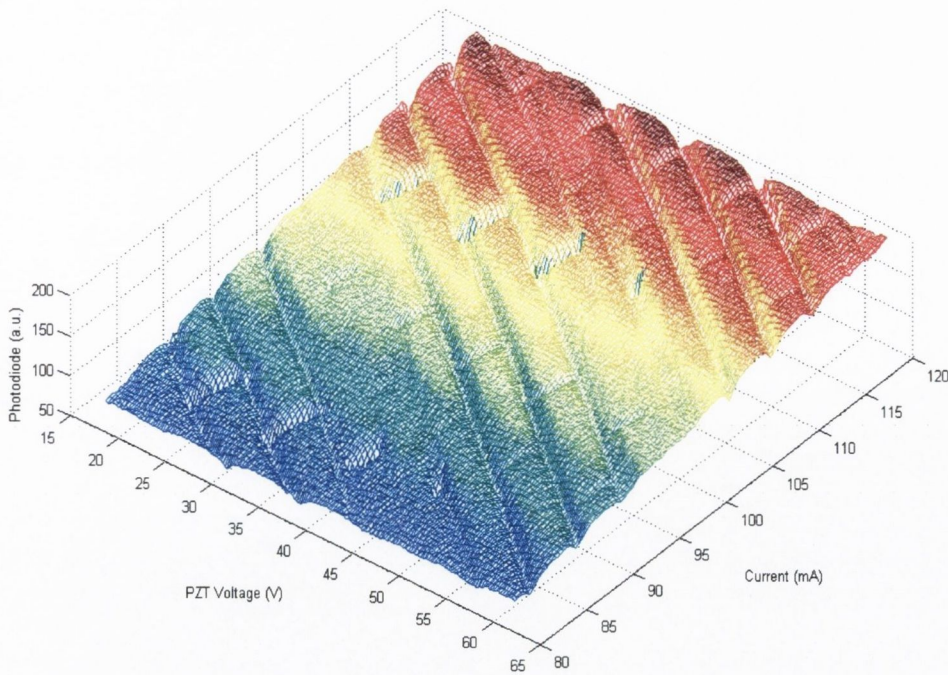Figure 5.14. *Mode profile of ECDL emission measured with the detection through water vapor cell at 24^0C from 80mA to 120mA and 18V to 62V as the current and PZT voltage are scanned. The points on the mode plane where water absorption lines are located are also clearly visible from the reduction in transmitted signal onto the photodiode.*

In order to demonstrate the performance of the mode referencing step a series of deliberate temperature changes to the ECDL heatsink were executed while the laser output was frequency stabilized. Figure 5.15 shows the output frequency of the ECDL while the device is frequency stabilized using the dual feedback loop and with the mode referencing switched on. For this measurement the heatsink temperature is varied from 23^0C to 24^0C in steps of 0.1^0C by simply adjusting the temperature controller (ILX Lightwave Model LDT 320). In terms of the emission wavelength of the ECDL, a 1^0C temperature change corresponds to a change of approximately 0.03nm in emission wavelength of the laser or in terms of frequency, 10.3GHz. In comparison to absorption line profiles of low pressure gases which usually have FWHM values of hundreds of MHz, the change in temperature of the ECDL by 1^0C is sufficient enough to shift the emission wavelength of the device well away from the absorption line-centre. It is clear that the output frequency of the stabilized ECDL does not vary by more that 5MHz for the duration of the test of 30 minutes. From the trace it is evident that the initial starting point corresponds to locking the absorption line centre and then a 0.1^0C change in temperature occurs. The frequency offset of the laser then increases but with the dual locking and referencing in operation the frequency error is again reduced until another temperature increase. The change in temperature to the heatsink of the device essentially

causes the contour mode profile to change and this requires a change in the operating points of the current and PZT voltage if frequency locking to the desired frequency is to be maintained. The mode referencing tracks the change in mode profile position with temperature and then with the dual feedback locking loop, the necessary changes to the injection current and PZT voltage are made.
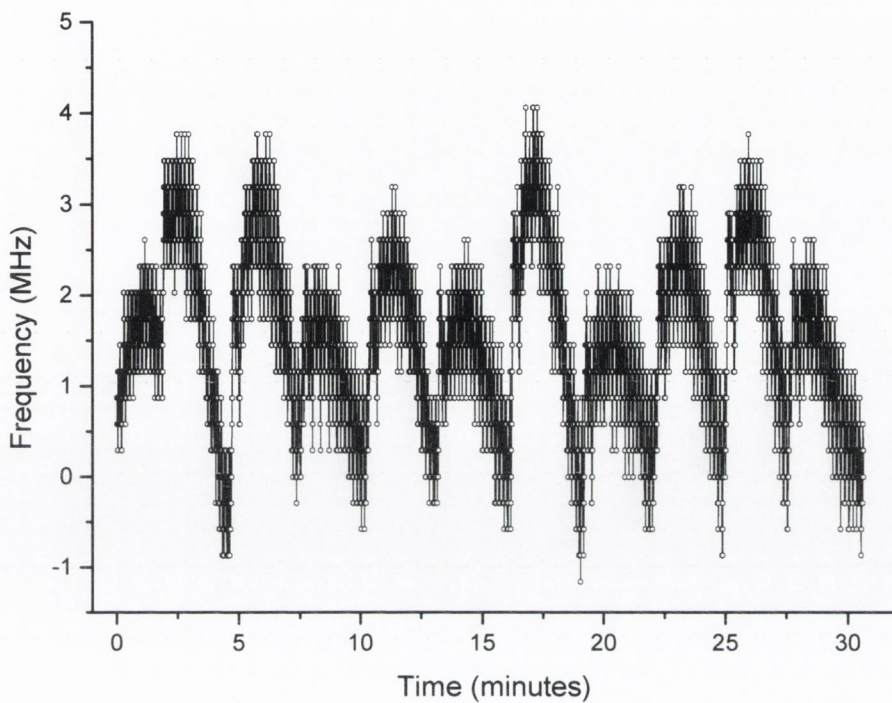
Figure 5.15. *Measured frequency drift of the ECDL output as the temperature is changed from 23^0C to 24^0C, in steps of 0.1^0C over a 30 minute period with the mode referencing technique enabled.*

Figure 5.16 shows the variation in the injection current and PZT voltage for the duration of the test as the temperature is changed in increments of 0.1^0C for a total of 1^0C. The increase in temperature from 23^0C to 24^0C results in a compensating increase in PZT voltage from 28.4V to 35V and a decrease in injection current from 110.5mA to 107.3mA. Figure 5.16 also shows the constant variation of the injection current resulting from the small modulation on the a_0 term of the 2nd order polynomial fit and hence, the wavelength tuning path. Finally, the trace in figure 5.17 shows the output power of the ECDL, recorded with the internal monitor photodiode, as the temperature changes are made. An overall reduction in output power occurs as the mode referencing causes a change to both the current and PZT voltage while constantly maintaining frequency stabilization to the desired wavelength of 935.684nm.

Figure 5.16. *Injection current and PZT voltage variation as the mode referencing step is in operation for the induced changes in the heatsink temperature of the ECDL.*

Figure 5.17. *Internal monitor photodiode of ECDL showing a reduction in output power as the frequency locking and the mode referencing track the induced temperature changes.*
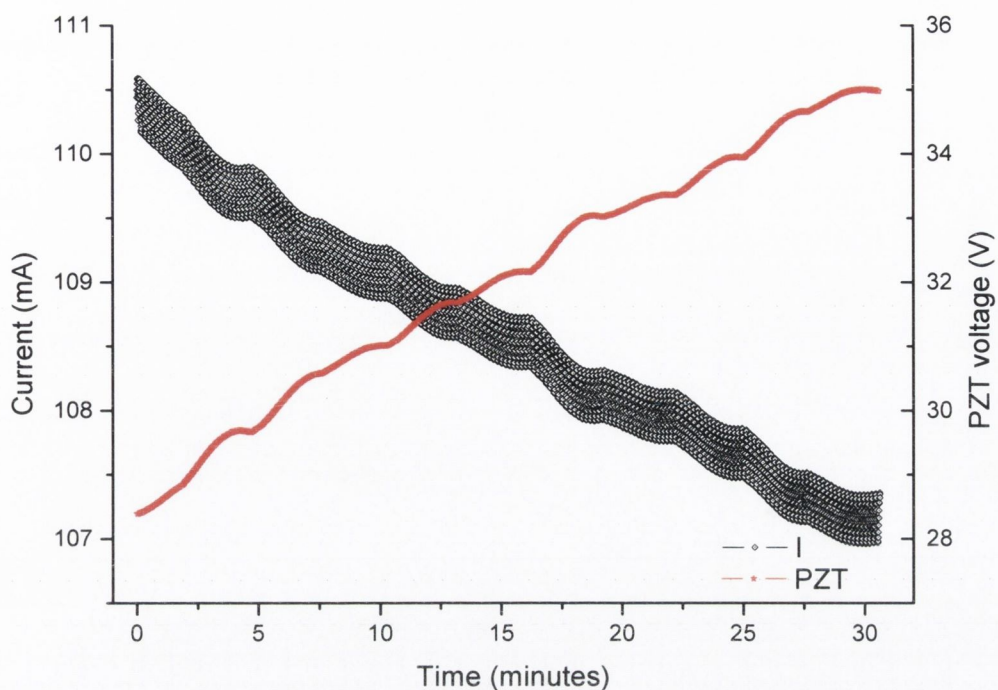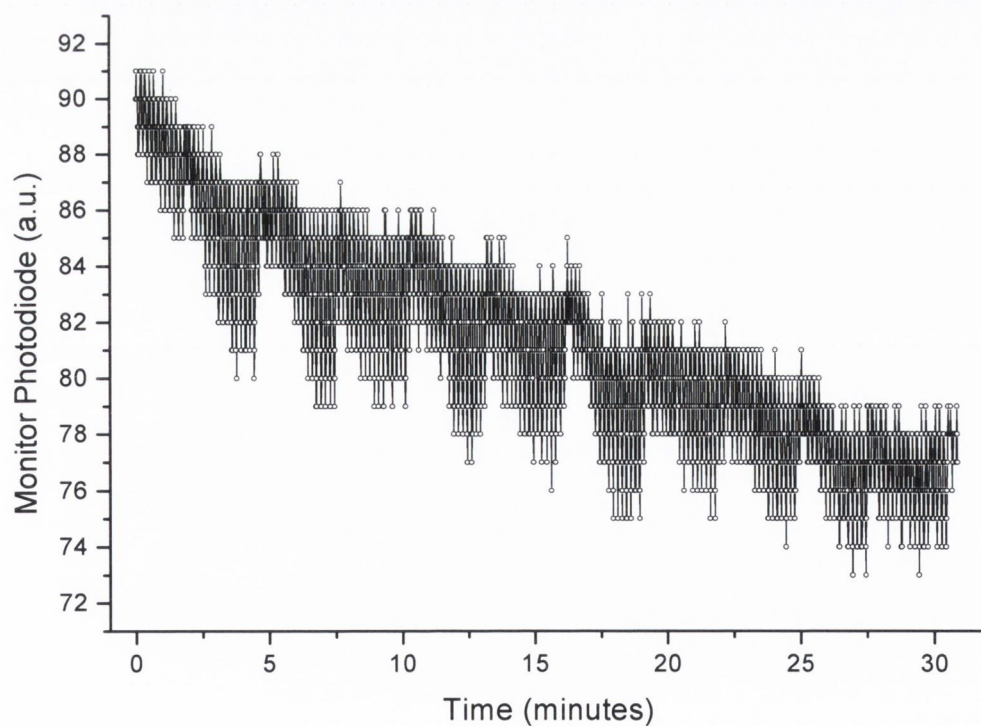
To understand the capability of the mode-referencing step in operation, the initial and final Current/PZT voltage values after the 1^0C temperature change are indicated on the contour mode map in figure 5.18, along with several water absorption lines. With the 1^0C change in the laser heatink temperature, it is clear to see that without the mode-referencing step in place, the ECDL would be lasing at a different wavelength and a totally different lasing mode, and hence the frequency stabilization of the device would fail.
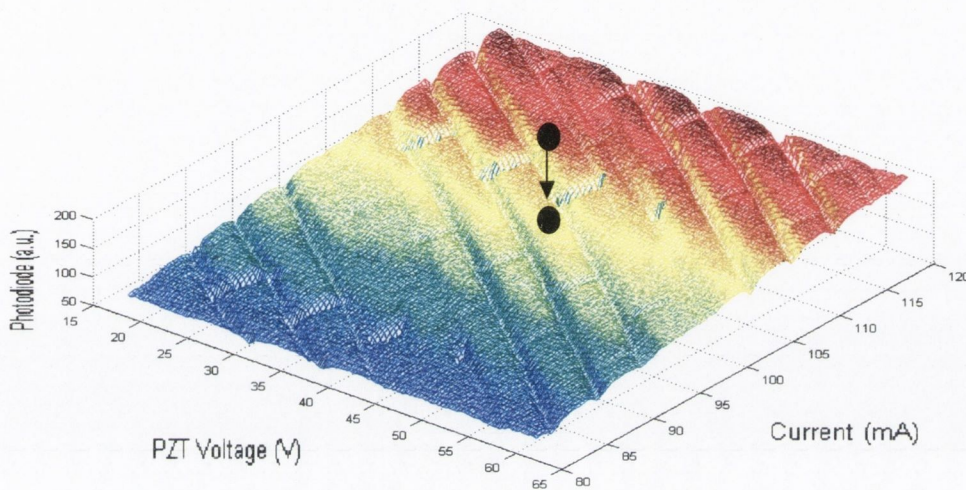
Figure 5.18. *Mode profile of ECDL emission with the initial and final Current/PZT voltage values before and after the 1^0C change in heatsink temperature.*

5.5 Conclusions

The frequency control of an ECDL locked to a H_2O absorption line at 935.684nm has been greatly enhanced with the introduction of a dual feedback locking loop. An improvement in the spectral performance of the device, with regard to frequency stability and wavelength switching speeds has been demonstrated. With the slow feedback loop it is possible to reduce any large drift of the laser frequency over large timescales (hours). The performance of the slow loop was tested by frequency locking the ECDL for 11 hours without any failure of the system with a rms value measured to be 19.61MHz. The combined dual feedback loop shows frequency accuracy with a rms value of 1.69MHz while the response time of the dual locking, is a factor of ten less than the slow loop, at approximately 0.1s. However it is noted that the result of the switching speeds is

admittedly slow in comparison to other laser devices but of secondary importance to the actual frequency locking accuracy of the laser output. For the purpose of providing a frequency stabilized injection seed laser for H_2O sensing at 935nm, the locking accuracy of 1.69MHz more than suffices for the space-based project. By comparison, for certain applications where switching the wavelength quickly is paramount, excellent switching speeds with values of 2-2000nm/s are specified for the New Focus, Venturi tuneable laser emitting at a wavelength of 1550nm, (Model TLB-6600), for example.

The use of a novel mode referencing technique has been introduced, and is clearly shown to aid in the frequency stabilization of the output of an ECDL in conjunction with a dual feedback locking loop. The addition of the mode referencing step has greatly improved the operation and reliability of the frequency stabilization system that controls the frequency output of the laser. Its performance was tested by frequency locking the ECDL and inducing a series of deliberate temperature steps from 23^0C to 24^0C in increments of 0.1^0C, to the device heatsink without any failure of the locking system. The laser output frequency was maintained to within 5MHz of the H_2O absorption line at 935.684nm for the 30 minute duration of the test and the output SMSR can be deemed $\geq$ 40dB, similar to the recorded values shown in figure 4.11, in chapter 4. In comparison, Sarlet *et al.* in [27], observed frequency deviation within $\pm$ 1 GHz for the mode stabilization of a SSG-DBR laser by varying the laser temperature submount by 10^0C. The FWHM of a typical Doppler broadened absorption line is typically several hundred MHz wide so an error of 5MHz in the frequency locking accuracy of the ECDL is sufficient for the determination of gas concentration analysis or maintaining an accurate frequency stabilized laser source. Therefore, with the addition of this mode referencing technique to the frequency locking set-up it is possible to operate the ECDL without having to repeat measurements of the mode contour profile, and thus maintain frequency stabilization. The essence of the technique is that it allows the frequency locking to continue uninterrupted which is critical for long term space-based missions. This contrasts with other schemes where the frequency locking has to be periodically turned off to determine if there is any drift in operational characteristics that need to be corrected to ensure continuation of the frequency locking. This technique has the potential to be applied to other tuneable laser diodes so that time consuming and tedious task of repeating the device operating characterization can be avoided.

5.6 References

[1] Y. T. Zhao, J. M. Zhao, T. Huang, L. T. Xiao and S.T. Jia "Frequency stabilization of an external cavity diode laser with a thin Cs vapour cell", *J. Phys. D: Appl. Phys.* vol. 37, pp. 1316-1318, 2004.

[2] M.W. Fleming and A. Mooradian, "Spectral characteristics of external-cavity controlled semiconductor lasers," *IEEE J. Quantum Electron.*, vol. 17, pp. 44-59, 1981.

[3] Schilt S, Thevenaz L, Robert P "Wavelength modulation spectroscopy: combined frequency and intensity laser modulation", *Applied Opt.*; vol. 42, pp. 6728-6738, 2003.

[4] M. Ogusu, K. Ide, and S. Ohshima, "Fast and precise wavelength switching of an SG-DBR laser for 1.07-b/s/Hz DVMM systems," *Optical Fiber Communication Conference, Technical Digest*. OFC/NFOEC, Vol. 2 March 2005.

[5] Shan Huang; Huafeng Zhao; Lin Xue; "Frequency stabilization of FBG external cavity laser diode," *Circuits and Systems,. APCCAS '02. Asia-Pacific Conference on*, vol. 1, pp. 565 – 567, 2002.

[6] Sarah L. Gilbert, Shelley M. Etzel, and William C. Swann, "Wavelength accuracy in WDM: Techniques and standards for component characterization " *Optical Fiber Communication Conference (OFC 2002),* invited paper, pp. 391-393, 2002.

[7] Sakai, Y.; Yokohama, I.; Kominato, T.; Sudo, S.; "Frequency stabilization of laser diode using a frequency-locked ring resonator to acetylene gas absorption lines", *Photonics Technology Letters, IEEE*, vol. 3, pp. 868 – 870, 1991.

[8] J. R. Leigh, *Control Theory 2nd edition*, chap. 3, Institution of Electrical Engineers (2004).

[9] L.S. Rothmana, D. Jacquemarta, A. Barbeb, D. Chris Bennerc, M. Birkd, L.R. Browne, M.R. Carleerf, C. Chackerian Jr.g, K. Chancea, L.H. Couderth, V. Danai, V.M. Devic, J.-M. Flaudh, R.R. Gamachej, A. Goldmank, J.-M. Hartmannh, K.W. Jucksl, A.G. Makim, J.-Y. Mandini, S.T. Massien, J. Orphalh, A. Perrinh, C.P. Rinslando, M.A.H. Smitho, J. Tennysonp, R.N. Tolchenovp, R.A. Tothe, J. Vander Auweraf, P. Varanasiq, and G. Wagner, " The HITRAN 2004 molecular spectroscopic database," *Journal of Quantitative Spectroscopy & Radiative Transfer,* vol. 96, pp. 139–204, 2005.

[10] T. Sato, M. Niikuni, S. Sato, and M Shimba, "Frequency stabilization of a semiconductor laser using Rb-D1 and D2 absorption lines," *Electron. Lett.* vol. 24, pp. 429-431, 1988.

[11] Cunyun Ye, *Tunable external cavity diode lasers*, chap. 4, World Scientific (2004).

[12] Kristen A. Peterson and Daniel B. Oh "High-sensitivity detection of CH radicals in flames by use of a diode-laser-based near-ultraviolet light source", *Optics Letters*, vol. 24, pp. 667, 1999.

[13] Grady J. Koch "Automatic laser frequency locking to gas absorption lines", *Optical Engineering* , vol. 42, pp. 1690-1693.

[14] O. Ishida and H. Toba, "200 kHz absolute frequency stability in 1.5 μm external-cavity semiconductor laser," *Electronics Letters*, vol. 27, pp. 1018-1019, 1991.

[15] T. Sato, M. Niikuni, S. Sato, and M Shimba, "Frequency stabilization of a semiconductor laser using Rb-D1 and D2 absorption lines," *Electron. Lett.* vol. 24, pp. 429-431, 1988.

[16] Sollberger, A.; Heinamaki, A.; Melchior, H.; "Frequency stabilization of semiconductor lasers for applications in coherent communication systems", *Lightwave Technology, Journal of*, vol. 5, pp. 485 – 491, 1987.

[17] Prasad, C.R.; Fromzel, V.A.; Smucz, J.S.; Hwang, I.H.; Hasselbrack, W.E.; "A diode-pumped Cr:LiSAF laser for UAV-based water vapor differential absorption lidar (DIAL)", *Geoscience and Remote Sensing Symposium, Proceedings. IGARSS IEEE International,* vol. 4, pp. 1465 – 1467, 2000.

[18] JAYARAMAN, V, CHUANG, Z.M., and COLDREN, L.A.: 'Theory, design, and performance of extended tuning range semiconductor lasers with sampled gratings', *IEEE J Quantum Electron,* vol. 29, pp.1824-1834, 1993.

[19] F. Favre and D. Le Guen, "82 nm of continuous tunability for an external cavity semiconductor laser," *Electronics Letters,* vol. 27, pp. 183-184, 1991.

[20] R. Wyatt and W. J. Delvin. "10kHz Linewidth 1.5μm InGaAsP External Cavity Laser with 55 nm Tuning Range." *Electronic Letters,* vol. 19, pp. 110-112, 1983.

[21] B. Boggs, C. Greiner, T. Wang, H. Lin and T.W. Mossberg, "Simple high-coherence rapidly tunable external-cavity diode laser'', *Opt. Lett.* vol. 23, pp. 1906, 1998.

[22] Delorme, F.; Terol, G.; de Bailliencourt, H.; Grosmaire, S.; Devoldere, P.; "Long-term wavelength stability of 1.55-μm tunable distributed Bragg reflector lasers" *Selected Topics in Quantum Electronics, IEEE Journal of,* vol. 5, pp. 480 – 486, 1999.

[23] Woodward, S.L.; Parayanthal, P.; Koren, U.;"The effects of aging on the Bragg section of a DBR laser", *Photonics Technology Letters, IEEE,* vol. 5, pp. 750 – 752, 1993.

[24] H. Mawatari, M. Fukuda, F. Kano, Y. Tohmori, Y. Yoshikuni, and H. Toba, "Lasing wavelength changes due to degradation in buried heterostructure distributed Bragg reflector lasers," *J. Lightwave Technol.,* vol. 17, pp. 918–923, 1999.

[25] S. A. Al-Chalabi, J. Mellis, M. Hollier, K.H. Cameron, R.Wyatt, J. E. Regnault, W. J. Devlin, and M. C. Brain, ''Temperature and mechanical vibration characteristics of a miniature long external cavity semiconductor laser,'' *Electron. Lett.* vol. 26, pp. 1159–1160, 1990.

[26] Ishii, H.; Kano, F.; Yoshikuni, Y.; Yasaka, H.; "Mode stabilization method for superstructure-grating DBR lasers" *Journal of Lightwave Technology*, vol. 16, pp. 433 – 442, 1998.

[27] G. Sarlet, G. Morthier, and R. Baets, "Wavelength and mode stabilization of widely tunable SG-DBR and SSG-DBR lasers," *Photonics Technology Letters, IEEE*, vol. 11, pp. 1351-1353, 1999.

Chapter 6

Application of a Gas Absorption Line as a Frequency Discriminator for Diode Laser Noise Measurements

6.1 Introduction

The ability to accurately quantify and characterize the spectral noise properties of laser diodes is of vital importance in laser based spectroscopic studies. The main focus of this chapter concerns the investigation and assessment of a technique involving a H_2O absorption line at 1.393μm to study and measure the noise properties of a DFB diode laser. In addition, the free running frequency stability of the ECDL and DFB lasers both emitting at 935nm is also examined. In particular, the noise associated with frequency fluctuations in the output of a diode laser is explored with the ultimate aim of determining the spectral linewidth of the device using the gas absorption line frequency discriminator method. The spectral linewidth is used to define the phase noise of the spectral output of a semiconductor diode laser [1-3]. The source of the phase noise has already been discussed in section 4.3 and is not detailed at length here, but it is suffice to say that it arises from carrier density, and spontaneous emission events of the gain medium into the lasing cavity [4-6]. There already exist many well established and proven techniques used to measure the spectral linewidth of semiconductor diode lasers such as heterodyne and self-homodyne methods [7-9]. The self-homodyne technique involves splitting the output of the source under test with one part of the beam passing through a delay arm of several kilometres of fibre and the other through a shorter arm with a polarization controller. The detection technique relies on the fact that the phase of both beams becomes uncorrelated provided the delay time is much larger for the longer arm than the coherence length of the laser. The light from the fibre delay line can thus be regarded as that from an independent local oscillator, which is as noisy as the signal

under test. The two signals are mixed at the photodetector and the resulting interference signal is analysed with an electrical spectrum analyser.

By comparison, the heterodyne method typically involves beating the laser signal under test with a local oscillator laser source with a narrow spectral linewidth. The local oscillator wavelength must be tuned close to the signal laser frequency to allow the mixing product to fall within the bandwidth of the detector, with the resultant beat signal viewed on an electrical spectrum analyser. As discussed in chapter 5, a gas absorption line can be successfully used as a frequency reference for stabilization of the output emission frequency of a laser source [10]. In addition to its use as an absolute frequency reference, an absorption line can also be employed to act as a frequency discriminator to measure frequency fluctuations in the output of a semiconductor laser [11].

In this chapter, a novel technique to measure the spectral linewidth of a DFB laser emitting at $1.393\mu m$, with a water absorption line acting as a frequency discriminator is considered. The idea for this measurement evolved from studies of the free running frequency stability of laser diodes employing a gas absorption line. Analysis of the results is presented and the technique is compared to a more traditional and proven spectral linewidth measurement scheme. Examples of more traditional frequency discriminators, that convert frequency fluctuations into intensity fluctuations, include high finesse Fabry-Perot cavities or unbalanced interferometers [12]. However, they are susceptible to thermal and mechanical influences, which can alter their accuracy unlike a gas absorption line at a fixed pressure and temperature. In a similar manner, the technique involves measuring the maximum frequency modulation to amplitude modulation (FM-AM) conversion by tuning the emission wavelength of the source under test to the exact point on the absorption line where this maximum frequency modulation to amplitude modulation conversion occurs. By measuring the maximum intensity fluctuations and having accurate and absolute knowledge of the absorption line profile in question, a value for the instantaneous noise frequency of the laser source under test can be determined.

For a laser source to act as an injection seed laser in a frequency stabilization system, the free running emission frequency stability of a laser is a very important measurement. The ability to quantify the free running frequency drift of a laser source is important if the laser is to function in a system for very long time periods, as would be the case for any

space based mission. Therefore, the free running frequency drift of an ECDL and DFB laser were measured using a H_2O absorption line as an absolute wavelength reference. The technique involves setting the laser wavelength to the centre of a gas absorption line and monitoring the transmitted signal. The emission output from two lasers, both emitting at 935nm, is directed through a gas cell with any drift in the laser frequency observed by a change in the amplitude of absorption/transmitted signal. There is no active wavelength stabilization applied to the laser for the duration of the measurement and the pressure and temperature of the gas cell are kept constant.

6.2 *Laser noise spectral density and spectral linewidth*

The technique that employs a gas absorption line to measure the spectral linewidth of a laser diode, is similar to that used by previous authors where frequency fluctuations are measured using a Fabry-Perot resonator that acts as a frequency discriminator [13]. The output radiation from a laser has some nominal centre frequency at which it operates. Of course there exists some instantaneous noise defined by the spectral linewidth of the laser.

The electric field of the output of a laser above threshold can be represented by,

$$E(t) = E_0(t)cos(2\pi v_0 t + \delta\varphi(t)) \tag{6.1}$$

where $E_0(t)$ and $\delta\varphi(t)$ are slowly varying real functions of time and v_0 is the constant laser frequency. Of course for an ideal device the intensity and phase noise are both zero but this is not possible in practice. Consequently, the instantaneous frequency of the laser output can be written as,

$$v(t) = v_0 + \delta\varphi(t)/dt = v_0 + v_n(t) \tag{6.2}$$

where $v_n(t)$ is the frequency noise. In order to quantify the noise of the output of a laser diode it is the frequency or phase noise that needs to be characterised as the spectral linewidth of a laser source is fundamentally related to the frequency or phase noise. The

phase/frequency fluctuations of the output of a laser can be treated in terms of phase noise spectral density $S^\varphi(f)$ with units of rad^2/Hz, where f denotes the Fourier frequency. The spectral density of a random signal is defined as the Fourier transform of its autocorrelation function [14].

$$S^\varphi(f) = 2 \int_{-\infty}^{\infty} R^\varphi(\tau) \exp(-2\pi i f \tau) d\tau \tag{6.3}$$

where $R^\varphi(\tau)$ is the autocorrelation of the phase noise. The autocorrelation function of the instantaneous frequency deviation $\delta\varphi(t)$, of the optical phase is given by,

$$R\varphi(\tau) = <\delta\varphi(t)\, \delta\varphi(t + \tau)> \tag{6.5}$$

where τ is a delay time and the angled brackets represent temporal averaging. Obviously, depending on the situation it may be more appropriate to think in terms of frequency deviations $\delta f(t)$ instead of phase deviations and so the corresponding frequency noise spectral density with units of Hz^2/Hz is defined as,

$$S^v(f) = S^\varphi(f) \cdot f^2 \tag{6.6}$$

The relevant noise properties of laser sources can be treated in terms of either frequency noise spectral density or phase noise spectral density. However, the focus of the work in this chapter is concerned with determining a spectral linewidth value by measuring the instantaneous frequency fluctuations of a DFB laser with respect to the optical carrier frequency.

6.2.1 Gas absorption line frequency discriminator

The method employed to measure the frequency noise of a semiconductor DFB laser involves a H_2O absorption gas line at a fixed temperature and pressure. The interest in developing a new linewidth measurement technique lies with the expense that is incurred in purchasing kilometres of fibre at non-communication wavelengths (e.g. 935nm), in order to measure spectral linewidths of devices using traditional self-homodyne techniques. In addition, it is not always possible to carry out the heterodyne technique. This is due to the fact that a narrow linewidth ECDL operating at the same wavelength of the laser under test may not always be available. The experimental set-up for this technique involves passing the output of the laser through low-pressure gas cell where any frequency variations in the output of the laser will be converted to amplitude variations in the transmitted signal at a certain position on the side of the gas line similar to the technique in [15,16]. The non-stabilized central frequency of the laser emission is set to the side of the water absorption line where maximum frequency to intensity fluctuations occurs. The amplitude change can be then detected, provided a suitable photodetector is used with the resultant transmitted signal recorded. An illustration of the frequency variations to amplitude variations is shown in Fig. 6.1.
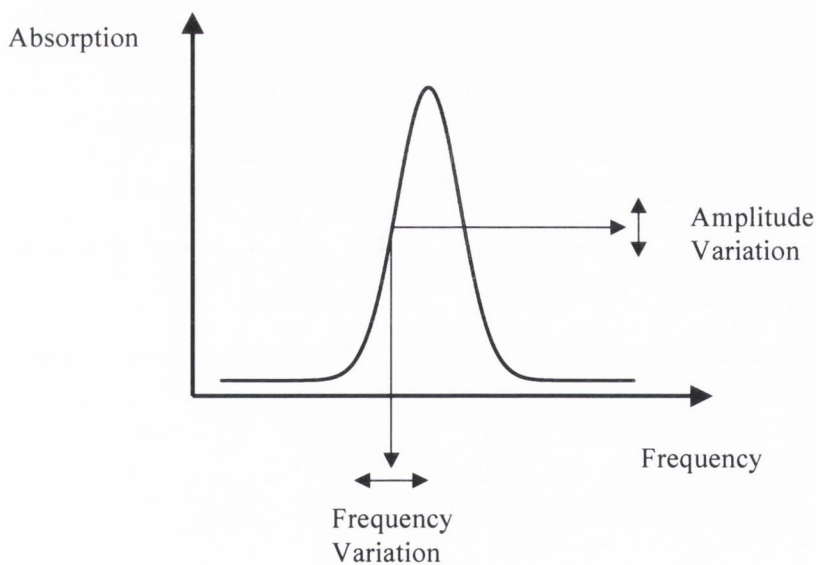

Figure 6.1. *Doppler lineshape for the spectral distribution of the absorbed intensity with the frequency to amplitude conversion also indicated.*

127

The conversion of the frequency modulation (FM) to amplitude modulation (AM) at a particular frequency depends on the slope (or derivative) of the absorption at that frequency. The gas cell used is a single-pass cell 1metre in length with angled Brewster windows to help minimize interference fringes. The main limiting factor is the amplitude noise of the laser and the noise floor on the photodetector. If the noise is too large, then the FM to AM converted signal will be difficult to detect as it is buried in the laser noise. This problem is overcome by incorporating into the experimental set-up an auto-balanced photodetector, details of which are described in section 6.3.1. In order to get a clearer insight into the significance of the slope of a typical absorption line profile, a mathematical model was developed for the FM-AM converted signals using the following equations.

From figure 6.1,

$$\frac{\Delta I}{I_0} = \frac{i_{FM} + i_{NOISE}}{I_0} \qquad (6.7)$$

$$\frac{\Delta I}{I_0} = \text{AM converted signal} = M \qquad (6.8)$$

$$\Rightarrow \frac{\Delta I}{I_0} = \frac{1}{I_0}\left(\frac{dI}{d\omega}\right)\Delta\omega \qquad (6.9)$$

where $\Delta\omega$ = frequency variations corresponding to laser linewidth.

Beer-Lambert law states $\quad I = I_0 e^{-\alpha L} \qquad (6.10)$

Let $\quad e^{-\alpha L} = e^{-\alpha(\omega)} \qquad (6.11)$

$\text{Slope of Absorption} = \frac{dI}{d\omega} = I_0\alpha(\omega)\frac{d\alpha}{d\omega} \qquad (6.12)$

$$\alpha(\omega) = \alpha_p e^{-\left(\frac{\omega}{\gamma_{ED}}\right)^2} \qquad (6.13)$$

where, α_p = peak absorption, ω = frequency

γ_{ED} = 1/e Doppler halfwidth = $\gamma_D /(\ln 2)^{1/2}$

$$\frac{d\alpha}{d\omega} = \alpha(\omega)\left(\frac{2\omega}{\gamma_{ED}^2}\right) \qquad (6.14)$$

$$\Rightarrow \frac{dI}{d\omega} = I_0 \alpha^2(\omega)\left(\frac{2\omega}{\gamma_{ED}^2}\right) \qquad (6.15)$$

From the model, it is possible to locate the exact frequency on the side of the gas line where the optimum FM-AM conversion occurs. The laser can then be accurately tuned with injection current to this point on the side of the gas line and by measuring the AM signal, the instantaneous frequency fluctuation of the laser can be calculated using the known value (from the model) of $\frac{dI}{d\omega}$ at that point. From equation 6.8,

$$M = \alpha^2(\omega)\left(\frac{2\omega}{\gamma_{ED}^2}\right)\Delta\omega \qquad (6.16)$$

By differentiation, $\quad M' = \left[2\alpha(\omega)\frac{d\alpha}{d\omega}\left(\frac{2\omega}{\gamma_{ED}^2}\right) + \left(\frac{2\omega}{\gamma_{ED}^2}\right)\alpha^2(\omega)\right]\Delta\omega \qquad (6.17)$

At a maximum,

$$2\alpha(\omega)\frac{d\alpha}{d\omega}\left(\frac{2\omega}{\gamma_{ED}^2}\right) = -\left(\frac{2\omega}{\gamma_{ED}^2}\right)\alpha^2(\omega) \qquad (6.18)$$

$$\Rightarrow \frac{4\omega^2}{\gamma_{ED}^2} = -1 \qquad (6.19)$$

$$\Rightarrow \frac{2\omega}{\gamma_{ED}} = \pm 1 \qquad (6.20)$$

Therefore, maximum FM to AM conversion occurs at,

$$\omega = \pm\frac{\gamma_{ED}}{2} \qquad (6.21)$$

where $\gamma_{ED} = 1/e$ Doppler halfwidth.

Figure 6.2 shows the simulated results from the model of the H_2O absorption profile showing the Doppler lineshape of the absorption profile and the clearly indicated positions on either side of line centre where the maximum frequency modulation to amplitude modulation can occur. The trace for the simulated conversion values follow a typical $1f$ demodulated signal and is used to calculate the slope of the absorption line. Once, the gas cell pressure and temperature are maintained constant, the slope of the H_2O absorption line can be then calculated from the model which in turn is used to measure the frequency noise of a device under test.
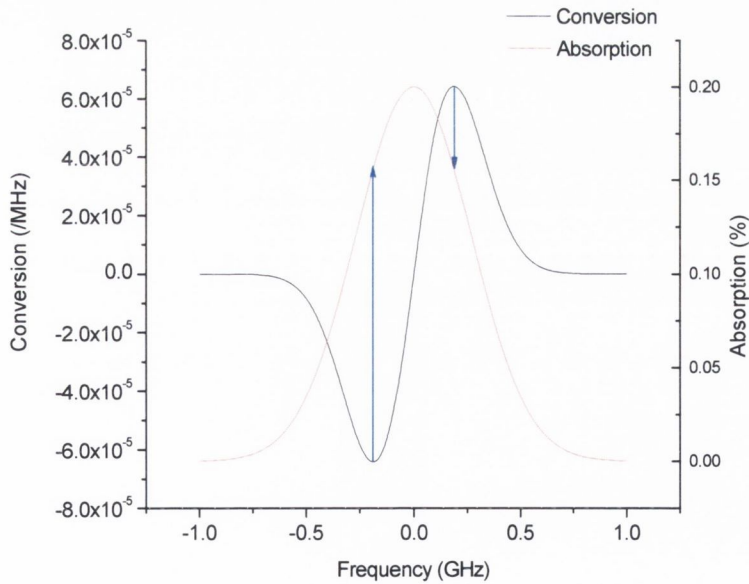

Figure 6.2. *Simulated results of model showing the absorption and optimum FM-AM conversion frequencies on the side of the gas absorption line.*

6.3   1.39μm DFB laser spectral characteristics

A distributed feedback (DFB) laser diode was chosen to act as the test device for the linewidth measurement technique on the side of a gas absorption line. The device was supplied by Aero-laser and showed good SMSR >35dB at an emission wavelength of 1.393μm, at room temperature. The device wavelength tuning characteristics with injection current were measured using a multi-wavelength meter (HP 86120B) with a maximum resolution of 0.001nm, in slow mode operation. The DFB laser wavelength tuning rate was measured to be 2.09×10^{-2} nm/mA over the range of 100mA to 150mA. To measure the direct detection of water vapour at 1.39μm, the emission output of the DFB laser was passed through a 1metre long gas cell containing water vapour at approximately 25mbar at a constant temperature and detected with a photodiode. Figure 6.3 shows the results of both the linear wavelength tuning of the laser with injection current and the direct detection of the H_2O absorption signal.
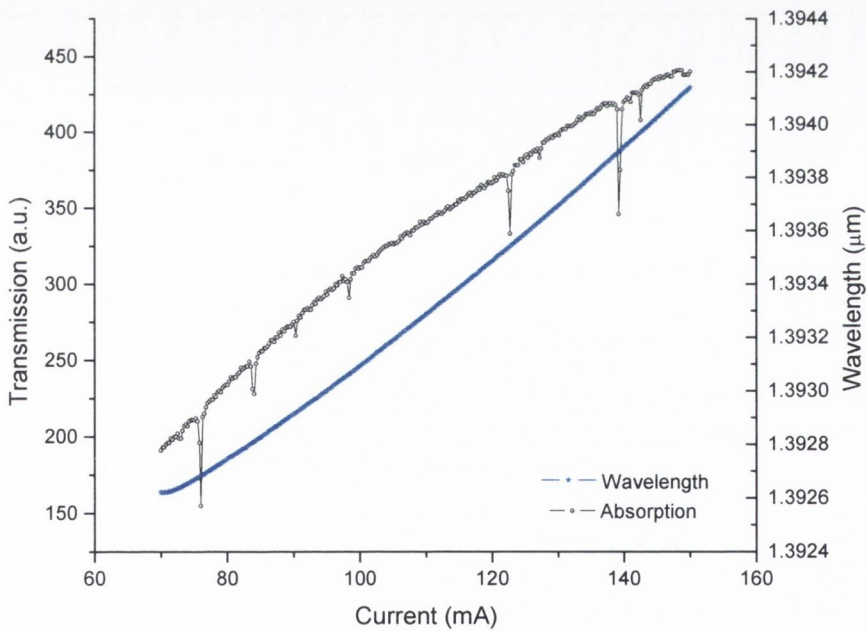

Figure 6.3. *Linear wavelength tuning behaviour of DFB laser and the direct detection of water vapour through 1 metre gas cell at 25mbar and 22^0C showing the numerous H_2O absorption lines present at this wavelength.*

6.3.1 *Experimental set-up and balanced detector operation*

In order to improve the frequency/phase noise measurement technique, an ultra low noise current source (ILX Lightwave, Model LDX 3620) was used to minimize the bias current fluctuation. The DFB laser temperature is controlled by means of a Peltier cooler and a temperature controller. The experimental set-up to measure the frequency/phase noise of the single frequency DFB laser is shown in figure 6.4. The output from the laser is split using a 50/50 beam splitter with one portion of the beam passing through a 1m gas cell containing H_2O vapour at 25mbar and the other is directly detected with the reference photodiode of a balanced detector. This measurement technique is facilitated by a New Focus balanced detector (Nirvana Model 2017), which enables the reduction of the common-mode laser noise by more than 50 dB at frequencies from DC to 125 kHz in either simple balanced mode, or by utilizing the auto-balancing circuit. The balanced detector cancels noise, such as laser intensity noise, common to both the reference and signal beams and therefore eliminates this from the overall detected measurement.
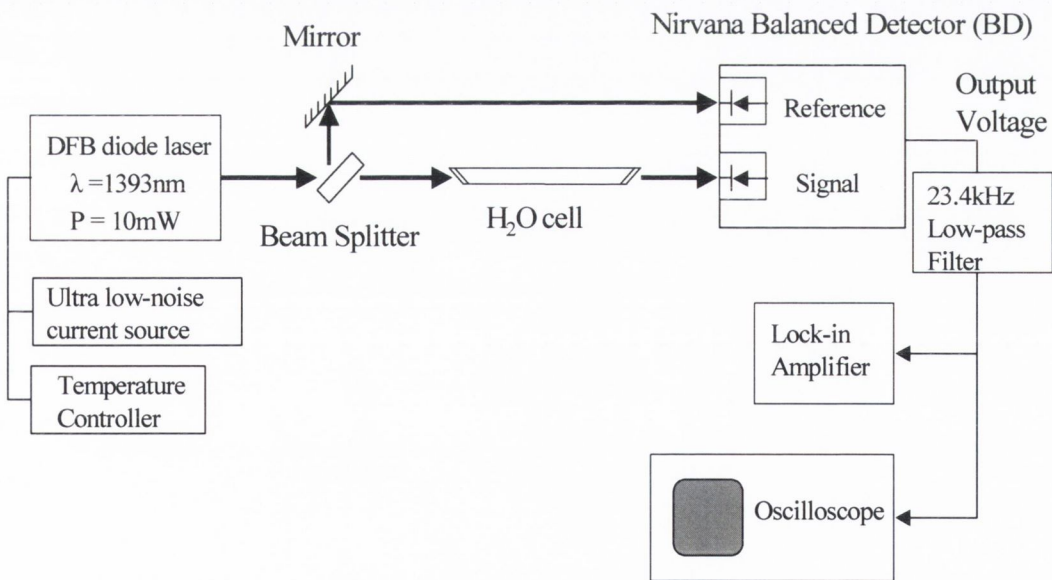

Figure 6.4. *Experimental set-up for frequency noise measurements of 1.39μm DFB using a New Focus balanced detector and H_2O absorption line with the optical path drawn as darker arrows.*

In the self-homodyne linewidth measurement technique, the delay line in the experimental set-up ensures that both arms of the interferometer are recombined in an uncorrelated state. As a result the optical interference between the two arms and hence the spectral linewidth or noise of the laser is measured. With the gas absorption line method, the balancing effect of the Nirvana detector guarantees that all intensity noise fluctuation in the laser output is balanced in addition to the actual laser output frequency. The resultant signal of the photodetector records the amplitude of the instantaneous frequency noise of the laser. The instantaneous frequency noise of the DFB laser is calculated from both the model, where the slope of the absorption line is determined, and the output of the balanced detector. The slope of the absorption line is determined by the pressure and temperature of the gas in 1 metre cell. As a result, the pressure and temperature of the water vapour in the gas cell was fixed to provide a slope where maximum FM-AM conversion occurs. According to the balanced detector specifications, optimum noise reduction is achieved when the power split ratio between the signal and reference photodiodes is equal to 2. By careful and accurate adjustment of the signal levels onto each photodiode the desired two to one ratio is obtained. A more detailed description of the optimum operation of the balanced detector can be found in [17].

From the model of the H_2O absorption line profile, the position on the side of the absorption line for optimum frequency modulation to amplitude modulation was determined and by careful adjustment of the low noise current source, it was possible to tune the emission wavelength of the laser to that frequency and thus record the noise amplitude. By inputting into the model the various parameters such as peak absorption, linewidth and absorption path length, it was possible to calculate the resulting conversion factor in units of V/Hz. The emission wavelength of the DFB laser, with the laser temperature fixed at 20^0C, was tuned with injection current across the H_2O line to compare the model results with experimental data. Figure 6.5 shows the results of the recorded balanced signal and direct detection of the H_2O line at 1.393μm. It is evident from the trace that the auto-balancing of the photodetector works very well with an amplitude change occurring on either side of the line centre as expected.
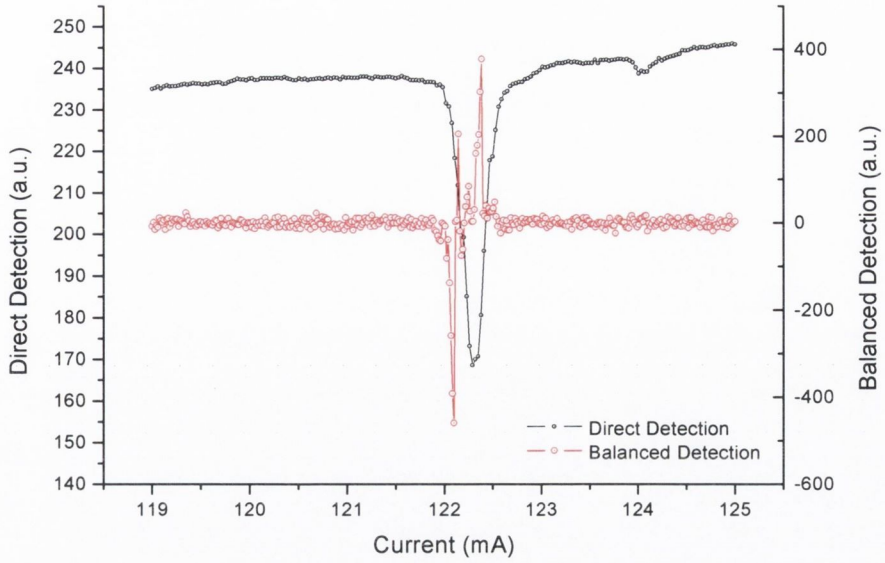
Figure 6.5. *Balanced detector output and direct detection of a H_2O absorption line at 1.393 μm as the wavelength of the DFB is tuned with injection current at constant temperature.*

A more detail view of the balanced detector output as the emission wavelength of the device is scanned across the line is shown in figure 6.6, where the amplitude change was recorded with a digital oscilloscope (Tektronix Model TDS 380). From the trace, the conversion of frequency modulation on the output of the laser to amplitude modulation of the detected signal, on the side of the H_2O absorption line is clearly observable where the zero on the x axis corresponds to the centre of the absorption line.
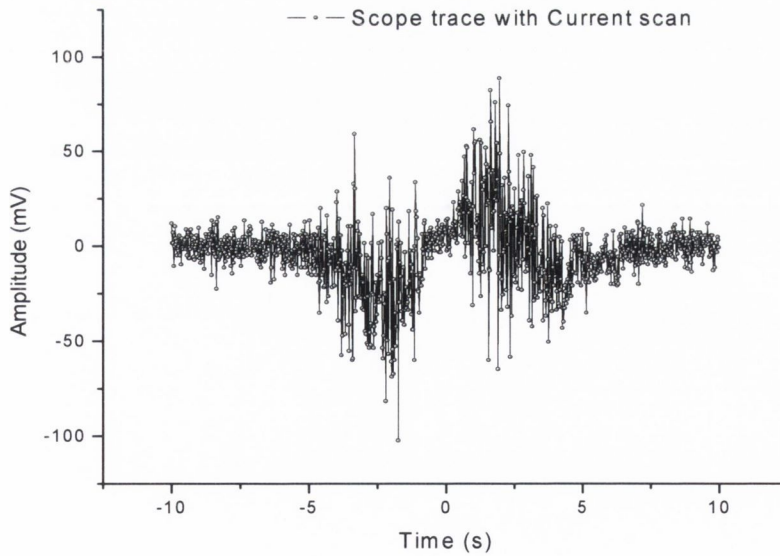

Figure 6.6. *Output of Nirvana balanced detector measured with a fast oscilloscope as the DFB wavelength is tuned linearly with injection current.*

This result agrees well with the simulated model where the maximum frequency to amplitude conversion occurs, as clearly indicated by the arrows in figure 6.2. In order to quantify these frequency fluctuations, and hence determine a value for the linewidth, the emission wavelength of the DFB laser under test was tuned with injection current to the point where maximum frequency modulation to amplitude modulation conversion occurs. The resultant signal from the balanced photodetector was recorded up to a maximum limit of 20kHz at a sampling rate of 40kHz. In order to remove any higher frequency components from the measurement, the signal was also filtered with a low pass filter at 23.4kHz. The injection current to the DFB laser at this point was approximately 138mA and the temperature was fixed at 20^0C. The value for the slope of the absorption line profile was calculated from the simulated model and thus it was possible to convert the amplitude fluctuations detected with the balanced detector, into frequency fluctuations of the instantaneous laser noise. The trace in figure 6.7 shows the magnitude of the instantaneous frequency noise fluctuations calculated from a combination of the slope of the water absorption line and the amplitude of the auto-balanced detector signal.
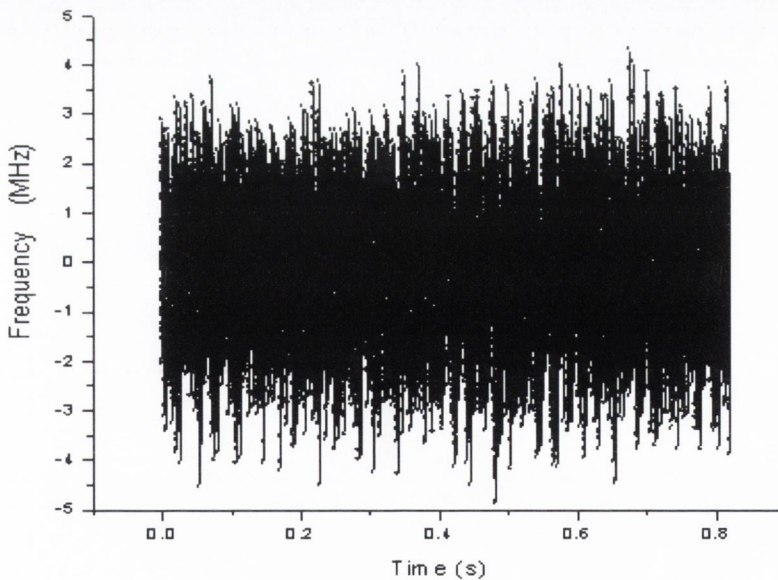

Figure 6.7. *Instantaneous frequency noise measurement of DFB laser diode at a constant injection current of 138mA and temperature of 20^0C on the side of H_2O absorption line at 1.393μm using the Nirvana balanced photodetector.*

From the data in figure 6.7, a value of 1.21MHz was obtained for the rms of the frequency noise. For a laser diode spectral linewidth measurement, it is critical that the effect of 1/f noise is isolated or filtered from the actual data that represents the linewidth. For coherent systems, the effect of the Lorentzian component of the laser lineshape resulting from white frequency noise, is much more critical in terms of device performance, whereas the 1/f frequency noise is less significant [18]. Similarly, the measurement recorded with the balanced detector/absorption line combination is processed to ensure that it represents white frequency noise only. A Fourier transform of the data in figure 6.7 was performed resulting in the trace in figure 6.8. The 1/f noise from 0Hz to 15kHz was filtered and removed so that a more precise value for the spectral linewidth of the DFB laser was determined. Typically, the 1/f noise is observed for frequencies lower than approximately 10kHz [19]. The data from 15kHz to 20kHz was considered for determining the spectral linewidth of the laser as the roll off of the 1/f noise ends at 15kHz as is clearly observable from the trace in figure 6.8. Ideally, extending the level plateau to include more data above the 1/f roll off would benefit the measurement, although this was not possible with the 20kHz limit of the lock-in amplifier in question.
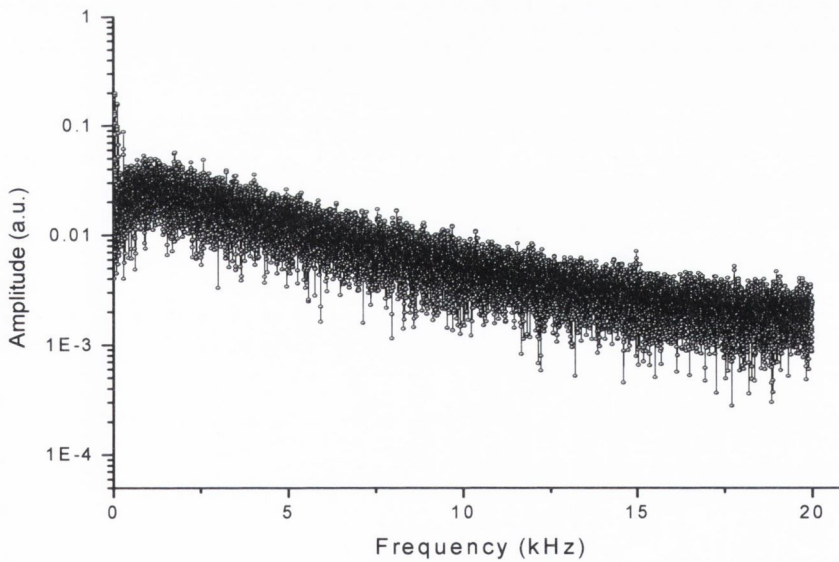

Figure 6.8. *Fourier transform of instantaneous frequency noise in figure 6.7.*

136

An inverse Fourier transform of the data in the 15kHz to 20kHz region was carried out in order to determine the instantaneous frequency fluctuations of the laser output for that frequency range. To extract spectral linewidth information from the data, a histogram of the laser frequency variation provides the distribution of the individual frequency components, as shown in figure 6.9. A Gaussian lineshape function was fitted to the data and a value of 0.52MHz was obtained for the FWHM of the trace. Therefore, for this measurement technique, the spectral linewidth of the DFB laser emitting at 1.39μm is determined to be 0.52MHz.
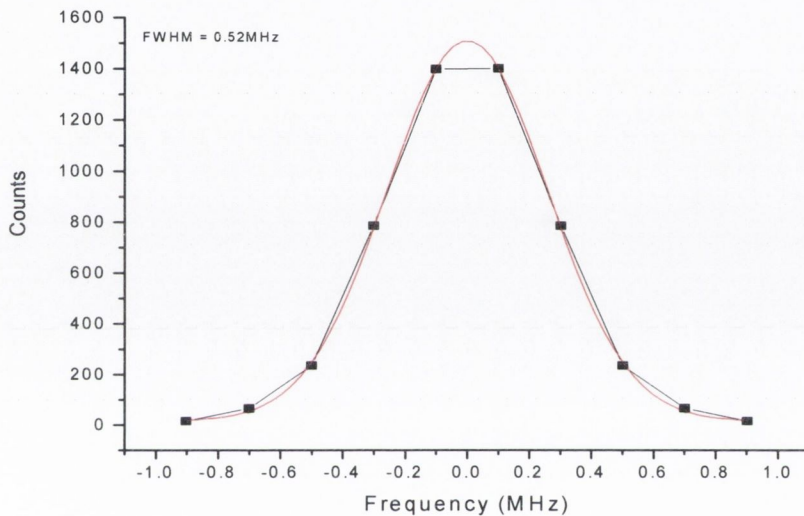

Figure 6.9. *Frequency distribution of the instantaneous noise measured by a simple histogram and a Gaussian fit giving a value of 0.52MHz for the FWHM.*

In order to compare results and test the validity of the measurement technique using the gas absorption line, the spectral linewidth of the DFB laser was measured simultaneously with the frequency noise measurement in figure 6.7, using a long arm homodyne technique and a fibre optic interferometer (Agilent Model 11980A).

The experiment consists of fibre coupling the output of the DFB laser and connecting the fibre to the input arm of the interferometer. A built in 50/50 splitter separates the beam into two arms with one delayed by passing it through approximately 5km of fibre, which corresponds to a delay of 25μs. The other arm is significantly shorter and consists of a polarization controller. The polarization adjustment operates on the principle of rotating

an optical birefringence in the plane of propagation of the entering light energy. This birefringence is realized by rotating a looped optical fiber. The physical stress in the fiber induces a birefringence in the refractive index properties of the fiber, causing a polarization shift. The two signals travel along separate fibre paths where the difference in the path lengths ensures there is no coherence relationship between the two beams when they recombine. The signals, which are thus uncorrelated, are then combined with a polarization stage that is used to optimise the output magnitude of the combined signal. The signal was detected with a 1GHz bandwidth photodetector and the spectrum was viewed with an electrical spectrum analyser. The details and theory of this method have already been discussed in chapter 4 and are not given here. The graph in figure 6.10 shows the resulting spectrum which was fitted with a Lorentzian profile. A value of 1.75MHz was determined for the linewidth of the DFB laser diode. The injection current to the laser was fixed at 120mA for this measurement, but the fact that the device did not have an optical isolator made the measurement more difficult and could result in feedback into the laser cavity from the collimating optics.
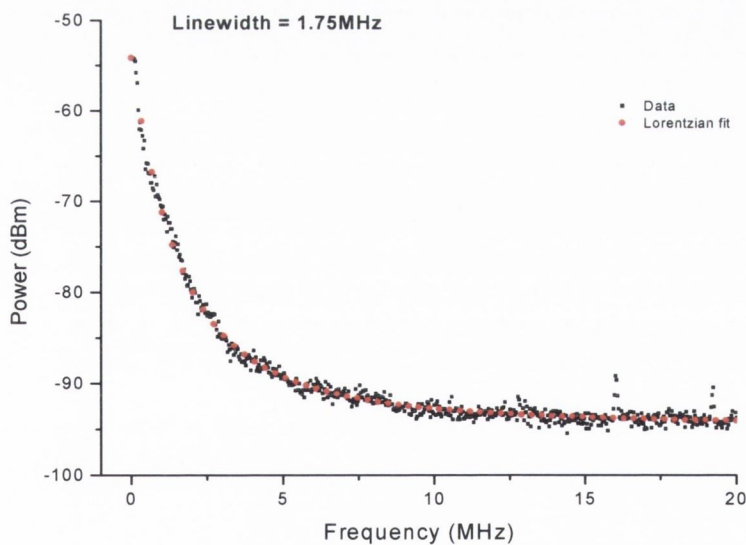

Figure 6.10. *Spectral linewidth of the 1.39μm DFB laser using a long arm homodyne technique at 20°C measured simultaneously with the frequency noise using the H₂O absorption line method.*

The self-homodyne and gas absorption line as a frequency discriminator techniques resulted in values for the spectral linewidth of a DFB laser of 1.75MHz and 0.52MHz respectively. The values differ by 1.23MHz but show reasonable agreement.

6.4 Frequency stability measurements

For any laser source to function as a frequency reference or as injection seed laser, it is essential to gain an indication of the unstabilized frequency drift of the device. In this section, the free running frequency drift of both an ECDL and DFB laser both emitting single mode at 935nm, are examined. In chapter 5, a frequency stabilization scheme to overcome the free running drift of an external cavity diode laser, was presented. The output of the laser was frequency locked to a gas absorption line using wavelength modulation spectroscopy and resulted in frequency stabilization of less than 3MHz. This value was deemed more than sufficient for successful operation of the laser for an injection seed laser role. The free running emission frequency stability of a laser can also be measured using a suitable water vapour absorption line as an absolute wavelength reference. For the measurement the temperature and pressure of the water vapour in a gas cell are held constant to ensure spectral and amplitude stability of the absorption line. The emission frequency of the laser is set to a value equal to that at the centre of a water absorption line and the transmitted power signal of a photodiode is monitored. The laser emission is directed through a gas cell and laser frequency variations are converted to changes in amplitude of the absorption/transmitted signal. These frequency variations are converted to amplitude variations and are detected with a photodiode as already indicated in figure 6.1. The results for the ECDL device are shown in figure 6.11. Below the 5 hour mark on the trace, the frequency decreases to 0Hz which corresponded to the laser frequency drifting across the absorption line centre.
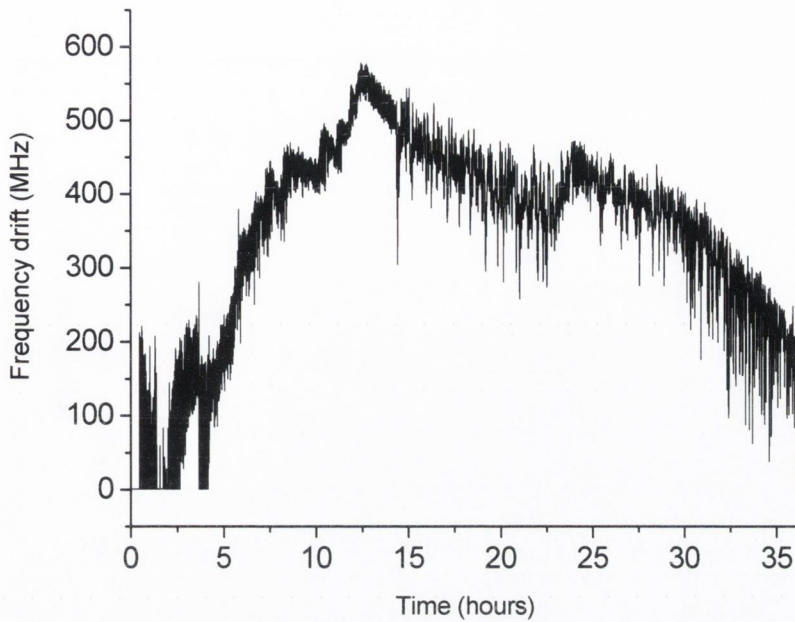
Figure 6.11. *Frequency drift of ECDL versus time for approximately 36 hours.*

The ECDL was continuously operated without adjustment for the duration of the test and the full frequency drift measured over the 36 hours period is approximately 540MHz. The frequency drift of the laser was measured by monitoring the absorption signal. By relating the signal strength to the width of the gas absorption line the frequency drift of the laser was calculated. An identical test was also carried out on a DFB laser diode emitting at 935nm. In the same manner, the output frequency of the DFB laser was tuned to the centre of a water absorption line with the absorbed transmitted signal monitored for the duration of the test. Figure 6.12 displays the results of the frequency drift for a period of 62 minutes where the maximum drift recorded was measured to be 340MHz. Because the ECDL was the laser source used for the injection seed source role, a more thorough and longer lasting frequency drift time period was performed. The analysis of the frequency drift of the ECDL lasted for 36 hours compared to 62 minutes for the DFB laser diode.
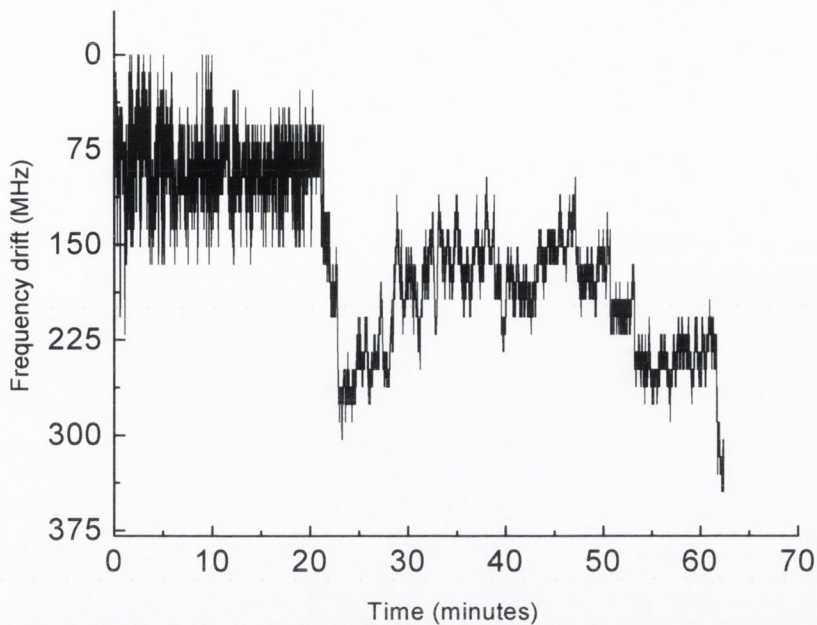
Figure 6.12. *The measured free running frequency drift of the DFB laser diode at 935nm over a period of 62 minutes showing a maximum drift of 340 MHz.*

6.5 Conclusions

A spectral linewidth measurement technique using a gas absorption line as a frequency discriminator has been investigated as an alternative method to the more common methods. Techniques such as the delayed self-homodyne employ kilometres of fibre generating extra cost for the experimental set-up. This is especially true at wavelengths far from the typical 1550nm telecommunication standard. The measurement of a DFB laser diode frequency noise has been successfully demonstrated by incorporating a water vapour absorption line as a frequency discriminator. By introducing an autobalancing photodetector, the frequency noise of the laser output was measured as an amplitude fluctuation. This amplitude fluctuation is then converted to a frequency by combining the auto balanced output signal and the simulated results of the absorption line in question, to extract the slope in terms of V/Hz. By constructing a histogram of the resultant frequency noise, analysis of the data resulted in a value of 0.52MHz for the laser linewidth of the

laser source. As already discussed, this linewidth value is narrow for a typical DFB laser diode but the absence of an optical isolator in the device packaging could result in external optical feedback having the effect of linewidth narrowing. However, it is noted that without any Fourier analysis to filter the 1/f noise of the instantaneous frequency noise recorded in figure 6.7, a histogram of this recorded signal resulted in a linewidth of 2.43MHz. This value is similar to the measurement taken simultaneously with a delayed self-homodyne technique where a value of 1.75MHz for the linewidth of the laser was measured.

Further investigation and development of this technique is required for a more complete validation before it can be employed with complete confidence for spectral linewidth measurements. However, the technique using the gas absorption line has already been shown to show reasonable agreement, within 1.23MHz of the standard self-homodyne measurement technique. If found to operate conclusively in a successful manner, this linewidth measurement technique using a gas absorption line as a frequency discriminator could be of great benefit to researchers employing lasers for operation outside the usual telecommunications wavelengths. For example, an experiment to measure the spectral linewidths of two lasers, whose linewidth values are already known and differ by an order of magnitude, would help to authenticate the technique. If both lasers operated without fibre coupling, then the ability to match the power split ratio of the balanced detector would also be improved. The measured frequency noise of the laser with a larger linewidth would show more frequency noise in comparison to the narrower linewidth laser. Unfortunately, two such lasers were not immediately available but would be of interest in the future.

Finally, the free running frequency drift of an ECDL and a DFB both emitting at 935nm were also examined using a water vapour absorption line. This measurement is critical before any frequency stabilization is implemented to a laser source. An initial investigation of each device was made and the measurements provided the original idea for the spectral linewidth measurement technique detailed in this chapter. The ECDL showed a maximum drift of 540MHz over a 36 hour period and the DFB laser showed a maximum of 340MHz drift over a 62 minute period.

6.6 References

[1]   C. H. Henry, "Theory of the phase noise and power spectrum of a single mode injection laser," *IEEE J. Quantum Electron.,* vol. QE-19, p. 1391, 1983.

[2]   Y. Yamamoto, T. Mukai, and S. Saito, "Quantum phase noise and linewidth of a semiconductor laser," *Electron. Lett.,* vol. 17, p. 327, 1981.

[3]   C.H. Henry, "Phase noise in semiconductor lasers," *Journal of Lightwave Technology*, vol. 4, pp. 298-311, 1986.

[4]   J.Armstrong: "Theory of interferometric analysis of laser phase noise", *Journal of Optical Society of America*, vol. 56, pp. 1024-1031, 1966.

[5]   Dandridge, A. B. Tveten "Phase noise of single-mode diode lasers in interferometer systems", *Appl. Phys. Lett.*, vol. 39, pp. 530-532, 1981.

[6]   K. Vahala, A Yariv, "Semiclassical theory of noise in semiconductor lasers--Part II", *IEEE Journal of Quantum Electronics*, vol. 19, pp. 6, 1983.

[7]   Nazarathy, M.; Sorin, W.V.; Baney, D.M.; Newton, S.A.; "Spectral analysis of optical mixing measurements", *Journal of Lightwave Technology*, vol. 7, pp. 1083 – 1096, 1989.

[8]   T.Okoshi,K. Okikuchi, A. Nakayama, "Novel method for high resolution measurement of laser output spectrum", *Electronic Letters*, vol. 16, pp 630-631, 1980.

[9]   D. M. Baney and W. V. Sorin, "Linewidth and power spectral measurements of single-frequency lasers,"*Hewlett-Packard J.*, pp. 92–96, 1990.

[10] Sudo, S.; Sakai, Y.; Yasaki, H.; Ikegami, T.; "Frequency stabilization of 1.55 μm DFB laser diode using vibrational-rotational absorption of $^{13}C_2H_2$ molecules", *Photonics Technology Letters, IEEE*, vol. 1, pp. 392 – 394, 1989.

[11] Bava, E.; Galzerano, G.; Svelto, C.; "Frequency-noise sensitivity and amplitude-noise immunity of discriminators based on fringe-side Fabry-Perot cavities"; *IEEE Transactions on Ultrasonics, Ferroelectrics and Frequency Control*, vol. 49, pp. 1150 – 1159, 2002.

[12] M.E Tobar,; "Fabry-Perot resonator with interferometric read-out for low noise applications", *IEEE Transactions on Ultrasonics, Ferroelectrics and Frequency Control*, vol. 47, pp. 495 – 501, 2000.

[13] K. Kikuchi and T. Okoshi, "Estimation of linewidth enhancement factor of AlGaAs lasers by correlation measurement between FM and AM noises," *Quantum Electronics, IEEE Journal of*, vol. 21, pp. 669-673, 1985.

[14] L. S. Cutler, C. L. Searle: "*Some Aspects of the Theory and Measurement of Frequency Fluctuations in Frequency Standards*", *Proc. of the IEEE*, vol. 54, pp. 136 – 154, 1966.

[15] T. L. Myers, R. M. Williams, M. S. Taubman, C. Gmachl, F. Capasso, D. L. Sivco, J. N. Baillargeon, and A. Y. Cho, "Free-running frequency stability of mid-infrared quantum cascade lasers ," *Opt. Lett.*, vol. 27, pp. 170-172, 2002.

[16] R. M. Williams, J. F. Kelly, J. S. Hartman, S. W. Sharpe, M. S. Taubman, J. L. Hall, F. Capasso, C. Gmachl, D. L. Sivco, J. Baillargeon, and A. Y. Cho, "Kilohertz linewidth from frequency-stabilized mid-infrared quantum cascade lasers ," *Opt. Lett.*, vol. 24, pp. 1844-1846, 1999.

[17] New Focus, Inc., "Nirvana. auto-balanced photoreceivers, Model 2007 & 2017 user's manual".

[18] L. B. Mercer, "1/f frequency noise effects on self-heterodyne linewidth measurements," *Lightwave Technology, Journal of*, vol. 9, pp. 485-493, 1991.

[19] K. Petermann, "Laser Diode Modulation and Noise", Kluwer Academic Publishers, Dordrecht, Co-publication with KTK, pp. 172, 1988.

Chapter 7

Conclusion

7.1 Review

Gas sensing using semiconductor diode lasers has had a very successful history thanks to the development and research carried out by the telecommunications industry [1]. Fortunately, this development has resulted in a technology that can also be implemented to monitor and detect a variety of different absorbing species over a wide range of wavelengths. Numerous types of laser devices have been developed over the years as an outcome, and two in particular feature predominantly in this thesis. The distributed feedback (DFB) laser diode forms the backbone of fibre transmission applications with its excellent single mode, high power operation but has also been effectively applied in the gas sensing field. In addition, an external cavity diode laser (ECDL), a device often used for sensing applications, has featured strongly in this work. The ECDL offers some beneficial spectral properties in comparison to the DFB laser, with its narrow spectral linewidth and the option of a wide wavelength tuning range.

The principal objectives of this thesis includes, the investigation of the suitability of these two laser diode sources to function as injection seed lasers for a water vapour experiment in space. The ECDL was implemented in a frequency stabilization scheme where the performance of the frequency locked source was examined. The development of a novel mode referencing technique greatly improves the frequency locking accuracy of the ECDL and is also of great benefit to the uninterrupted, long term operation of the laser, as required for many space-based missions. Finally, a new technique to measure the spectral linewidth of a DFB laser using a H_2O absorption line at 1.39µm as a frequency discriminator was also explored.

In chapter 4, background information regarding the water vapour sensing experiment in space is outlined. The spectral characteristics of the two candidate injection seed lasers, an ECDL and a DFB laser diode, both emitting at 935nm, are studied to assess their suitability for H_2O sensing applications. Their operational characteristics are measured including, SMSR, wavelength tuning range, output power, and spectral linewidth. Further

146

tests are also carried out on the ECDL which involves monitoring its spectral performance under near vacuum (<1mbar) conditions and some issues relating to the effect of external optical feedback on the device output. The results confirm what was initially suspected. Even though the ECDL showed superior spectral performance in terms of wavelength tuning over a wider range and a narrow spectral linewidth, the architecture of the device is far too complex and fragile for space flight conditions. The sensitivity of the external grating position and the fibre coupling stage mean that it would be totally unsuitable for operation as an injection seed laser in space. By comparison, even with it's less impressive spectral characteristics, the more robust and compact nature of the DFB makes it an ideal laser source to act as an ISL for this mission.

The frequency stabilization of the ECDL is outlined in chapter 5. The dynamics of the feedback locking loop along with the overall accuracy and performance of the frequency locked system are measured. A water absorption line at 935.684nm was targeted using WMS with the voltage to the piezo modulated at 14kHz [2,3]. The resulting zero crossing point of the *1f* harmonic signal of the absorption line was used to lock the frequency of the laser. A dual feedback loop approach combining a slow and fast loop was adopted for accurate control of the laser output frequency. The slow loop tunes along the wavelength tuning contour path with combination of injection current and grating adjustment, and a second faster loop drives the grating only. It was therefore possible to continuously lock the frequency of the ECDL to within 1.69MHz of the reference locking frequency, for a period of 4 minutes, which lies well within the precision needs for LIDAR applications [4]. In addition a mode referencing technique was devised to improve the long-term performance of the frequency locked ECDL. For any space-based mission, it is common for missions to last several years and so the laser device chosen to function as an ISL must be able to operate without fail over long periods. The initial results for the mode referencing, in combination with the frequency locked laser, demonstrate a system that can operate without any re-characterization of the device. In-situ monitoring of the laser output power meant that it was possible to fix the operating current and piezo values of the laser to the centre, and hence optimum, position of the lasing mode. It was therefore possible to maintain the output frequency of the laser to within <5MHz of the reference frequency even when the temperature of the laser mounting was varied by 1^0C in steps of 0.1^0C.

The details of a novel technique to measure the spectral linewidth of a DFB laser diode are discussed in chapter 6. The method involves using a H_2O gas absorption line profile

to act as a frequency discriminator. Frequency variations in the laser output are converted into intensity variations by tuning the emission wavelength of the laser under test to a point on the side of the gas absorption line where the maximum frequency to intensity modulation occurs. The intensity modulation is measured using an auto-balancing photodetector. A value of 0.52MHz was determined for the spectral linewidth of the laser by measuring the maximum intensity fluctuations and having accurate and absolute knowledge of the absorption line profile in question. Further investigation of the technique is obviously required to conclusively authenticate this approach, but if proved successful, it could provide researchers with a useful technique for measurement of spectral linewidths of lasers outside the usual telecommunications wavelengths. The free running frequency drift of both the ECDL and DFB laser both emitting at 935nm was also investigated. The measurement of the unstabilized frequency drift of any laser source functioning as a frequency reference is crucial. Using a gas absorption line as a frequency discriminator, a maximum value of 540MHz over a 36hour period and 340MHz over a 62 minute period was recorded for the ECDL and DFB laser respectively.

7.2 Future proposals and outlook

Some topics that could be further developed are now outlined.

The application of the mode referencing technique to a widely tuneable laser, other than an ECDL would be of great interest. For the case where a laser device is to function as a frequency reference, the fact that device ageing and external environmental influences cannot affect the laser performance for very long time periods (months) would be of great benefit. Also, knowing that only one initial characterization of the laser was necessary would be of great help in several research fields, not only gas sensing applications.

As discussed in section 3.3, the subject of security, particularly in the transportation industry is currently one of the most popular topics where development in THz sources and detectors is thriving. The ability to detect and view harmful instruments or hazardous materials and narcotics has provided law enforcement agencies throughout the globe with an instrument to counteract these threats. For that reason, looking at extremely high detection sensitivities of the fundamental absorption bands in the 2.5μm - 20μm wavelength region would be of enormous benefit [5].

Throughout this work, the issue of external feedback was a source of constant frustration. Consequently, while attempting to implement laser based gas sensing experiments, the operation and wavelength tuning performance of several lasers suffered. A solution to this issue would be the development of a laser source, perhaps based on the slotted structure of a SFP laser that was specifically designed with a high level of insensitivity to feedback. This could be achieved by designing a laser with a low linewidth enhancement factor and thus, negating the need for expensive and bulky optical isolators in the device packaging.

Finally, the mid-infrared region (2.5μm - 20μm) of the spectrum where the strongly absorbing fundamental absorption bands of many important gas species lie can now be targeted using quantum cascade lasers (QCL). The advent of QCLs has resulted in a device that can operate in the mid-infrared region in continuous wave (CW) mode and at room temperatures. Consequently, much research in this field remains to be undertaken and at present the future for laser based gas sensing is vibrant.

7.3 References

[1]   Russell D. Dupuis, " The Diode Laser—the First Thirty Days Forty Years Ago", *IEEE LEOS Newsletter*; Vol. 17,1, Feb. 2003.

[2]   L.S. Rothmana, et al, " The HITRAN 2004 molecular spectroscopic database," *Journal of Quantitative Spectroscopy & Radiative Transfer,* vol. 96, pp. 139–204, 2005.

[3]   D. S. Bomse, A. C. Stanton, and J. A. Silver, "Frequency-Modulation and Wavelength Modulation Spectroscopies - Comparison of Experimental Methods Using a Lead-Salt Diode-Laser," *Applied Optics*, vol. 31, pp. 718-731, 1992.

[4]   C. Cahen and G. Megie, ''A spectral limitation of the range resolved differential absorption lidar technique,'' *J. Quant. Spectrosc. Radiat Transf.,* vol. 25, pp. 151–157, 1981.

[5]   Woolard, D.L.; Brown, R.; Pepper, M.; Kemp, M.; "Terahertz frequency sensing and imaging: a time of reckoning future applications?", *Proceedings of the IEEE,* vol. 93, pp. 1722 – 1743, 2005.